THE CENTRAL NERVOUS CONTROL OF WALKING IN THE LOCUST, *SCHISTOCERCA AMERICANA*

Thesis by Sylvie Adrienne Ryckebusch

In Partial Fulfillment of the Requirements

for the Degree of

Doctor of Philosophy

California Institute of Technology

Pasadena, California

1994

(Defended 2 March 1994)

Acknowledgements

I could not have done this work alone. So many people contributed in important ways that I could not name them all here. I am very indebted to all of those friends and colleagues who helped and encouraged me in the last six years.

Carver Mead had the difficult task of teaching the naive graduate student that I was how science was done. He was a great teacher and a source of inspiration. For this and much more I am very grateful.

Gilles Laurent deserves a much more eloquent "thank you" than I am capable of writing. He taught me all I know about neurophysiology. I only wish I could have been a better student. Despite the considerable pressures he was under, his support and encouragement never wavered. *Merci,* Gilles, for your guidance and your friendship.

Eve Marder and Mike Nusbaum encouraged me to finish, by tantalizing me with visions of the "afterlife."

Without all of the friends who lured me away from the lab, I might have finished this thesis much sooner. Thank you for giving me so many opportunities to be delinquent. Achim, Fiona, Pietro, and Steve[1] deserve a special place in heaven (if your sins do not bar entry) for tolerating me at my worst. I'm looking forward to our future reunions

[1]Thanks for offering me a Holodeck and so much more

in exotic lands.

Sans ma famille, enfin, je n'aurais pas eu le courage d'entreprendre de si longues études. Merci, Maman, Papa, Annie, Jacques, Anne, David, et Diane, pour votre amour et votre soutien. Bon courage à mes nièces, Jenifer et Sarah, et à mon neveux, Coulter. Je souhaite que vous éprouviez les joies de la découverte.

Pour mon père,
qui a l'âme d'un scientifique

Abstract

Rhythmic motor behaviors in all animals appear to be under the control of "central pattern generator" circuits, neural circuits which can produce output patterns appropriate for behavior even when isolated from their normal peripheral inputs. Insects have been a useful model system in which to study the control of legged terrestrial locomotion. Much is known about walking in insects at the behavioral level, but to date there has been no clear demonstration that a central pattern generator for walking exists. The focus of this thesis is to explore the central neural basis for locomotion in the locust, *Schistocerca americana.*

Rhythmic motor patterns could be evoked in leg motor neurons of isolated thoracic ganglia of locusts by the muscarinic agonist pilocarpine. These motor patterns would be appropriate for the movement of single legs during walking. Rhythmic patterns could be evoked in all three thoracic ganglia, but the segmental rhythms differed in their sensitivities to pilocarpine, their frequencies, and the phase relationships of motor neuron antagonists. These different patterns could be generated by a simple adaptable model circuit, which was both simulated and implemented in VLSI hardware. The intersegmental coordination of leg motor rhythms was then examined in preparations of isolated chains of thoracic ganglia. Correlations between motor patterns in different thoracic ganglia indicated that central coupling between segmental pattern generators is likely to contribute to the coordination of the legs

during walking.

The work described here clearly demonstrates that segmental pattern generators for walking exist in insects. The pattern generators produce motor outputs which are likely to contribute to the coordination of the joints of a limb, as well as the coordination of different limbs. These studies lay the groundwork for further studies to determine the relative contributions of central and sensory neural mechanisms to terrestrial walking.

Contents

Acknowledgements iii

Abstract vi

1 Introduction 1

1.1 Central pattern generators 1

Isolating nervous systems from peripheral inputs 2

Evoking central rhythms 3

Comparing intact and isolated rhythms 4

1.2 Terrestrial locomotion 5

Central pattern generators in terrestrial walkers 6

Insect walking 8

1.3 Overview of this thesis 9

2 Locomotor Rhythms Evoked in Locust Thoracic Ganglia 11

2.1 Summary and conclusions 11

2.2 Introduction 13

2.3 Methods 14

2.4 Results 19

Pilocarpine induces rhythmic activity 19

Description of the rhythm 24
Coupling between hemiganglia of the same segment 42
Coupling to ventilation 44
2.5 Discussion 45
Pharmacologically-induced rhythm and walking patterns 47
Common inhibitors 50
Intrasegmental coupling 51
Intersegmental coupling 51
Walking and related behaviors 52

3 An Adaptive Circuit Model for Segment-Specific Motor Patterns 54
3.1 Summary and conclusions 54
3.2 Introduction 55
3.3 Methods 58
Electrophysiology 58
Computer simulations 59
VLSI implementation 62
3.4 Results 62
Segment-specific rhythmic motor patterns 62
A simple configurable model circuit 68
VLSI implementation 74
Mathematical analysis 78
3.5 Discussion 83
Locomotor rhythm generation in thoracic segments 83
Adaptable neural circuits 85
Design of realistic walking robots 87
Appendix A: A mathematical description of the levator-depressor model . 88

Appendix B: A bursting neuron using summating synapses 91

4 Coordination of Segmental Leg Central Pattern Generators 94

4.1 Summary and conclusions 94

4.2 Introduction 95

4.3 Methods 97

Electrophysiology 97

Data analysis 98

Cross-correlation of neuronal spike trains 99

4.4 Results 103

Rhythmic activity in isolated thoracic ganglia 103

Effects of sectioning thoracic connectives on rhythmic activity 106

Intrasegmental correlations 107

Intersegmental correlations 109

Correlations between non-adjacent hemisegments 116

4.5 Discussion 118

Limitations of the cross-correlation technique 121

Intersegmental coordination and the implications for behavior 123

Neural basis of intersegmental coordination 126

Concluding remarks 129

5 Conclusions 130

5.1 Central control of leg movements during walking 130

5.2 Segment-specific tuning of fictive motor patterns 134

5.3 Coordination of segmental central pattern generators 136

Bibliography 139

Chapter 1

Introduction

1.1 Central pattern generators

It has now been established in over 50 species of animals distributed among 11 classes and 4 phyla that repetitive movements are under the control of neural circuits known as "central pattern generators" (review: Delcomyn 1980). The attempt to define what constitutes a central pattern generator (CPG) has been a subject of heated debate for over 20 years. What is now generally accepted is that the central nervous system does not require feedback from sensory organs to generate the essential rhythmic motor commands underlying a wide variety of repetitive behaviors, such as locomotion, respiration, and feeding. It is also clear, however, that rhythmic patterns generated in nervous systems isolated from their normal peripheral inputs differ in important ways from those observed in an intact animal, because centrally generated rhythmic patterns must be shaped by sensory feedback to produce behavior which is adapted to the requirements of the animal and its environment. It seems then that "central pattern generation" is a useful concept, provided that the broader behavioral context within which these circuits operate is not ignored.

Three tasks are involved in showing that a particular motor pattern is under the control of a central pattern generator: (1) developing a preparation in which the nervous system is isolated from peripheral inputs; (2) finding a stimulus which can initiate and maintain rhythmic outputs; and (3) demonstrating that the patterns thus obtained are related to the rhythmic behavior of interest. Although these issues are of general relevance to all central pattern generators, I will focus here on the issues of particular relevance to the study of central pattern generators underlying terrestrial locomotion.[1]

Isolating nervous systems from peripheral inputs

A convincing demonstration of the existence of a central pattern generator involves showing that in nervous systems that are completely isolated from normal peripheral inputs, rhythmic patterns appropriate for the behavior can still be recorded in motor nerves. Whenever possible, such a demonstration is carried out in an isolated nervous system preparation. This technique has been most successful in invertebrate preparations (e.g., Sillar and Skorupski 1986), which survive the disruption of a normal supply of blood and oxygen much better than vertebrate preparations. Alternatively, the ability of the nervous system to produce patterned motor output is studied in preparations in which the sensory afferents to the nervous system are severed (Grillner and Zangger 1975; Pearson and Iles 1970; Székely et al. 1969). Since it is not usually possible to deafferent a nervous system completely while retaining normal motor outputs, there may still be some contribution of sensory signals to the patterning of the motor output. A third technique commonly used in vertebrate preparations is the use of paralytic agents to selectively eliminate patterned sensory feedback related

[1]Citations in this chapter are examples from work on walking animals, except where otherwise noted. Given the large number of publications relevant to central pattern generation and to terrestrial walking, review articles are cited whenever possible.

to the movement (Viala and Buser 1969, Grillner and Zangger 1979, Jacobson and Hollyday 1982). While this technique has the advantage of allowing preparations to be minimally dissected, the effects of paralytic agents on the brain can produce spurious results. In addition, unless paralysis is used in conjunction with deafferentation, effects on the rhythmic motor pattern due to abnormal sensory information from the skin and other receptors cannot be ruled out. In vertebrates, "central" control of motor behaviors in the narrowest sense also implies that supraspinal influences are not involved in shaping motor programs. In addition to the isolation from sensory inputs, a demonstration that central pattern generator circuits are entirely contained within the spinal cord involves transecting the spinal cord below the brainstem region and showing that the rhythmic motor pattern persists. However, such preparations do not usually exhibit spontaneous rhythmic motor outputs, but require external stimulation. Electrical stimulation of descending nerve fibers or the use of certain pharmacological agents (e.g., glutamate, dopamine, NMDA) has been shown to restore rhythmic activity in such "spinal" preparations (Grillner and Zangger 1979; Pearson and Rossignol 1991; Shik and Orlovsky 1976; review: Grillner and Wallén 1985).

Evoking central rhythms

The absence of rhythmic activity in an isolated nervous system does not imply that a central pattern generator does not exist. For example, when isolated leech nerve cords failed to show rhythmic activity, researchers prematurely concluded that a central pattern generator did not exist (Gray et al. 1938). Later studies, however, were able to establish the existence of a CPG in the same preparation (Kristan and Calabrese 1976). Many factors can influence whether or not rhythmic patterns are observed. Since descending inputs from higher brain areas are important in the initiation and

maintenance of rhythmic activity, as has been shown both in invertebrate (Wiersma and Ikeda 1964; Roeder 1937) and vertebrate (reviews: Grillner 1981; Grillner and Wallén 1985) preparations, the nervous system deprived of such inputs could be in a depressed state, lacking the excitation necessary to activate the pattern generating circuitry. Electrically stimulating those descending neural pathways can often then activate centrally-generated rhythms (Jacobson and Hollyday 1982; Shik and Orlovsky 1976; other references in Grillner and Wallén 1985). More commonly, pharmacological agents are used to initiate locomotor rhythms (Pearson and Rossignol 1991; Barbeau and Rossignol 1991; Sqalli-Houssaini et al. 1993; Grillner and Zangger 1979), although the sites of action of these agents are not usually known. It is then incumbent on the experimenter to show that the artificial stimulation actually activates neural pathways which would normally be involved in initiating and maintaining rhythmic activity. Since this is difficult to do, most studies attempt to show that the centrally generated rhythms are similar to those obtained in an intact animal or in a preparation in which a different stimulus was used to activate the central rhythms.

Comparing intact and isolated rhythms

Once it has been established that a nervous system does not require peripheral or descending inputs in order to generate patterned rhythmic output, it still must be shown that this rhythmic pattern is related to the motor behavior being studied. The tacit assumption made when comparing motor rhythms produced by isolated nervous systems to those observed in intact animals is that if the patterns are "similar," one can assume that the same premotor circuitry is being activated in both cases. That this assumption is a reasonable one has been borne out in studies of central pattern generators that have been described at the cellular and synaptic level (e.g., crustacean gastric mill: Turrigiano and Heinzel 1993; leech heartbeat: Calabrese

and Arbas 1989; *Tritonia* swimming: Getting and Dekin 1985b; other references in Getting 1988). The central problem, which has been the focus of much controversy, is to define what is meant by "similar," since rhythmic patterns are almost always altered when sensory feedback is eliminated. This debate is essentially equivalent to the argument over the definition of a central pattern generator circuit (i.e., the narrower the definition of the central pattern generator circuit, the more different its output pattern is likely to be from the intact motor pattern). Now that it is generally accepted that both central and sensory mechanisms are important in the production of motor behaviors, it is equally clear that different systems rely to varying degrees on one or the other mechanism. In systems which rely more on central than sensory mechanisms to shape the basic motor output, the effects of deafferentation can be expected to be minimal. In systems such as walking systems that rely heavily on sensory feedback, the elimination of such feedback should lead to drastic alterations of the motor output. In fact, a comparison of rhythms obtained in isolation to those obtained in intact animals should provide important clues about which aspects of the rhythmic behavior are most dependent on sensory versus central mechanisms. The challenge then is to understand the contribution of each mechanism—central or sensory—to the formation of the final motor output.

1.2 Terrestrial locomotion

The ability of metazoan animals to move distinguishes them from most other life forms. In order to move, metazoans have evolved a variety of appendages adapted to their natural habitat, such as legs, wings, and fins. Despite the huge variety of locomotor strategies, it seems that the basic rhythmic movements that underlie most forms of locomotion are under the control of central pattern generators. The best studied locomotor CPGs are those which control flight in insects (Wilson 1961; re-

view: Robertson 1986) and swimming in a variety of animals, including vertebrates (reviews: Grillner 1981; Arshavsky et al. 1993; Grillner et al. 1991) and invertebrates (reviews: Arshavsky et al. 1993; Friesen 1989; Getting and Dekin 1985b). Less is known about the central control of legged terrestrial locomotion. Terrestrial locomotion is more complex in some ways than locomotion in a uniform medium such as air or water. A walking animal has to support its weight to maintain a distance from the ground, above small obstacles that would impede its progress. In addition, walking animals have evolved multi-functional jointed appendages that must be coordinated appropriately to ensure forward propulsion without loss of stability. Since terrestrial environments are generally unpredictable and irregular, terrestrial walkers have evolved a variety of sophisticated exteroceptive sensory organs to detect environmental changes. A central locomotor program must therefore be flexible and easily modified by peripheral feedback. Because of the greater reliance of walking on sensory feedback, it has been more difficult to demonstrate the existence of central motor programs for walking than for other rhythmic motor patterns.

Central pattern generators in terrestrial walkers

There are few clear demonstrations that walking is under the control of central pattern generators. In most of these cases, evidence for the existence of a central pattern generator is limited to the control of a single limb. Evidence that individual limb pattern generators are centrally coupled in patterns appropriate for leg coordination during walking is more scarce. In addition, unlike studies of central pattern generators in molluscs and crustacea, the neural basis for central pattern generation in terrestrial locomotion is largely unknown. In all of the systems which have been studied, the large number of neurons involved often precludes analysis of the circuit at the cellular and synaptic level.

The best studied vertebrate central pattern generators for locomotion are those of cats, turtles, tadpoles, dogfish, and lamprey (reviews: Grillner 1981; Grillner and Wallén 1985). By far the largest body of work on walking in vertebrates comes from studies on cats, in which the central origin of the control of individual limbs during walking is well established (reviews: Grillner 1981; Grillner and Wallén 1985; Rossignol et al. 1993). Motor rhythms have been shown to exist in deafferented, paralyzed cats, provided that descending pathways from the brainstem are stimulated electrically (Shik and Orlovsky 1976) or pharmacologically (Grillner and Zangger 1979; Pearson and Rossignol 1991; Barbeau and Rossignol 1991). There is some evidence as well that central mechanisms can coordinate the legs in the absence of peripheral feedback (Grillner and Zangger 1979). However, very little is known about the cellular basis of central pattern generation in vertebrates. In the spinal cord, a large number of segmental interneurons that are part of or driven by the CPG are active during fictive locomotion, but neither the specific input nor the projections of these interneurons have been identified (reviews Grillner 1981; Grillner and Wallén 1985). It is unlikely that a detailed understanding of central pattern generation in mammals can be achieved with present techniques, given the complexity of mammalian neural circuitry. For this reason, lower vertebrates such as lamprey and *Xenopus* embryos are considered more favorable preparations in which to study vertebrate central pattern generation. Invertebrate preparations, on the other hand, can be used to further our understanding of issues specifically related to the neural control of terrestrial locomotion. Since the same environmental constraints are imposed on all walkers, it is possible that the same general classes of solutions to problems related to walking are used both by invertebrate and vertebrate nervous systems.

Insect walking

Insect walking has fascinated neuroethologists for several centuries, and in recent years has also captured the interest of engineers seeking to build legged mobile robots. Insects are in many ways ideal preparations for the study of terrestrial walking systems, since they retain the ability to walk even after extensive lesions and limb amputations. The different parts of the leg and their sensory organs, which for the most part are located in or below the chitinous cuticle, are easily accessible. The segmental nature of the nervous system, with single ganglia controlling each pair of legs, allows individual segments to be studied in partial or complete isolation. A large number of behavioral studies on cockroaches, locusts, and stick insects have yielded a good functional description of walking (reviews: Graham 1985; Cruse 1990).

On the neuronal level, much is known about the control of an individual leg. In particular, the sensory-motor pathways underlying local reflexes of the legs are starting to be well understood in the locust (Burrows 1992). Very little is known, however, about the effects of central inputs on the different components of the local neural circuits which have been described, since central and peripheral influences are inextricably linked during walking (Wolf and Laurent 1994). The contributions of different pools of premotor interneurons to the generation of motor rhythms are not known. In addition, although qualitative descriptions of the mechanisms of interleg coordination have existed for some time (review: Cruse 1990), little is known about the relative contributions of central and sensory mechanisms to achieve this coordination. In order to further our understanding of the neural control of walking, a preparation is needed in which central mechanisms involved in walking can be studied in the absence of sensory feedback.

There is currently no clear evidence in any insect that isolated nervous systems can generate leg motor rhythms related to walking. This failure to demonstrate the

existence of a central pattern generator appears to be due in part to the absence of spontaneous activity of motor rhythms in isolated insect nervous systems. When rhythmic activity in motor neurons was reported, it was generally so irregular that it was not clear whether this activity was related to walking. In stick insects, in fact, leg motor rhythms recorded in deafferented preparations resembled rocking—a behavior characterized by a rhythmic movement of the body from side-to-side—rather than walking (Bässler and Wegner 1983). The most convincing evidence for a central pattern generator was obtained in cockroaches (Pearson and Iles 1970, 1973; Pearson 1972), but the evidence for a walking CPG was ambiguous enough that Pearson subsequently argued against it (Pearson 1985). It is surprising that, despite the paucity of evidence supporting the central pattern generator hypothesis, the existence of hemisegmental CPGs is generally accepted.

1.3 Overview of this thesis

Chapter 2

I first demonstrate that in the presence of the muscarinic agonist pilocarpine, leg motor neurons in isolated thoracic ganglia of the locust express rhythmic activity similar to that which occurs during walking in an intact animal. These results are the first evidence obtained in an isolated insect nervous system that there are central pattern generating networks in each hemiganglion which can rhythmically drive leg motor neurons in a "walking-like" pattern. Differences between the "fictive" locomotor rhythm and walking are discussed.

Chapter 3

I then show that there are differences between the fictive locomotor rhythms recorded in the three thoracic ganglia that control the front, middle, and hind legs. Arguing that the central pattern generating circuits underlying these three segmental rhythms should be similar, I developed a simple model circuit whose output can be tuned to any of the three segmental activity patterns by modifying a single synaptic weight. This model was simulated on a computer, and an analog VLSI circuit implementation was then built and tested in collaboration with Michael Wehr (Caltech).

Chapter 4

Finally, I present evidence in preparations consisting of isolated chains of thoracic ganglia that the fictive locomotor rhythms generated by the three thoracic ganglia are centrally coupled. I argue that interlimb coordination during walking is influenced in part by the central coupling of hemisegmental central pattern generators. Other roles for the central coupling, such as load compensation and the maintenance of posture, are also discussed.

Chapter 2

Locomotor Rhythms Evoked in Locust Thoracic Ganglia

2.1 Summary and conclusions

1. When an isolated metathoracic ganglion of the locust was superfused with the muscarinic cholinergic agonist pilocarpine, rhythmic activity was induced in leg motor neurons. The frequency of this induced rhythm increased approximately linearly from 0 to 0.2 Hz with concentrations of pilocarpine from 10^{-5} to 10^{-4}M. Rhythmic activity evoked by pilocarpine could be completely and reversibly blocked by 3×10^{-5}M atropine, but was unaffected by 10^{-4}M d-tubocurarine.

2. For each hemiganglion, the observed rhythm was characterized by two main phases: a levator phase, during which the anterior coxal rotator, levators of the trochanter, flexors of the tibia, and common inhibitory motor neurons were active; and a depressor phase, during which depressors of the trochanter, extensors of the tibia, and depressors of the tarsus were active. Activity in depressors of the trochanter followed the activity of the levators of the trochanter with a

short, constant interburst latency. Activity in the levator of the tarsus spanned both phases.

3. The levator phase was short compared to the period (0.5 to 2 sec, or 10% to 20% of the period), and did not depend on the period. The interval between the end of a levator burst and the beginning of the following one thus increased with cycle period. The depressor phase was more variable and was usually shorter than the interval between successive levator bursts.

4. Motor neurons in a same pool often received common discrete synaptic potentials (e.g., levators of trochanter or extensors of tibia), suggesting common drive during the rhythm. Co-active motor neurons on opposite sides (such as left trochanteral depressors and right trochanteral levators), however, did not share obvious common PSPs. Depolarization of a pool of motor neurons during its phase of activity was generally accompanied by hyperpolarization of its antagonist(s) on the same side.

5. Rhythmic activity was generally evoked in both hemiganglia of the metathoracic ganglion, but the intrinsic frequencies of the rhythms on the left and right were usually different. The activity of the levators of the trochanter on one side, however, was strongly coupled to that of the depressors of the trochanter on the other side.

6. The locomotory rhythm was weakly coupled to the ventilatory rhythm, such that trochanteral levator activity on either side never occurred during the phase of spiracle opener activity, corresponding to inspiration.

7. The rhythmic activity observed *in vitro* bears many similarities to patterns of neural and myographic activity recorded during walking. The similarities and differences are discussed.

2.2 Introduction

During terrestrial locomotion, central commands and sensory feedback are integrated in the central nervous system to generate appropriate limb movements (Rossignol et al. 1988). In the locust, the sensory-motor pathways underlying local reflexes of the legs are starting to be well understood (Burrows 1992). Sensory information about the movement and position of a leg is integrated primarily by spiking local interneurons. They in turn make synapses onto nonspiking local interneurons, which also receive direct afferent input (Burrows et al. 1988; Laurent and Burrows 1988a) and organize movements in sets of coordinated motor pool activations (Burrows and Siegler 1976; Burrows 1980). Intersegmental interneurons are in turn responsible for controlling the gain of local reflexes in phase with sensory activity in adjacent segments (Laurent 1987; Laurent and Burrows 1989a,b). Thus, local circuits controlling each leg can be modulated by sensory information from other legs to ensure that reflex movements are appropriate to the behavior of the animal. Very little is known, however, about the effects of central inputs on the different components of these local circuits, since central and peripheral influences are inextricably linked during walking behavior (Wolf 1992). To examine these influences separately, it would be desirable to develop a deafferented preparation which produced patterned neural activity similar to that recorded during walking. This was the object of the work reported here.

Central pattern generators (CPGs) have been shown to generate rhythmic motor patterns in many vertebrate and invertebrate preparations (Delcomyn 1980). While some rhythmic motor patterns are spontaneously active in isolated nervous systems (*Helisoma* feeding: Kater and Rowell 1973; crayfish swimmeret beating: Ikeda and Wiersma 1964; leech heartbeat: Thompson and Stent 1976; rat breathing: Suzue 1984; cockroach ventilation: Myers and Retzlaff 1963; lobster stomatogastric pyloric and gastric rhythms: Selverston et al. 1976), others require external stimulation

such as the application of pharmacological agents (cat walking: Grillner and Zangger 1979; crayfish walking: Chrachri and Clarac 1990; locust flight: Stevenson and Kutsch 1987, lamprey swimming: Poon 1980; *Xenopus* swimming: Dale and Roberts 1984). Such pharmacologically-induced rhythms are often very similar to the motor rhythms recorded *in vivo* or in spontaneously active preparations. Although longer cycle periods and small differences in the structure of a pattern are sometimes observed (Grillner and Zangger 1979; Chrachri and Clarac 1990; Stevenson and Kutsch 1987), such differences are not necessarily a direct effect of using a drug to induce rhythmic activity, as similar observations have been made in deafferented preparations where rhythmic activity was induced without using pharmacological agents (Stevenson and Kutsch 1987). Although the existence of a central pattern generator for walking in insects has been suggested (Pearson and Iles 1970), no detailed study of such circuits has been carried out, since spontaneous rhythmic activity of the leg motor neurons is rarely observed in isolated ganglia or deafferented insects. We describe here a new preparation in which rhythmic activity in leg motor neurons can be induced in an isolated thoracic ganglion of the locust under the action of the muscarinic agonist pilocarpine. This preparation could be used to study the influence of centrally generated patterns of neural activity on the neural pathways underlying local reflexes. Certain of these results have been presented in abstract form (Ryckebusch and Laurent 1991).

2.3 Methods

Experiments were performed on adult locusts *Schistocerca americana* of either sex, from our crowded laboratory colony. The results presented here were gathered from 118 different experiments.

The preparation. Most experiments were performed in an *in vitro* thoracic preparation (for details see Laurent 1990). Briefly, the meso- and metathoracic ganglia were

removed from the thorax of the animal with the surrounding tracheal supply and air sacs undisturbed, and were pinned down in a chamber lined with Sylgard 184 (Dow Corning Co., Midland, MI). Leg motor nerves were carefully stripped of their surrounding connective tissue with a small hooked pin. The preparation was superfused with locust saline (mM: NaCl: 140; KCl: 5; $CaCl_2$: 5; $NaHCO_3$: 4; $MgCl_2$: 1; HEPES: 6.3; pH 7.0) supplemented with 2.5% (wt/vol) sucrose. Air was supplied to the ganglia by teasing open the tracheae at the surface of the saline. Stock solutions of 10^{-2}M pilocarpine hydrochloride, atropine sulfate, and d-tubocurarine chloride (Sigma) were prepared in advance, and were added to the saline to final bath concentrations of 10^{-5} to 10^{-4}M. To perform intracellular recordings, the ventral surface of the metathoracic ganglion was treated with 1% (wt/vol) protease (Sigma, Type XIV) for 30 sec, and then was washed thoroughly. In most experiments, the connectives between meso- and metathoracic ganglia were cut at the beginning of an experiment. The preparation remained healthy for at least 4 or 5 hours at a room temperature of 20 to 26°C. Tarsal motor neurons were studied in a similar preparation, except that the ganglion was left in the thorax of the animal. The leg was extended and immobilized, and a window was cut in the ventral surface of the distal end of the tibia to expose the tarsal muscles and nerves. In some of these experiments, the main leg nerve (N5B) was cut at mid-tibia.

Electrophysiology. The electrical activity of different leg motor nerves was monitored extracellularly using polyethylene suction electrodes. *En passant* recordings were made with differential steel hook electrodes. Simultaneous intracellular recordings were made from the soma of leg motor neurons, identified using the following criteria: (1) one-to-one correlation between intracellularly recorded action potentials and spikes recorded in one or several of the nerves; (2) position of the soma in the ganglion (Burrows and Hoyle 1973; Tyrer and Gregory 1982; Siegler and Pousman 1990a,b); (3) characteristic pattern of PSPs. (For example, flexor tibiae motor neu-

rons could be recognized by EPSPs evoked centrally by spikes in the fast extensor tibiae (FETi) motor neuron (Burrows et al. 1989).) In some cases we identified motor neurons by correlating intracellularly recorded junction potentials (JPs) in the muscle with spikes recorded *en passant* from a motor nerve. Intracellular recordings were made with 50–90 MΩ glass microelectrodes filled with 3M potassium acetate. Data were recorded on an eight-channel Digital Audio Tape recorder sampled at 5 kHz (Sony/Biologic), and were displayed on a Gould TA4000 chart recorder.

Anatomy and nomenclature. The muscles are numbered according to Snodgrass (1929). Muscle names are those given by Snodgrass (1929), except where a variant is now more commonly used in the literature. The nerves are numbered according to Bräunig (1982). Motor neurons are designated by commonly used abbreviations or by the name of the muscle group that they innervate. Detailed descriptions of the innervation of the leg musculature can be found in Campbell (1961), Bräunig (1982), and Siegler and Pousman (1990a). Their results for leg nerves and muscles relevant to this paper are summarized in Table 1.

Analysis. Data were analyzed off-line on a Macintosh II microcomputer, after digitization at 2 to 8 kHz with a National Instruments NBMIO16L AD/DA interface. The software packages used for data analysis were Spike Studio (Eli Meir, Cornell University), MatLab (The MathWorks), and Kaleidagraph (Abelbeck Software). We analyzed continuous recordings which varied from 2 to 20 minutes in duration, chosen on the basis of overall regularity.

The activity of a motor neuron refers to the production of action potentials, as recorded extracellularly from the motor nerves or intracellularly from the soma of motor neurons. Most muscles are innervated by both slow and fast motor neurons, which could usually be distinguished on the basis of their different spike thresholds, as well as of the relative sizes of the extracellularly recorded spikes. Slow motor neurons often had smaller amplitude spikes when recorded extracellularly, had a lower

Table 1. Nomenclature and known innervation of leg muscles

Muscle[A]	Function	Nerve	Excitatory MN	Inhibitory MN
M121	anterior rotator coxa	$3C_1$	2^B	$CI_1{}^C$
M131	levator trochanteris	3B	7^B	$CI_1{}^C$
M132	levator trochanteris	4A	6^B	$CI_1{}^C$
M133a	depressor trochanteris	5A	2^B	$CI_1{}^C$
M133b/c	depressor trochanteris	$3C_3$	3^B	
M133d	depressor trochanteris	$3C_2a$	3^B	$CI_1{}^C$
M136	flexor tibiae	$5B_2$	$9+^D$	$CI_{2,3}{}^C$
M135	extensor tibiae	3B, $5B_1$	2^E	$CI_1{}^C$
M137	levator tarsus	$5B_2a$	1^F	$CI_{2,3}{}^C$
M138	depressor tarsus	$5B_2a$	$5+^F$	$CI_{2,3}{}^C$

[A] Snodgrass 1929

[B] Bräunig 1982

[C] Hale and Burrows 1985

[D] Phillips 1981

[E] Burrows and Hoyle 1973

[F] Siegler 1982

Abbreviations

ant rot coxa	anterior rotator coxa
CI	common inhibitor
dep	depressor
Df	fast depressor trochanteris
dmn	dorsal median nerve
Ds	slow depressor trochanteris
EJP	excitatory junction potential
FETi	fast extensor tibiae
IJP	inhibitory junction potential
L	left
lev	levator
PSP	post-synaptic potential
tar	tarsus
troch	trochanter
R	right
SETi	slow extensor tibiae

threshold, and were often active during much of the cycle. Activity of some of the motor pools consisted of "bursts" of activity in the fast motor neurons and modulated tonic activity in slow motor neurons. In that case, the onset and end of a burst were defined by the larger amplitude spikes. This choice was generally unambiguous. For some motor neurons whose activity often consisted of few spikes (e.g., SETi), the beginning and end of a burst were more difficult to define, as is reflected in the broad distribution of burst onsets in the phase histograms (see below). Although we chose to analyze our most regular patterns, we used all the bursts within a segment of data in our analysis, even if their timing in the cycle did not conform to expectations.

The centrally generated rhythm observed in the present experiments was characterized by two main phases, hereafter referred to as the **levator** and **depressor** phases, corresponding to the activities of levators and depressors of the trochanter. The onset of a burst of activity in trochanteral levators was chosen as the reference

for the rhythmic activity. This is equivalent to using the tibial flexor bursts, since levators and flexors were active in phase (see Results). Activity of trochanteral levators could easily be recorded extracellularly from nerves 3B or 4A. Since no difference was found between the activity patterns of trochanteral levators recorded from these two nerves, we used both groups interchangeably as a reference. In addition, levator bursts had well-defined onsets and offsets, which was not necessarily the case for the motor neurons active during other phases of the rhythm. A period is defined as the interval from the onset of a levator burst to the onset of the next levator burst. All phases were computed from -0.5 to 0.5, where 0 is the onset of a levator burst, and the period is normalized to 1.

2.4 Results

Pilocarpine induces rhythmic activity

Spontaneous activity in leg motor neurons in an isolated metathoracic ganglion bathed in physiological saline rarely occurred in bursts, although rhythmic bursting often developed spontaneously after 1 to 2 hours *in vitro*. When spontaneous rhythmic activity was observed, the period between bursts was generally very long (30 seconds to several minutes) and variable. In normal saline, some slow motor neurons were tonically active and the fast motor neurons were silent. Bath application of the muscarinic agonist pilocarpine, however, reliably induced bursts of activity in leg motor neurons after several minutes. Figure 1 shows simultaneous extra- and intracellular recordings from leg motor neurons during rhythmic activity evoked by 2×10^{-5}M pilocarpine. The top four traces are extracellular recordings from nerves L3B (trochanteral levators, SETi), L5A (trochanteral depressors, CI_1), $L3C_1$ (coxal anterior rotators) and $R3C_1$. Intracellular recordings are both from trochanteral lev-

ator motor neurons on the left. The trochanteral levators were active in phase with the anterior coxal rotators, and preceded activity in the trochanteral depressors and tibial extensors (Fig. 1, first three traces). Both sides of the ganglion were generally rhythmically active, but often at different intrinsic frequencies (Fig. 1, fourth trace, and see below).

When leg motor neurons in a preparation consisting of both meso- and metathoracic ganglia bathed in low concentrations of pilocarpine (see below) showed only tonic activity, those in the metathoracic ganglion usually began to fire rhythmically (i.e., in bursts) within a few seconds of cutting the connectives between the two ganglia. If a rhythm was already established in the metathoracic ganglion, cutting the connectives between meso- and metathoracic ganglia induced a faster, more regular rhythm. Similarly, if the connectives between all three thoracic ganglia were intact, cutting the connectives between the pro- and mesothoracic ganglia induced a rhythm in the previously silent metathoracic ganglion. Cutting the connectives between meso- and metathoracic ganglia further increased the frequency of the metathoracic rhythm. Figure 2A shows an extracellular recording from metathoracic nerve R3B (trochanteral levators, SETi) in a preparation consisting of pro-, meso-, and metathoracic ganglia bathed in 5×10^{-5}M pilocarpine. In the top trace, the connectives between pro- and mesothoracic ganglia were cut at the time indicated by the vertical arrow. Connectives between meso- and metathoracic ganglia were intact. In the bottom trace, connectives between meso- and metathoracic ganglia were cut at the time indicated by the vertical arrow. The top and bottom traces were separated in time by about 8 minutes. Figure 2B shows the frequency of metathoracic levator bursts shown in A as a function of time after section of the thoracic connectives. We can see that (1) the effect of sectioning the connectives was immediate, and (2) a stable frequency (always higher than the frequency preceding the cut) was reached only one to three minutes after the section.

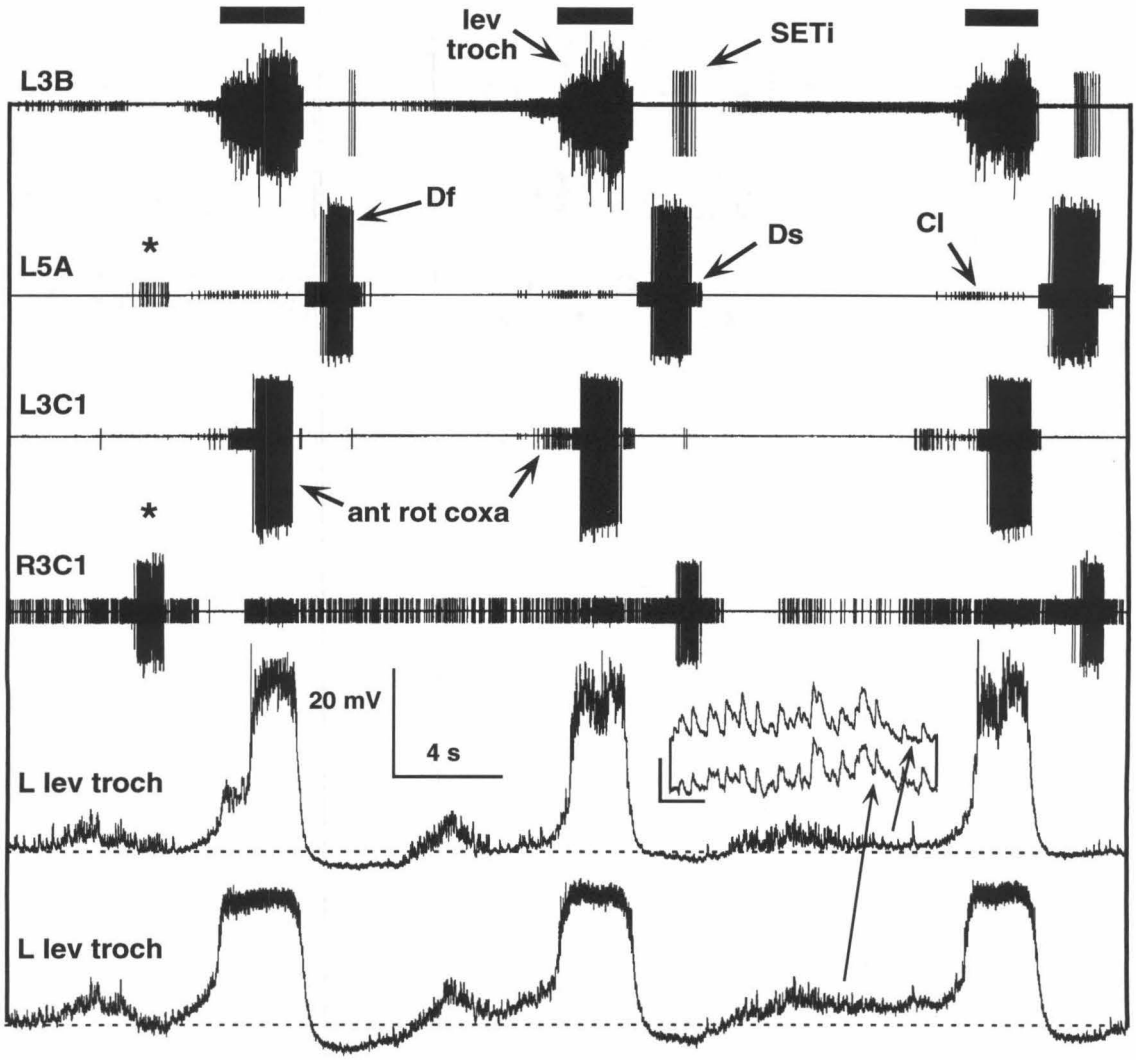
lev
troch
SETi
L3B
Df
Ds
CI
L5A
*
L3C1
ant rot coxa
*
R3C1
20 mV
4 s
L lev troch
L lev troch

Figure 1

Figure 1. Simultaneous extra- and intracellular recordings from leg motor neurons during rhythmic activity evoked by pilocarpine (2×10^{-5}M). Extracellular recordings are from nerves L3B (trochanteral levators, SETi), L5A (trochanteral depressors, CI_1), $L3C_1$ (coxal ant. rotators) and $R3C_1$. Intracellular recordings are both from trochanteral levator motor neurons (L lev troch) on the left. (Scale bars: 20mV, 4 sec). The inset is a magnified section of the intracellular recordings showing correlated PSPs in both traces (Scale bars: 5mV, 200 msec). Asterisk indicates coupling between left depressors and the right fast coxal rotator (right levator phase). Dark bars above the recording from L3B indicate the limits of trochanteral levator bursts as defined for the purposes of analysis (see Methods).

In a typical preparation, concentrations of ca. 10^{-5}M pilocarpine induced sporadic bursting activity similar to that observed in some preparations in normal saline. The burst frequency increased approximately linearly with pilocarpine concentration, saturating at 0.1 to 0.2 Hz at 10^{-4}M (Fig. 3A). Increasing the concentration further led to irregular burst durations and interburst intervals and to disruptions in the phase relationships between motor neurons. The average duration of levator bursts also increased with the concentration of pilocarpine (Fig. 3B), due in part to the recruitment of fast motor neurons that were silent at lower concentrations. Since the period decreased and the levator burst duration increased as the concentration of pilocarpine was raised, the trochanteral levators were active during a greater proportion of the cycle. Consequently, increasing the concentration of pilocarpine changed the phase relationships among different pools of motor neurons. The latency between the end of a levator burst and the beginning of trochanteral depressor and tibial extensor activity, however, was not affected (Figs. 7C and 8B).

The muscarinic antagonist atropine was added to the saline once the rhythmic activity induced by pilocarpine had been well established (Fig. 4A,B). In the presence of both atropine ([10^{-4}M]) and pilocarpine ([3×10^{-5}M]), rhythmic activity of motor

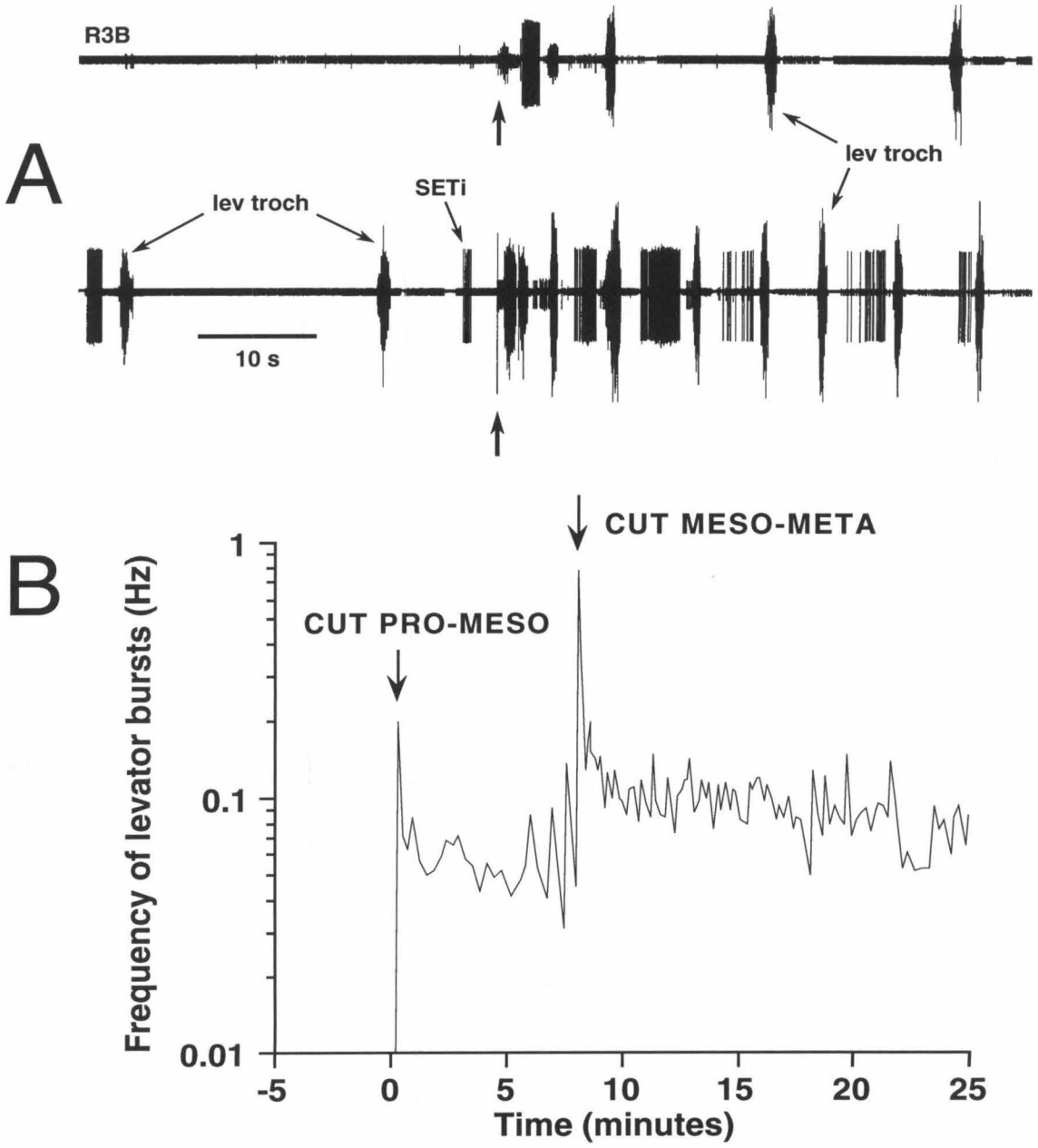
A
R3B
lev troch
lev troch
SETi
10 s
B
CUT MESO-META
CUT PRO-MESO
Frequency of levator bursts (Hz)
1
0.1
0.01
-5
0
5
10
15
20
25
Time (minutes)

Figure 2

Figure 2. Cutting the intersegmental connectives increases the frequency of the metathoracic rhythm. **A.** Recordings are from metathoracic nerve R3B (trochanteral levators, SETi). Top trace: connectives between pro- and mesothoracic ganglia were cut at the time indicated by the vertical arrow. Bottom trace: connectives between meso- and metathoracic ganglia were cut at the time indicated by the vertical arrow. The top and bottom traces are separated in time by about 8 minutes. Pilocarpine 5×10^{-5}M. (Scale bar: 10 sec.) **B.** Frequency of metathoracic levator bursts shown in **A** as a function of time after section of thoracic connectives. Arrows indicate times at which connectives were cut. Connectives between pro- and mesothoracic ganglia were cut at time 0. Connectives between meso- and metathoracic ganglia were cut about 8 minutes later. Note that the ordinate is in log units.

neurons ceased or diminished considerably, and Ds became tonically active (Fig. 4C). The neural activity then resembled that observed in the ganglion in saline (compare Figs. 4A and 4C). Superfusing the ganglion with pilocarpine alone then restored the rhythmic activity to previous levels (compare Figs. 4B and 4D). Adding the nicotinic antagonist d-tubocurarine to the bath in concentrations as high as 10^{-4}M had no noticeable effect on the rhythmic activity.

Description of the rhythm

Two groups of motor neurons could be distinguished by their patterns of discharge during rhythmic activity. The first group, which includes levators of the trochanter and flexors of the tibia, was characterized by short bursts of relatively constant duration. The activity of the second group, which includes depressors of the trochanter and extensors of the tibia, was of variable duration and often included a tonic component. The activity of this second group was strongly influenced by contralateral rhythmic activity. The patterns of discharge of the different motor pools will be described successively. For each group, we determined the phase of onset of activity

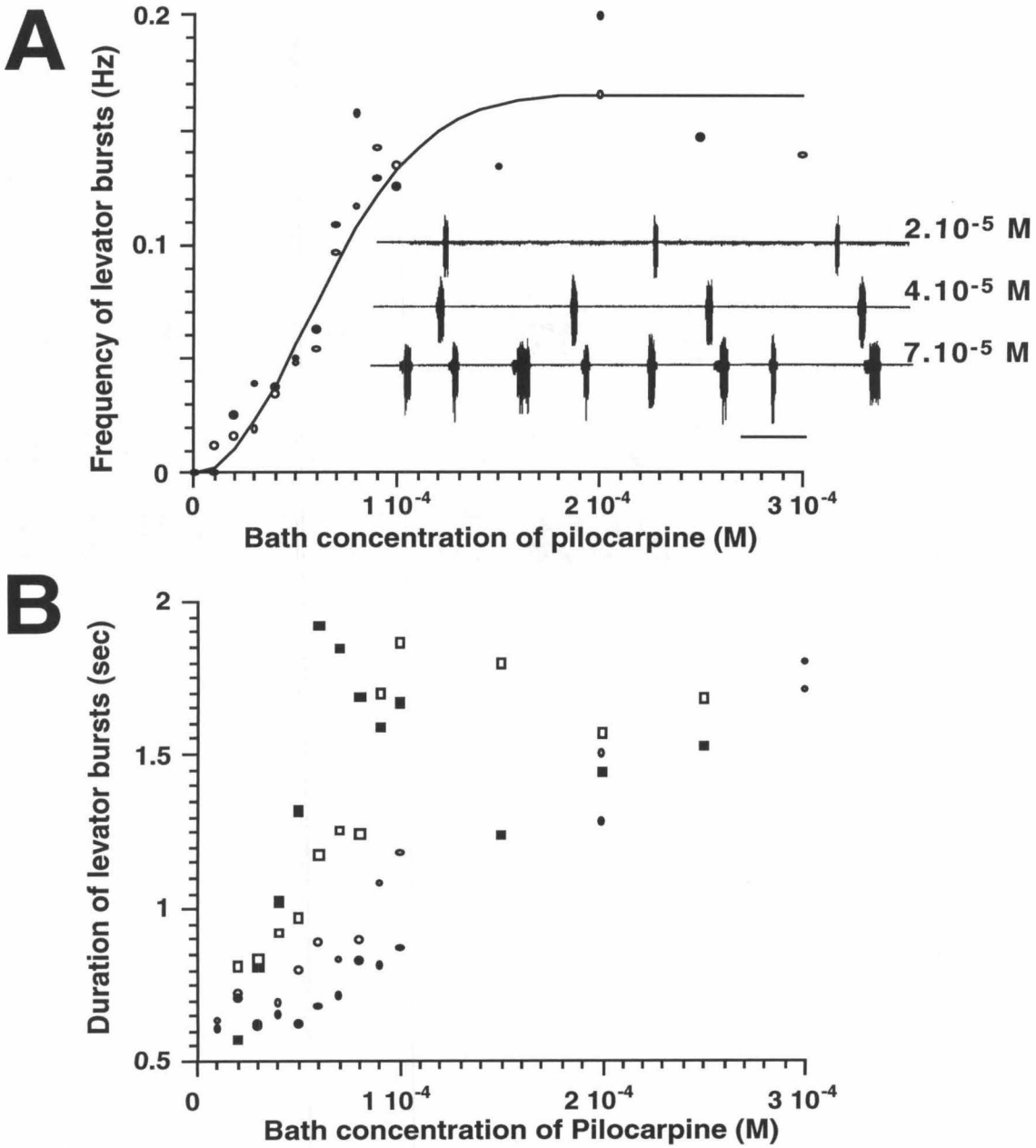
A
0.2
0.1
0
Frequency of levator bursts (Hz)
2.10-5 M
4.10-5 M
7.10-5 M
0
1 10-4
2 10-4
3 10-4
Bath concentration of pilocarpine (M)
B
2
1.5
1
0.5
Duration of levator bursts (sec)
0
1 10-4
2 10-4
3 10-4
Bath concentration of Pilocarpine (M)

Figure 3

Figure 3. Dose-response curves. **A.** Levator burst frequency (inverse of interburst interval) as a function of bath concentration of pilocarpine. Filled and open circles are data from two different experiments. Each data point represents an average frequency computed over 4 to 60 cycles. Standard deviations were usually very large, particularly at lower concentrations, since these data were averaged over the smallest numbers of cycles, and error bars were thus omitted for clarity. Solid line fitted by eye. Equation: $Ae^{-x^2/B}$; $A = 0.165$; $B = 6 \times 10^{-9}$ where x is concentration. Inset: Recordings from nerve 4A (trochanteral levators) for three different concentrations of pilocarpine. (Scale bar: 10 sec.) **B.** Levator burst duration as a function of concentration of pilocarpine. Circles and squares are data from two different experiments. Filled and open symbols are data from left and right hemiganglia respectively. Standard deviations were usually very large, particularly at higher concentrations of pilocarpine, and error bars were omitted for clarity.

of the different motor neurons in the cycle (cf. Methods), the latency between burst onsets, and the duration of bursts of activity. Subthreshold changes in membrane potential were determined from intracellular recordings.

Levators of the trochanter

The activity of the levators of the trochanter consisted of short bursts of spikes from up to seven motor neurons. For a fixed set of experimental conditions, large variations were observed in the period of the rhythmic activity from one cycle to the next (Figs. 5A,B), but the mean period did not change systematically with time (Fig. 5B). The ratio of levator burst duration to period ranged from 0.01, for the slowest rhythms, to 0.30. Typical values were 0.1 to 0.2. Although burst durations varied considerably during the course of a single experiment, or across different experiments, there was no correlation between the duration of the levator burst and the length of the period during which this burst occurred (Fig. 5C), for a *fixed* concen-

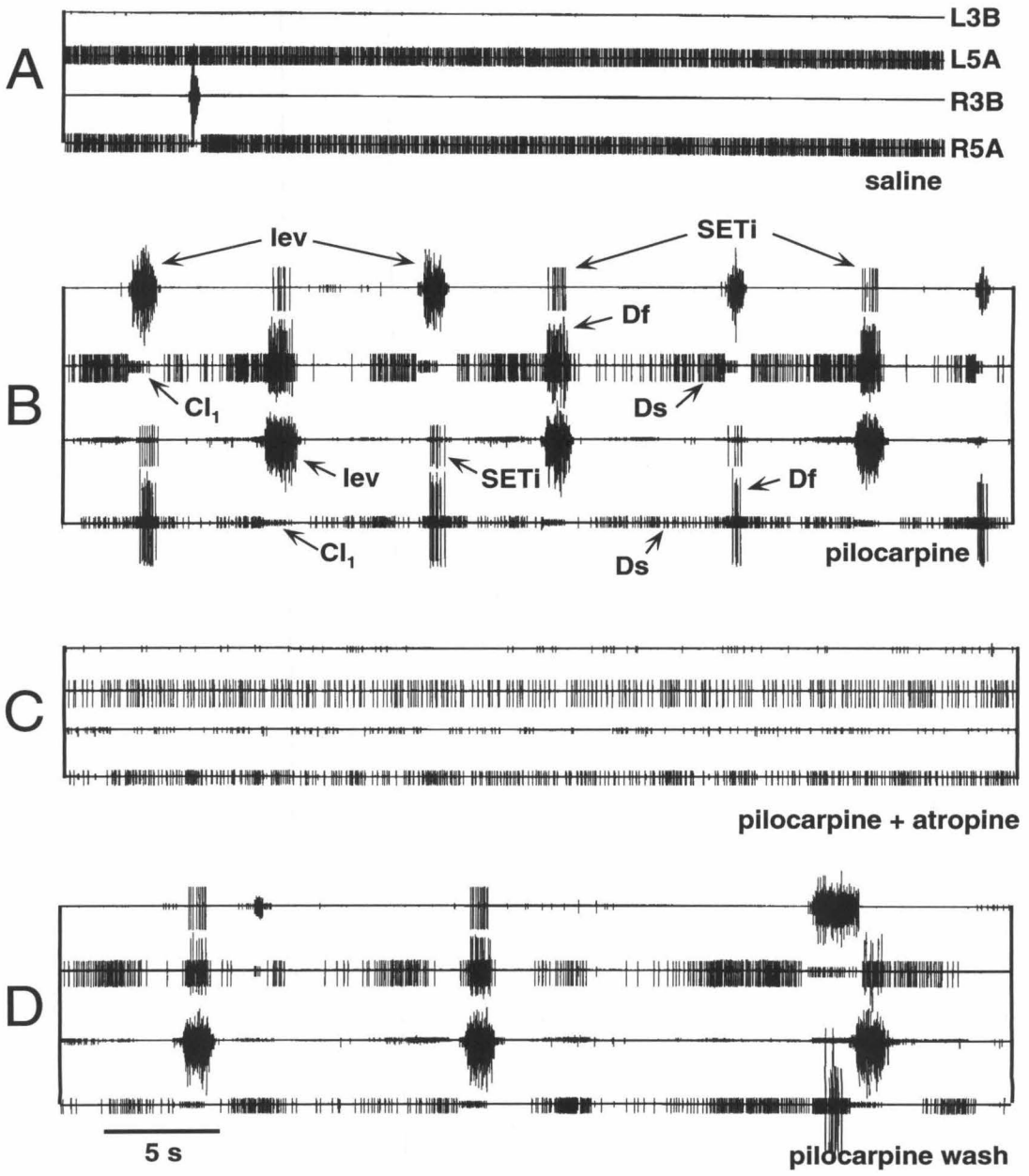
A
L3B
L5A
R3B
R5A
saline
B
lev
SETi
Df
Cl1
Ds
lev
SETi
Df
Cl1
Ds
pilocarpine
C
pilocarpine + atropine
D
5 s
pilocarpine wash

Figure 4

Figure 4. Atropine blocks the pilocarpine-induced rhythm. **A.** Extracellular recordings from motor nerves of an isolated metathoracic ganglion in saline. From top to bottom: metathoracic nerves L3B (trochanteral levators, SETi), L5A (trochanteral depressors, CI_1), R3B, and R5A (panels A through D). The tonically active neuron in L5A and R5A are the left and right trochanteral depressor Ds. (Scale bar: 5 sec.) **B.** Rhythmic activity in the same leg nerves as in A, after addition of 3×10^{-5}M pilocarpine. Note that, in this preparation, the activity of trochanteral depressors Ds and Df is strongly coupled to the contralateral levator activity. The firing frequency of Ds increases during contralateral levator bursts. **C.** Recordings from the same preparation 30 minutes after addition of 10^{-4}M atropine sulfate to the bath. Pilocarpine concentration is still 3×10^{-5}M. **D.** Recovery, 1 hour after washing with 3×10^{-5}M pilocarpine alone.

tration of pilocarpine.[1]

Intracellular recordings from levator motor neurons suggested that the activity during a burst was terminated by inhibitory inputs, as the membrane potential after a burst was generally more negative than was that preceding it (Fig. 1, bottom two traces). This inhibition coincided with activity of depressors of the trochanter (Fig. 1, second trace). Hyperpolarizing a levator motor neuron during a burst decreased its peak firing frequency, but did not disrupt the extracellularly recorded rhythm or the activity of other motor neurons. Recording intracellularly from two levator motor neurons simultaneously revealed similar patterns of PSPs, indicating common synaptic drive (Fig. 1, inset).

[1]This result does not contradict Fig. 3B, which shows that the average duration of levator bursts depended on the concentration of pilocarpine (and thus, on the average cycle period). This is because different numbers of motor neurons were active at different concentrations of pilocarpine, giving rise to variations in the burst durations, whereas a fixed number of motor neurons participated in a burst at any given concentration of pilocarpine.

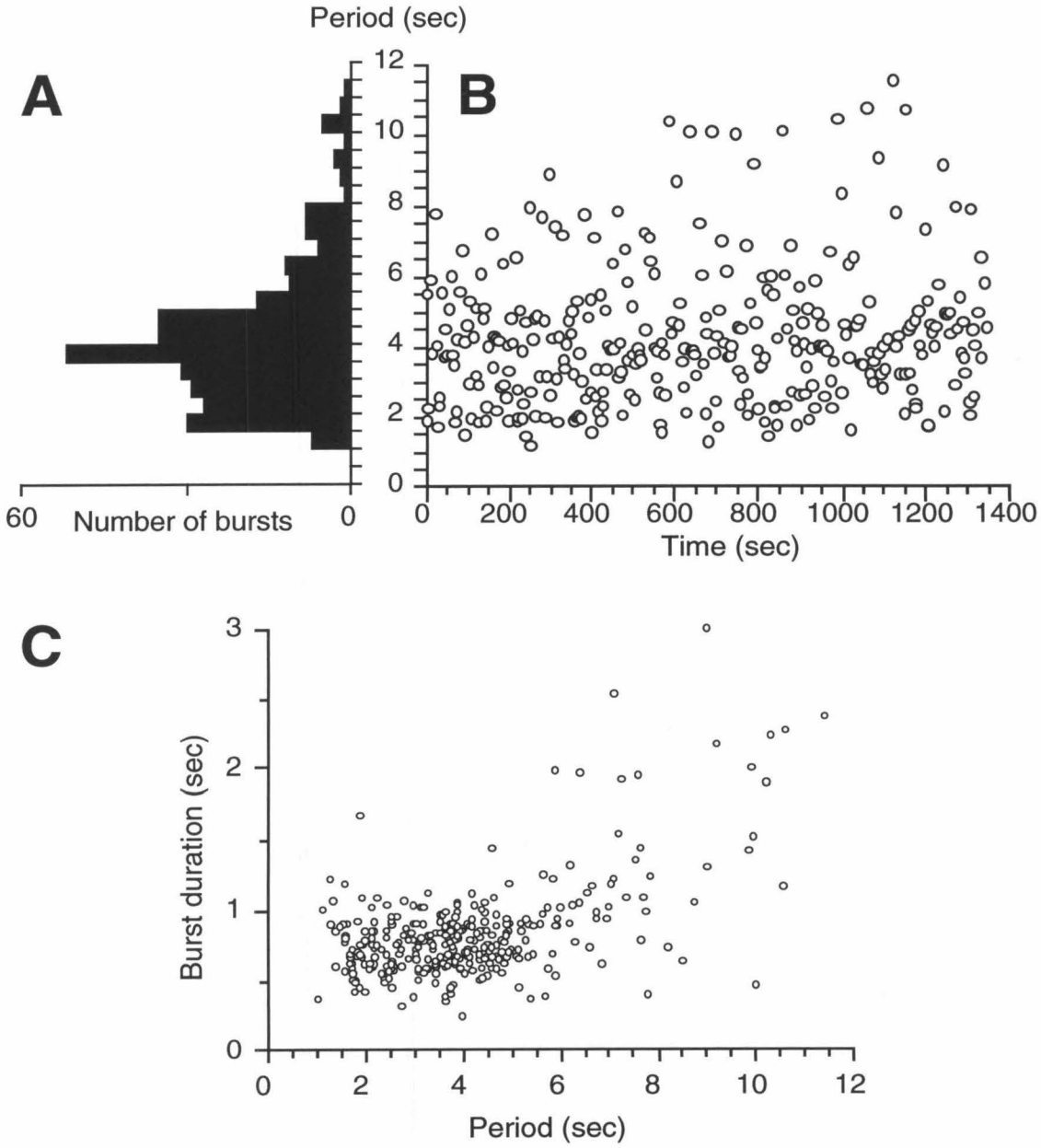
A
B
C
Period (sec)
12
10
8
6
4
2
0
60
Number of bursts
0
0
200
400
600
800
1000
1200
1400
Time (sec)
3
2
1
0
Burst duration (sec)
0
2
4
6
8
10
12
Period (sec)

Figure 5

Figure 5. Activity in the levators of the trochanter and cycle period. **A.** Frequency histogram showing the distribution of periods from a 23-minute continuous extracellular recording (324 cycles) of activity from nerve 3B (levators trochanteris, SETi). **B.** The variability of the period with time. Note that the average period remains more or less constant. **C.** The burst duration of trochanteral levators as a function of the cycle period. Note that the burst duration does not depend on the cycle period. Data from all graphs were computed from the same recording.

Flexors of the tibia

The tibial flexor motor neurons were active in phase with the levators of the trochanter (Figs. 6 and 8A), and the duration of their bursts was independent of the period. Flexor motor neurons were inhibited during activity of the extensors of the tibia, and the background of depolarizing PSPs seen between bursts disappeared during this inhibition (Fig. 8A).

Anterior rotators of the coxa

Both the slow and fast anterior coxal rotator motor neurons were active in phase with the ipsilateral levators of the trochanter (Fig. 1). The onset of activity in the fast anterior rotator often occurred slightly after the onset of a levator burst. The slow motor neuron was frequently active during much of the cycle. This pattern of activity is shown in Fig. 1, which contains extracellular recordings from nerve $3C_1$ on both sides of the ganglion. Whereas the slow rotator on the left side of the ganglion produced short bursts in phase with the ipsilateral trochanteral levators and the fast rotator, the slow rotator on the right side was active tonically, and its firing frequency was modulated in phase with the rhythmic activity of the right side of the ganglion.

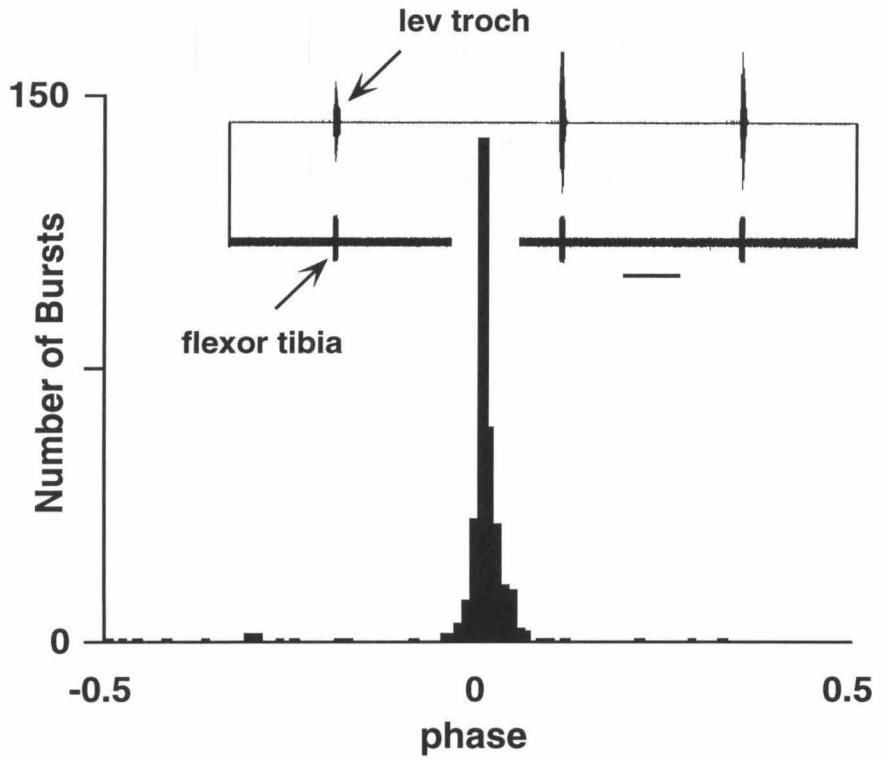

Figure 6. Flexors of the tibia are active with the levators of the trochanter. Phase histogram of tibial flexor burst onset. Reference (0) is ipsilateral trochanteral levator burst onset. Inset: Top: nerve 4A (trochanteral levators) Bottom: small branch of nerve $5B_2$ showing the activity of a single flexor tibiae motor neuron. (Scale bar: 5 sec.)

Depressors of the trochanter

All depressor trochanteris motor neurons were active during the same phase, although their spiking thresholds differed substantially.

M133a: In inactive preparations (no pilocarpine), Df was silent and Ds was tonically active (Fig. 4A). At low levels of activity, the tonic firing of Ds was interrupted during the bursts of trochanteral levator activity, followed by a transient increase in firing frequency (Fig. 7A, first trace). Variations of the instantaneous firing frequency of Ds were mirrored by those of the membrane potential of Df, which was hyperpolarized during a levator burst, and depolarized immediately after it (Fig. 7A, first and second traces). As the level of activity increased, the tonic firing of Ds ceased, and short, clearly defined bursts of spikes emerged. Df spikes were often observed when Ds reached its peak instantaneous firing frequency (Figs. 1, second trace and 7B, fourth trace). Depressor activity followed a levator burst after a short latency[2] (median 200 msec), such that activity in the two antagonistic groups did not overlap (Fig. 7C). A second depressor burst was sometimes observed during the latter half of a cycle (Figs. 1, second trace, and 7D, asterisks). This second burst generally coincided with a levator burst on the contralateral side (see below) and always ended before the onset of the ipsilateral levator burst.

M133b/c and M133d: At 10^{-5}M to 10^{-4}M pilocarpine, little spike activity was usually recorded from depressors of the trochanter in nerves $3C_3$ and $3C_2a$. At concentrations greater than 10^{-4}M, however, activity from these depressors was recorded (Fig. 7B, second and third traces). All the motor neurons were phasically active, in phase with Ds and Df. Bursts were generally short, and coincided with the phase of peak activity

[2]Since the onset of depressor activity occurred at a constant latency, rather than at a constant phase, the phase histograms shown in Figs. 7D and 8C are broader than they would be for any given experiment, since they were constructed from data taken from many different experiments with different mean cycle periods.

in Ds (Fig. 7B).

Extensors of the tibia

The slow tibial extensor SETi was hyperpolarized during a levator burst (Fig. 8A, second trace). The onset of a burst of SETi spikes (of variable duration and number of spikes) followed the end of the trochanteral levator burst by 0.2 to 1 sec, with a median of 400 msec (Fig. 8B). SETi often discharged tonically at a low frequency during the interval between levator bursts (Figs. 2A and 8C). The onset of SETi activity was strongly correlated with that of the trochanteral depressor Ds (Fig. 8D). Consequently, activity in SETi was often correlated with activity in contralateral trochanteral levators (Figs. 4B and 4D). FETi was rarely depolarized above threshold, but its subthreshold activity mirrored activity in SETi (Fig. 8E). PSPs in FETi and spikes in SETi often occurred simultaneously (Fig. 8E, inset). FETi, like SETi, was inhibited during the levator phase (Fig. 8E, asterisk).

Tarsal motor neurons

The activity of the levator of the tarsus had both a tonic and a phasic component. Whereas it typically spiked at a low frequency during most of the cycle (Fig. 9A, third and fourth traces), the firing frequency increased transiently soon after the onset of a burst in trochanteral levator motor neurons (Fig. 9A). This burst of activity in the tarsal levator occurred during the transition between the trochanteral levator and depressor phases (Fig. 9C). The fast depressor of the tarsus produced a short burst of spikes in phase with trochanteral depressors (Figs. 9B,D). The duration of this burst did not depend on the length of the cycle. In some preparations, coupling to the contralateral rhythm was also observed. Activity in one of the slow tarsal depressors was analyzed. It was tonically active during the interval between trochanteral levator

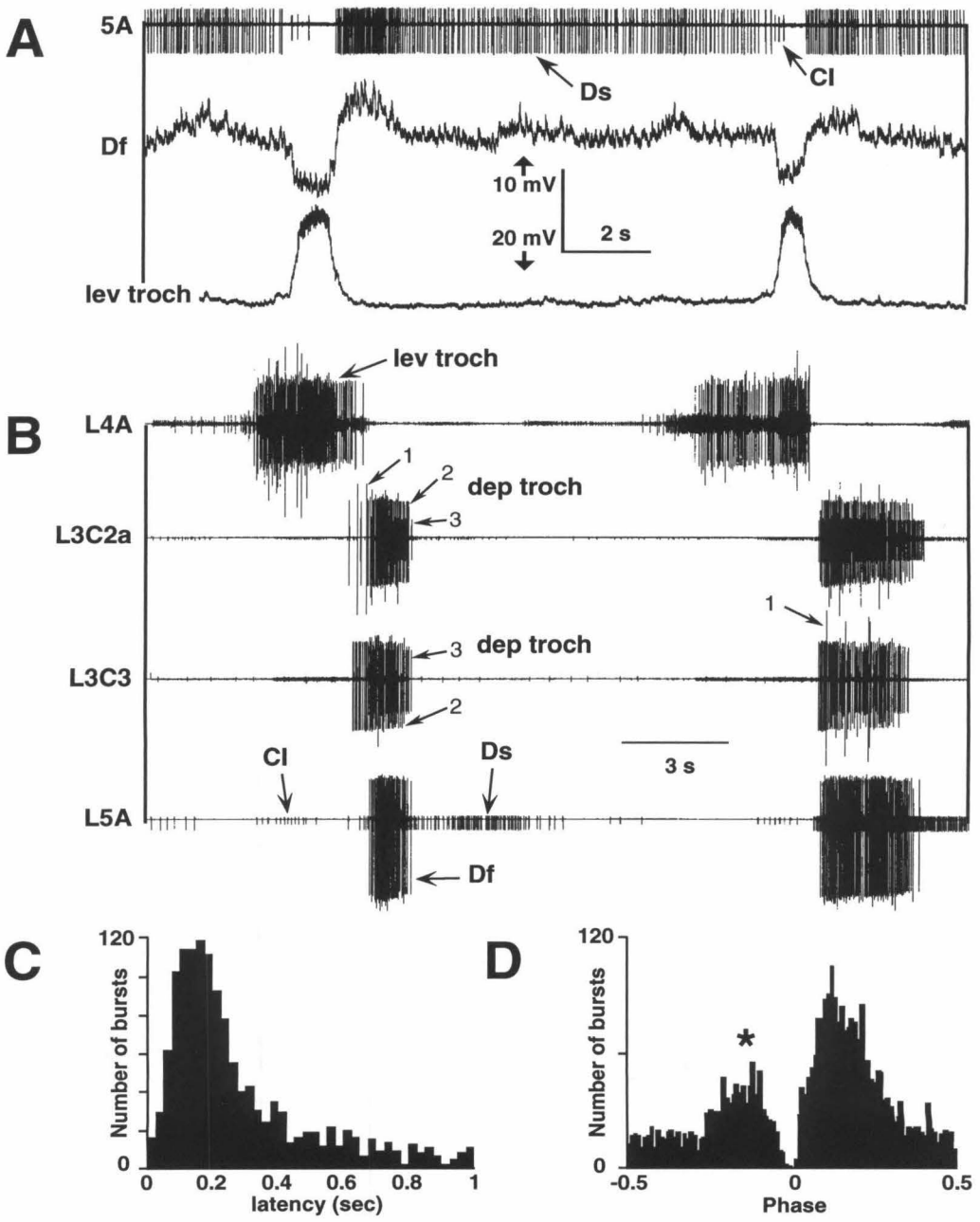
A
5A
Ds
Cl
Df
10 mV
20 mV
2 s
lev troch
B
lev troch
L4A
1
2
dep troch
3
L3C2a
1
3
dep troch
L3C3
2
Cl
Ds
3 s
L5A
Df
C
120
Number of bursts
0
0
0.2
0.4
0.6
0.8
1
latency (sec)
D
120
Number of bursts
*
0
-0.5
0
0.5
Phase

Figure 7

Figure 7. The depressors of the trochanter are inhibited during levator activity. **A.** Depolarization of a levator motor neuron corresponds to phasic inhibition of depressor motor neurons (Df and Ds). Repolarization of levator coincides with depolarization of depressors. Note CI spikes during levator bursts. Top to bottom: nerve 5A (trochanteral depressors, CI_1), intracellular recording from Df (Scale bars: 10mV, 2 sec), trochanteral levator motor neuron (Scale bars: 20mV, 2 sec). **B.** All trochanteral depressors are co-active in a burst following levator activity. From top to bottom: nerves 4A (trochanteral levators), $3C_2$a (trochanteral depressors), $3C_3$ (trochanteral depressors), 5A (trochanteral depressors, CI_1), all on left side. Three units (1–3) can be distinguished in second and third traces. Activity in motor neurons in nerves $3C_2$ and $3C_3$ usually was subthreshold for concentrations of pilocarpine 10^{-5} to 10^{-4}M. Pilocarpine 1.5×10^{-4}M. (Scale bar: 3 sec.) **C.** Frequency histogram of latencies between the end of a levator burst and the onset of the next depressor burst (N5A). The abscissa was truncated at 1 second for clarity, although depressor bursts can occur anywhere in the cycle, as discussed in the text. Data combined from 8 experiments. **D.** Phase of Ds and Df burst onsets relative to the preceding trochanteral levator burst onset. As discussed in the text, depressor bursts typically occur after levator bursts; the occurrence of bursts with negative phases (asterisk) is usually correlated with activity of contralateral levators. Ds and Df phase histograms had the same profiles, and were therefore combined in this figure.

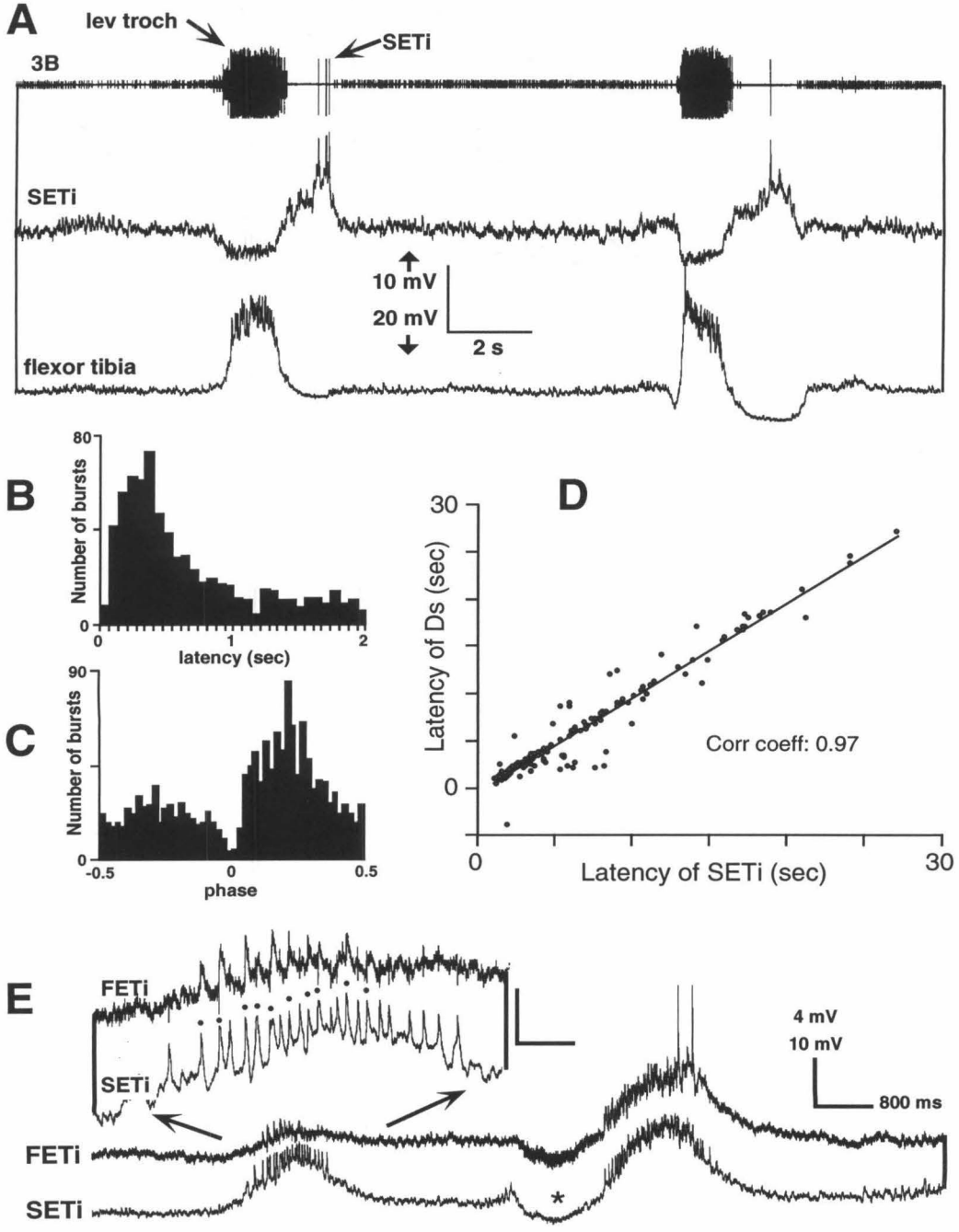
A
lev troch
SETi
3B
SETi
10 mV
20 mV
2 s
flexor tibia
B
Number of bursts
latency (sec)
C
Number of bursts
phase
D
Latency of Ds (sec)
Latency of SETi (sec)
Corr coeff: 0.97
E
FETi
SETi
4 mV
10 mV
800 ms
FETi
SETi

Figure 8

Figure 8. Activity in extensors of the tibia follows that in levators of the trochanter. **A.** SETi is inhibited during flexor activity. Flexor motor neuron is hyperpolarized during SETi activity. Top to bottom: nerve 3B (trochanteral levators, SETi), SETi, flexor motor neuron. SETi spikes can be seen in extracellular recording. (Scale bars: 10mV (SETi), 20mV (flexor); 2 sec) **B.** Frequency histogram of latencies of SETi burst onset computed from the end of the preceding trochanteral levator burst. Data combined from 7 experiments. The abscissa was truncated at 2 seconds for clarity, although SETi can be active anywhere in the cycle, as discussed in the text. **C.** Phase histogram of SETi bursts calculated in reference to ipsilateral trochanteral levator burst onsets. **D.** Correlation between Ds and SETi onset activity. Data are from a continuous recording in a single experiment. Abscissa: onset of SETi bursts. Ordinate: onset of Ds bursts. Times referenced to onset of levator bursts. Solid line is least-squares fit to the data. Correlation coefficient: 0.97; Slope: 1.00. **E.** Intracellular recordings from SETi and FETi show common PSPs. Top trace: FETi. Bottom trace: SETi. (Scale bars: 4mV (FETi), 10mV (SETi); 800 msec.) Asterisk shows inhibition of both motor neurons during activity in trochanteral levators (not shown). Inset is magnified section of previous traces showing common PSPs in both neurons (dots). PSPs are suprathreshold for SETi. (Scale bars in inset: 2mV (FETi), 5mV (SETi); 200 msec.)

bursts (Fig. 9E). It appeared to be inhibited during the higher frequency tarsal levator bursts, and to be excited transiently during the fast tarsal depressor phase (Fig. 9E). Its peak firing rate was reached after that in the fast depressor (compare Figs. 9D and 9E). The activity of the slow depressor was also clearly modulated in phase with the contralateral rhythm (compare Figs. 9E and 9F).

Common inhibitors

The three common inhibitory motor neurons had similar activity profiles. Detailed analysis was therefore restricted to CI_1, whose activity was usually recorded extracellularly on nerve 5A (Fig. 10A). In most rhythmic preparations, CI_1 produced a short burst of spikes that began slightly before a trochanteral levator burst (Figs. 10A and 10B), and that usually ended during the early part of the levator burst. In some preparations, the activity of the common inhibitory motor neurons also had a slow tonic component, modulated in phase with the rhythm. CI_2 and CI_3 were generally active in phase with CI_1, albeit slightly later in the cycle. Since CI_2 and CI_3 innervate the tarsal musculature, their activity was closely correlated with activity of tarsal levators and depressors, which were active slightly after the trochanteral levator and depressor motor neurons, respectively (Figs. 9A, bottom trace and inset). Intracellular recordings from CI_2 showed that the burst of spikes which preceded a trochanteral levator burst was terminated by strong inhibition during the latter part of the trochanteral levator burst. The strong correlation between the activity of common inhibitory and trochanteral levator motor neurons is shown in Fig. 10A, where simultaneous recordings were made from a motor neuron of each pool. Despite a highly irregular rhythm, the two motor neurons were phase locked and thus appeared to be driven by common inputs.

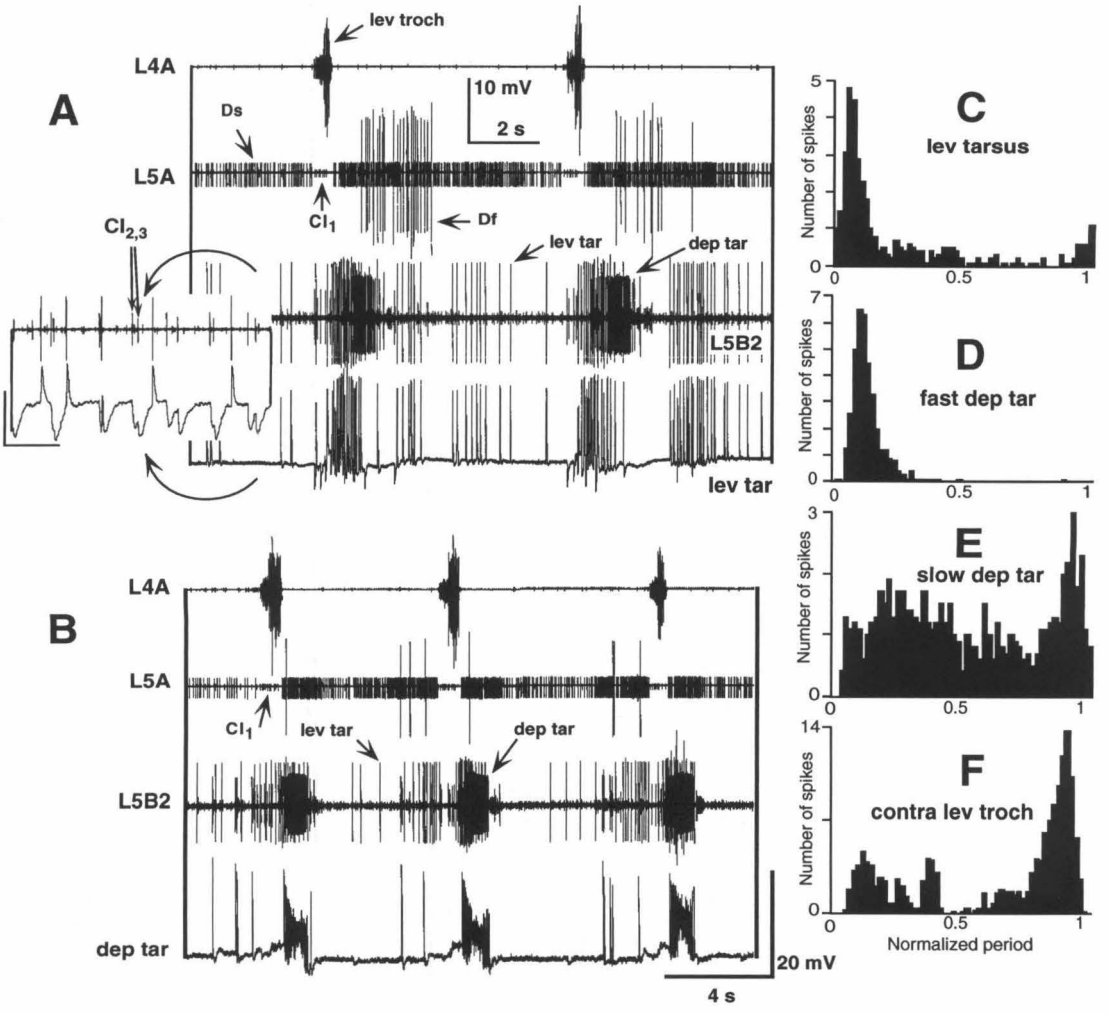
A
lev troch
L4A
10 mV
2 s
Ds
L5A
CI1
Df
CI2,3
lev tar
dep tar
L5B2
lev tar
B
L4A
L5A
CI1
lev tar
dep tar
L5B2
dep tar
20 mV
4 s
C
lev tarsus
D
fast dep tar
E
slow dep tar
F
contra lev troch
Number of spikes
Normalized period

Figure 9

Figure 9. Activity in tarsal motor neurons overlaps transition between trochanteral levator and depressor bursts. **A.** Tarsal depressor and levator activities overlap at transition between levator trochanter and depressor trochanter bursts. Top to bottom: L4A (trochanteral levators), L5A (trochanteral depressors, CI_1), $L5B_2$ (tarsal levator and depressors, CI_2 and CI_3), and intracellular recording from a tarsal levator muscle fiber (Scale bars: 10mV, 2 sec). Inset shows tarsal levator muscle fiber recording (bottom) on faster time base to show IJPs from CI_2 and CI_3 (downward deflections), and EJPs caused by the tarsal levator motor neuron (large extracellular spikes in $L5B_2$, top). (Scale bars in inset: 20mV, 400 msec.) **B.** Identification of depressor spikes from nerve $5B_2$ by intracellular recording of EJPs. Top to bottom: L4A (trochanteral levators), L5A (trochanteral depressors, CI_1), $L5B_2$ (tarsal levator and depressors), and intracellular recording from a tarsal depressor muscle fiber showing EJPs from the fast tarsal depressor motor neuron. (Scale bars: 20mV, 4 sec.) **C–F.** Statistical analysis of tarsal depressor activity during the rhythm. Frequency histograms for the activity in the tarsal levator (C), fast tarsal depressor (D), a slow tarsal depressors (E), and a contralateral trochanteral levator (F). Data were obtained from 10 cycles in a single experiment with periods ranging from 8 to 15 seconds. The reference time was the onset of ipsilateral trochanteral levator burst, and the period was normalized to 1. All the histograms were constructed from the same 10 cycles. Note correlation between slow tarsal depressor activity and both ipsi- and contralateral activities.

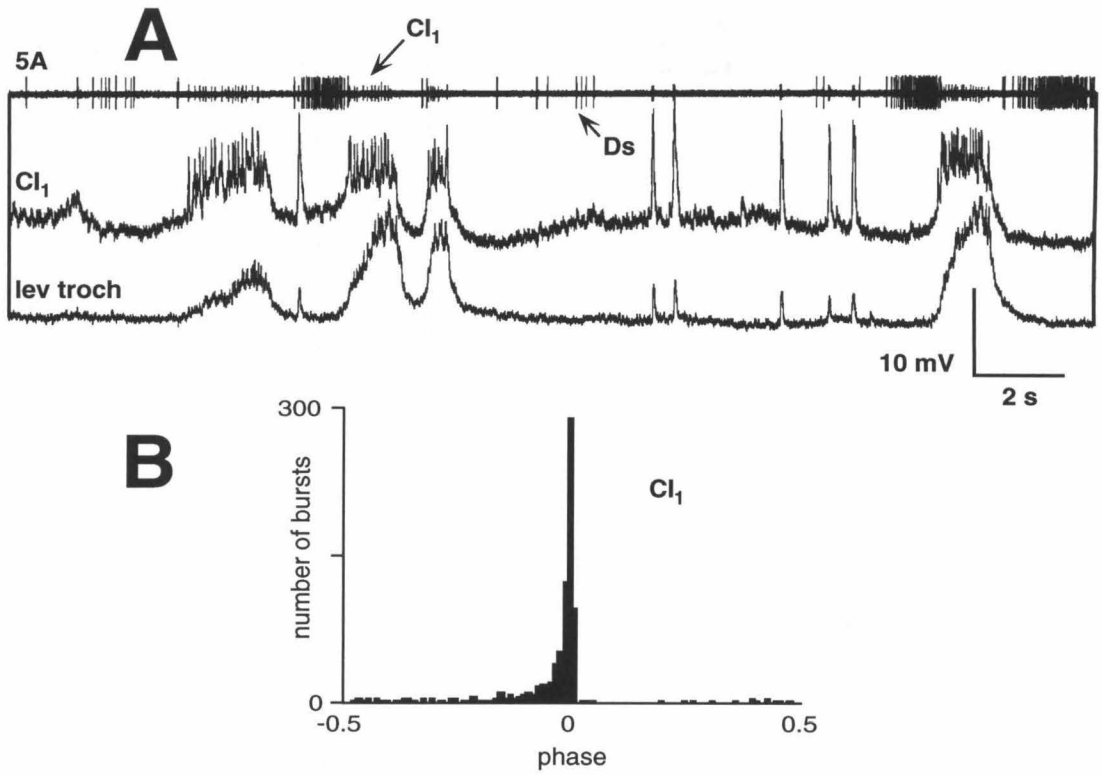

Figure 10. The common inhibitors are active during or just before the trochanteral levator phase. **A.** Simultaneous recordings from nerve 5A showing CI_1 and Ds activity, from CI_1 (intracellular recording), and a trochanteral levator. Note common drive to CI_1 and levator motor neuron. (Scale bars: 10mV, 2 sec.) **B.** Phase histogram of CI_1 onset activity with respect to onset of ipsilateral trochanteral levator bursts.

Coupling between hemiganglia of the same segment

In very few preparations, rhythms could be evoked in one side only of the metathoracic ganglion. In most preparations, rhythms were evoked in both sides, but in only a subset of these were the rhythms in both sides locked at a common frequency (Fig. 11A). In the latter case, the trochanteral levators on one side were active in phase with the trochanteral depressors on the other (Fig. 11A, shaded boxes). Because activity on one side consisted of a short levator burst preceding a depressor burst, activity on the other side then consisted of a depressor burst preceding a levator burst, usually followed by another depressor burst (Fig. 11A). One side of the ganglion thus appeared to impose its rhythm on the other. This apparent "domination" could flip from one side to the other, as shown in Fig. 11A, where the leading side changes from left to right around the time indicated by an arrow. In most preparations, both sides were active and oscillated at different frequencies. We made the following general observations:

1. When a levator burst occurred on one side, a depressor burst was generally observed simultaneously on the other side. This coupling can be seen in Fig. 1, where a burst of Ds spikes is evoked in nerve L5A (asterisks) during the contralateral levator phase, represented by the burst in nerve $R3C_1$ (since the fast rotator of the coxa is active in phase with trochanteral levators). In subsequent cycles, the right fast coxal rotator activity coincided with the left depressor activity (Fig. 1). This left-right coupling could also be seen from intracellular traces. In Fig. 11B, a trochanteral levator wave of depolarization was associated with a depolarization of a contralateral trochanteral depressor motor neuron (Fig. 11B). Common PSPs could not be seen, however.

2. Levator bursts were never observed simultaneously on both sides (Fig. 11C).

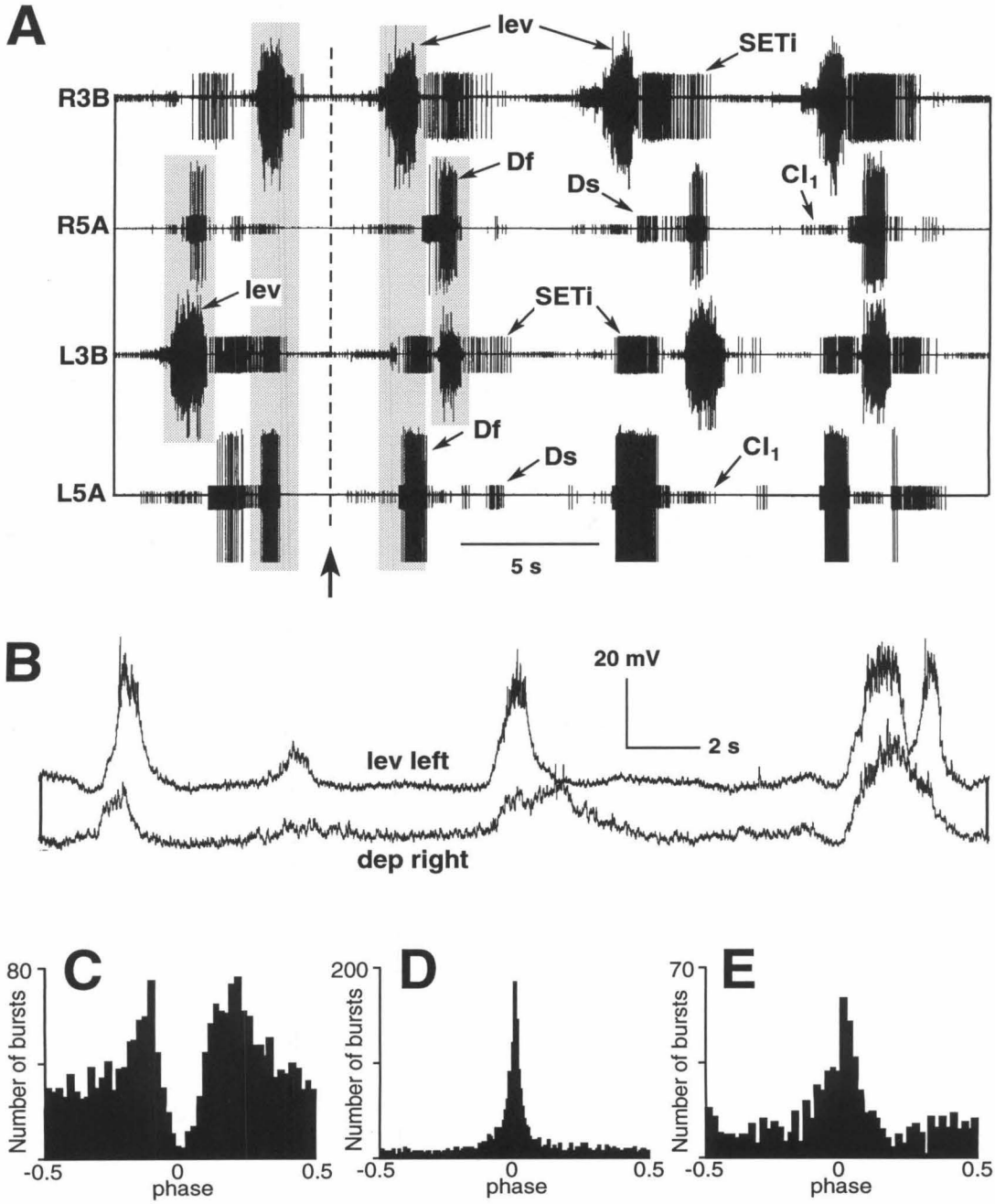
A
lev
SETi
R3B
Df
Ds
CI1
R5A
lev
SETi
L3B
Df
Ds
CI1
L5A
5 s
B
20 mV
2 s
lev left
dep right
C
80
Number of bursts
-0.5
0
0.5
phase
D
200
Number of bursts
-0.5
0
0.5
phase
E
70
Number of bursts
-0.5
0
0.5
phase

Figure 11

Figure 11. Rhythms in left and right hemiganglia are coupled. **A.** Change of dominant ganglion from left to right. Top to bottom: R3B (trochanteral levators, SETi), R5A (trochanteral depressors, CI_1), L3B, L5A. (Scale bar: 5 sec.) The bold arrow and dashed line indicate a reversal of dominance from left to right in leading the rhythmic activity. The leading hemiganglion expresses the "correct" sequence of activity, with levator burst preceding the depressor burst. The shaded boxes indicate the co-activation of levators on one side and depressors on the other. **B.** Intracellular recording from a trochanteral levator motor neuron on the left side (top trace) and the contralateral depressor Df (bottom trace). Although in phase, the two motor neurons do not receive obvious common PSPs. (Scale bars: 20mV, 2 sec.) **C.** Phase histogram of trochanteral levator onset of activity referenced to contralateral levators. **D.** Phase histogram of Ds and Df onset of activity referenced to contralateral levators. **E.** Phase histogram of SETi onset of activity referenced to contralateral levators.

3. Although the occurrence of a trochanteral levator burst on one side was generally a good predictor of a contralateral trochanteral depressor burst (Fig. 11D), the converse was not true. This left-right coupling between trochanteral levators and depressors thus appeared to be dominated by the levator "drives" on either side.

4. This contralateral influence of the trochanteral levators on the depressors was also observed with other motor neurons active during the trochanteral depressor phase, such as SETi. The probability of SETi being active was high during a contralateral levator burst (Fig. 11E). As for the trochanteral depressors, the converse left-right influence was not observed.

Coupling to ventilation

We monitored ventilation from the first metathoracic dorsal median nerve, which innervates opener and closer muscles of left and right third spiracles. This nerve

contains the axons of two opener and two closer motor neurons (Miller 1960; Lewis et al. 1973; Burrows 1982). In an isolated ganglion in normal saline, no rhythmic activity was observed on this nerve in most preparations. A ventilatory rhythm could be evoked reliably in the isolated ganglion, however, with the addition of ca. 10^{-5} M pilocarpine. The rhythm had a period of about 5 sec, and was characterized by a short burst of activity in opener motor neurons (corresponding to inspiration in the animal) and a longer burst in closer motor neurons (corresponding to expiration) (Fig. 12A). We verified the identity of the bursts by monitoring the mesothoracic dorsal median nerve, which contains only closer motor neurons active during the expiratory phase (Hoyle 1959; Miller 1960; Lewis et al. 1973; Burrows 1975) (Fig. 12B). We then monitored simultaneously the rhythmic output of left and right metathoracic levator motor neurons and that of the metathoracic median nerve (Fig. 12A); we observed long periods during which the leg and respiratory rhythms were coupled. Although their periods were substantially different, such that several respiratory cycles could occur during one leg activity cycle, bursts in levator motor neurons on either side were more likely to occur at a constant phase relative to the ventilatory rhythm (Fig. 12A). In particular, levator bursts on either side usually did not occur during the short inspiration phase (Fig. 12C).

2.5 Discussion

We have shown that pilocarpine reliably induces rhythmic activity in leg motor neurons in an isolated metathoracic ganglion of the locust. The rhythm is characterized by two phases of activity: a levator phase and a depressor phase. Most leg motor neurons showed rhythmic activity in phase with either the levators or the depressors of the trochanter, as summarized in Fig. 13 and below. Coupling was observed between the left and right hemiganglia such that depressors on one side were often active in

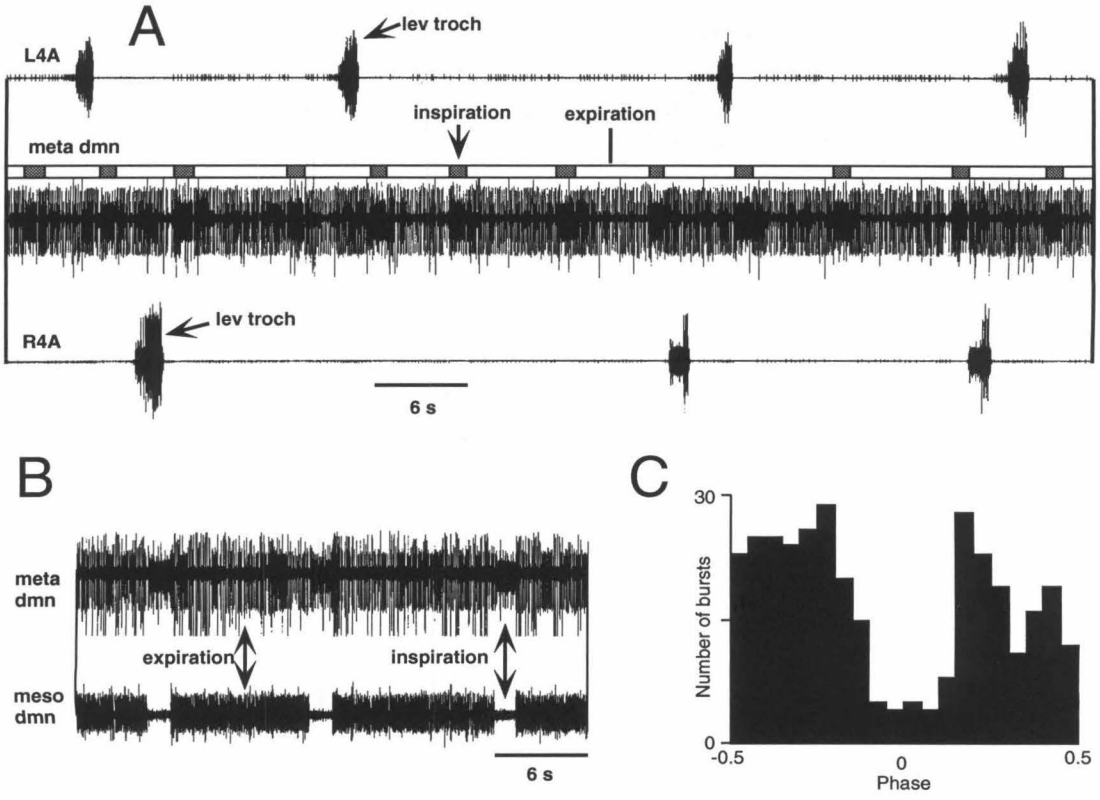

Figure 12. The locomotor rhythm is influenced by the ventilatory rhythm. **A.** Levator bursts on either side never occur during inspiration. Top to bottom: nerve L4A (trochanteral levators), metathoracic dorsal median nerve, nerve R4A. The inspiratory and expiratory phases of the respiratory rhythm are indicated by the dark (inspiration) and light (expiration) bars above the dorsal median nerve recording. (Scale bar: 6 sec.) **B.** Characterization of inspiration and expiration phases. Top trace: metathoracic dorsal median nerve. Bottom trace: mesothoracic dorsal median nerve. The mesothoracic median nerve contains only spiracle closer motor neurons, whereas the metathoracic median nerve contains both openers and closers. Connectives between meso- and metathoracic ganglia intact. (Scale bar: 6 sec.) **C.** Phase histograms of levator burst onsets referenced to onset of inspiratory burst. Data pooled from two preparations.

phase with levators on the other. These results confirm that central pattern generating networks exist in each hemiganglion, which can rhythmically drive leg motor neurons in a "walking-like" pattern. Some coupling to the ventilatory rhythm also was observed.

Pharmacologically-induced rhythm and walking patterns

Muscarinic acetylcholine agonists have also been used to induce central rhythms in crustacean isolated ganglia (Nagy and Dickinson 1983; Chrachri and Clarac 1990; Elson and Selverston 1992). Both nicotinic and muscarinic receptor types have been found in insect nervous systems, although little is known about the latter (Breer and Sattelle 1987; Gundelfinger 1992). In locust and in *Manduca sexta*, muscarinic receptors may be involved in the presynaptic regulation of release from cholinergic fibers (Breer and Knipper 1984; Trimmer and Weeks 1989). In addition, receptors have been found postsynaptically, where their role may be the regulation of excitability (Trimmer and Weeks 1989). Recent work has shown that muscarinic receptors are involved in the regulation of an inward current in insect motor neurons (David and Pitman 1992; Trimmer and Weeks 1991). Our results provide additional evidence that muscarinic receptors may be involved in the modulation of rhythmic motor patterns, although their sites of action in the nervous system and functional role have yet to be determined (Marder and Paupardin-Tritsch 1978).

The coordination of the activities of the different motor pools was generally similar to that observed in walking insects. In an intact insect, levators of the trochanter are in phase with flexors of the tibia during protraction of the hind leg. Depressors of the trochanter are in phase with extensors of the tibia during retraction (Burns, 1973; Burns and Usherwood 1979; Delcomyn and Usherwood 1973; Hughes 1952; H-J Pflüger, personal communication). The tarsal depressors are active during retraction,

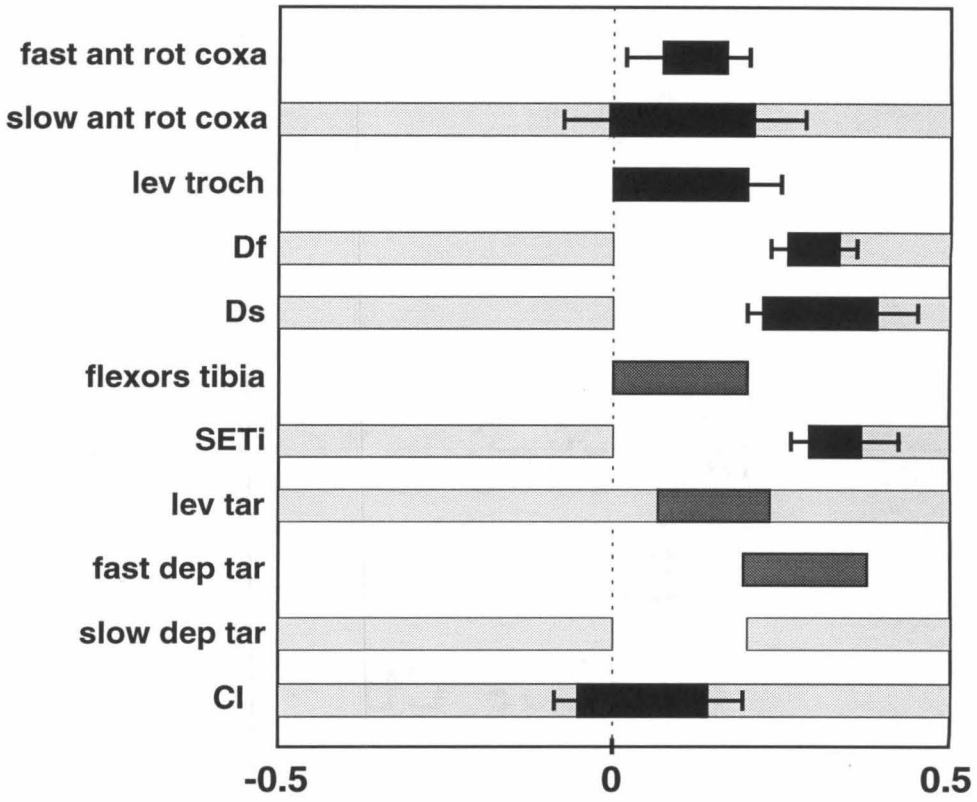

Figure 13. Summary of rhythmic activity induced by pilocarpine in the isolated preparation. Duration of spike activity in different leg motor neurons for a single normalized cycle in the isolated preparation. Solid bars and associated error bars were computed from a single continuous set of recordings in one representative experiment. (period: 15.3 ± 2 sec., n= 17 cycles) Error bars on the left are standard deviations of the latency of burst onset. Error bars on the right are standard deviations of burst duration. Dark stippled bars with no error bars were based on qualitative observations from intra- and extracellular recordings in other experiments. Light shaded bars for some motor neurons indicate times in a cycle during which spikes were also observed frequently. For example, Ds can be active during most of the cycle, but never during an ipsilateral trochanteral levator burst, when it is inhibited (Fig. 7A, 7C).

and are silent during protraction, whereas the tarsal levator is mainly active during protraction and is inhibited during the beginning of retraction (Laurent and Hustert 1988). This general description was also true in the present study. The duration of the trochanteral levator phase was independent of the cycle period, which is consistent with behavioral observations and electromyographical and neural recordings in intact walking insects (Burns 1973; Burns and Usherwood 1979; Delcomyn and Usherwood 1973; Graham 1972). The latencies from the end of a levator burst to the beginning of depressor/extensor bursts were constant, as in walking, although these latencies have not been measured for different walking speeds in an intact animal.

The rhythmic patterns of activity that we observed were more irregular than other centrally generated rhythmic patterns studied in insects (flight: Wilson 1961; ventilation: Myers and Retzlaff 1963, oviposition: Seymour 1990). This is not surprising in view of the higher plasticity and greater dependance of legged locomotion on sensory information. In addition, walking patterns are more variable in locusts than in cockroaches and stick insects, possibly because of the higher degree of specialization of the legs (Burns 1973; Burns and Usherwood 1979). There were both ipsi- and contralateral contributions to the observed irregularity. The output of a single pattern generator was inherently irregular, which was evident in the variability of the burst durations and interburst intervals for a single hemiganglion when no rhythmic activity was observed on the contralateral side. The coupling between left and right hemiganglia also appeared to perturb the rhythmic activity. Coupling between trochanteral levators and contralateral trochanteral depressors seemed to cause the irregular patterns of activity observed in trochanteral depressors and tibial extensors, but did not appear to affect the timing of the levator bursts. In an intact animal, the pattern generators for the different legs could be phase-locked by sensory inputs and mechanical coupling, whereas the coupling between different motor pools within a hemiganglion could be achieved primarily via non-sensory interactions.

Under all conditions, the frequency of the rhythm studied here was slower than that of walking in intact locusts (0.5 to 3 steps per second (Wolf 1990); 2 to 9 steps per second (Burns 1973)). This was mainly due to the long intervals between the end of a depressor burst and the beginning of the next levator burst. Rhythmic motor patterns evoked in deafferented preparations typically are slower than the corresponding motor pattern in intact animals (locust flight: Wilson 1961; lamprey swimming: Wallén and Williams 1984; cat walking: Grillner and Zangger 1979; oviposition: Seymour 1990). For most biphasic rhythmic motor patterns, deafferentation tends to lengthen the "power stroke" (here the depressor phase), i.e., the phase most sensitive to sensory cues. Indeed, sensory inputs appear to be critical during this phase, to trigger the transition to the next phase or to modify the position of the limb in response to changes in the terrain or the load on the limb (Cruse 1990). Such inputs were of course missing here, which may explain the characteristic patterns of the deafferented rhythm. The prolonged waiting period between the end of depressor activity and the next levator burst could therefore reflect the absence of sensory inputs signaling the end of retraction, which in an intact animal would be used to trigger the next leg protraction.

Common inhibitors

In intact locusts, the three common inhibitors are maximally active immediately before and during the protraction of the leg (Runion and Usherwood 1968; Burns and Usherwood 1979; Wolf 1990). In addition, these motor neurons are often tonically active at frequencies which vary with walking speed and the state of arousal of the animal (Burns and Usherwood 1979; Wolf 1990). They act to suppress tension in muscle fibers that have a tonic, or postural role, to enhance the action of fast muscle fibers during rapid movements (Wiens 1989; Wolf 1990). The activity of the common

inhibitors recorded here is consistent with this view, as they were maximally active slightly before a burst of activity in fast motor neurons. These observations show, as Wolf (1990) concluded from his experiments in walking locusts, that the common inhibitors and excitatory motor neurons are driven by the same central oscillator.

Intrasegmental coupling

Previous studies of the coupling between legs focused mainly on inter-, rather than intrasegmental, interactions (Pearson and Iles, 1973). Most of the evidence from intact and deafferented arthropods supports the view that the legs of the same segment are coupled primarily through reflex action, and that central coupling, if it exists, is "weak" (Pearson and Iles 1973; Bässler and Wegner 1983; Sillar et al. 1987). One surprising result of the present study is the strong coupling we observed between levators of the trochanter and contralateral depressors of the trochanter. Previous studies considered only coupling between putative "flexor burst generators" on both sides of the ganglion (Wilson 1966; Pearson and Iles 1970). This may explain why the levator and contralateral depressor interactions were never observed. Indeed, in the present study, coupling between levator bursts on opposite sides appeared to be mainly inhibitory (Fig. 11C). This would be sufficient to phase-lock the pattern generators on opposite sides if their natural frequencies were similar, as we observed. When the frequencies of the rhythmic activity on opposite sides differed, levator bursts on opposite sides appeared to be uncoupled, except for the fact that they never occurred simultaneously.

Intersegmental coupling

Although we did not study the coupling between segmental oscillators, cutting the thoracic connectives had a striking effect on the locomotor rhythm. The nature of

descending signals and their influence on walking have not been established clearly. Cutting the circum-oesophageal connectives triggers long sequences of walking in praying mantis (Roeder 1937) and stick insect (Graham 1979a,b), suggesting that descending inputs from the brain have an inhibitory influence on locomotory activity. By contrast, cutting the connectives between the suboesophageal and prothoracic ganglia inhibits walking (Roeder 1937). Because we explored the effects of cutting the connectives only between thoracic ganglia, we cannot assess the importance of the brain and suboesophageal ganglia on the locomotor rhythm. Our results clearly indicate, however, that progressively isolating the metathoracic ganglion from other thoracic ganglia increases the frequency of the locomotor rhythm. This result could be explained within a simple mathematical framework of systems of coupled oscillators such as that developed by Rand, Kopell, Ermentrout, and collaborators (Rand et al. 1988; Kopell 1988). Such formal analysis, applied to our results, should allow testable predictions to be made about the nature of intersegmental coupling. Intersegmental coupling will be reviewed in Chapter 4.

Walking and related behaviors

In a fully deafferented stick insect, Bässler and Wegner (1983) observed alternation between antagonistic muscles, but the patterns of activity were irregular and the coordination between legs resembled "seeking" or "rocking" movements, rather than walking. Rhythmic leg movements in decapitated cockroaches appeared more similar to righting than to walking (Zill 1986). It is indeed true that, although insect legs are used for walking, they are also used for grooming (Reingold and Camhi 1977), righting (Reingold and Camhi 1977; Sherman et al. 1977; Zill 1986), searching (Delcomyn 1987), kicking and jumping (Heitler and Burrows 1977), and swimming (Pflüger and Burrows 1978). These behaviors can be separated into two categories. In the first are

swimming, kicking, and jumping, all characterized by an initial flexion of the tibia, a co-contraction of flexor and extensor muscles that locks the leg in a flexed position while tension builds in the extensor muscle, followed by a powerful extension of the tibia due to very strong activity in both FETi and SETi (Heitler and Burrows 1977). In jumping and swimming, the two hind legs kick at the same time. The motor activity we recorded here differed in most respects from this description. First, as during walking, FETi was rarely depolarized above threshold. Second, flexors and extensors were never co-active. Third, the coordination between left and right legs did not correspond to the coordination reported for jumping and swimming.

Walking, searching, righting, and grooming form the second group of leg motor behaviors (Reingold and Camhi 1977; Sherman et al. 1977). The main difference among them seems to be in the inter-leg coordination. The fact that no strong coordination was found between left and right legs in deafferented cockroaches (Pearson and Iles 1973; Reingold and Camhi 1977) was the basis for the argument that the rhythmic leg activity did not resemble walking more than it resembled righting or grooming. In fact, our results showed strong coordination between rhythms evoked in the left and right hemiganglia. Without studying the intersegmental coordination, we cannot conclude yet that the rhythmic activity observed here is indeed a walking pattern. We can conclude, however, that the central pattern generator activated here produced a pattern of motor neuron activity that would be appropriate for the movement of a single leg or a segmental pair of legs during walking, without excluding other behaviors for which similar leg movements might be required.

Chapter 3

An Adaptive Circuit Model for Segment-Specific Motor Patterns

3.1 Summary and conclusions

Rhythmic motor patterns can be induced in leg motor neurons of isolated locust thoracic ganglia by bath application of pilocarpine. We observed that the relative phases of levators and depressors differed in the three thoracic ganglia. Arguing that the central pattern generating circuits underlying these three segmental rhythms are probably very similar, we developed a simple model circuit which can produce either of the three activity patterns and characteristic phase relationships by modifying a single synaptic weight. We show results of a computer simulation of this circuit using the neuronal simulator NeuraLOG/Spike. We built and tested an analog VLSI circuit implementation of this model circuit which exhibits the same range of "behaviors" as the computer simulation. This multidisciplinary strategy will be useful to explore the dynamics of central pattern generating networks coupled to physical actuators, and ultimately should allow the design of biologically realistic walking robots.

3.2 Introduction

It is now generally recognized that neural circuits are not hardwired ensembles of neurons with fixed properties, but rather form plastic and adaptable sets. Some of the clearest demonstrations of such neural plasticity have come from studies of central pattern generator circuits. Studies of the crustacean stomatogastric nervous system, for example, have established that the intrinsic properties of component stomatogastric neurons and the efficacies of their synaptic connections are subject to modulation by a large number of "neuroactive" substances, which can act on a wide range of temporal and spatial scales (Harris-Warrick et al., 1992). Altering neuronal and synaptic properties is one way of creating different "functional" circuits from a fixed set of interconnected neurons. The traditional concept of a central pattern generator as a hardwired neural circuit which produces a fixed output pattern is thus being replaced by that of a "family" of circuits, a set of modifiable neurons and connections, which can be reorganized to produce different outputs as external and internal conditions change (Harris-Warrick and Marder, 1991; Marder and Weimann, 1992). Some examples of neural circuits that are used to generate the motor patterns underlying multiple behaviors come from the studies of *Tritonia* withdrawal and swimming (Getting and Dekin, 1985a, b), crab forward and reverse scaphognathite beating (Simmers and Bush, 1983), *Pleurobranchaea* feeding, regurgitation, and rejection (McClellan, 1982), and the crustacean gastric and pyloric nervous system (Weimann et al., 1991).

Work on more complex central pattern generators (such as the flight system of the locust (Robertson, 1986) or the spinal cord of vertebrates (Grillner et al., 1991; Grillner and Wallén, 1985)) has shown that the identification of component neurons and their interconnections does not necessarily yield a clear functional understanding of the circuits. Such circuits are often more "complicated" than appears necessary to generate a limited set of observable behaviors. In addition, because a central pattern

generator circuit probably contains elements which serve several functions, it is hard to identify by inspection the components which are essential for the generation of a single behavior. In other words, the dissection of a complex circuit into its component parts does not necessarily lead directly to an understanding of the computational rules or algorithms that it employs. One of the clearest demonstrations of the limits of our intuition comes from a theoretical study of pairs of neurons connected through reciprocal inhibitory synapses (Wang and Rinzel, 1993). In this study, Wang and Rinzel showed that the behavior of such a circuit depends critically on the time constant of decay of the inhibitory synaptic conductance. If this time constant is short, the neurons oscillate in antiphase; if it is long, however, the neurons fire in synchrony, despite their inhibitory reciprocal coupling. Even seemingly simple ideas, therefore, need to be carefully tested and explored.

An alternative strategy to exhaustive electrophysiological analysis of complex circuits and characterization of their component neurons is to use a limited experimental data set to generate artificial models, whose behavior can then be exhaustively challenged. This strategy, in time, leads to new specific questions about the biological system that can be addressed experimentally, and to the gradual addition of constraints on the modelled circuit. We adopted such a multidisciplinary strategy in the study of central pattern generating circuits underlying terrestrial locomotion in insects. We focussed on the thoracic circuits controlling the three pairs of legs of locusts. Because the front, middle, and hind legs have unique morphologies and functional roles during walking, we focussed here on the differences between the patterns of rhythmic activity generated by the three segments. Arguing that, although different, these rhythms should be produced by similar central pattern generating networks (the three thoracic ganglia being essentially homologous repeats of a single ontogenetic design), we then attempted to design a simplified generic circuit capable of producing all three output patterns. This paper describes one such successful

circuit.

Although computer simulations are now widely used to model various aspects of neural systems, silicon (hardware) models are less commonly used. Yet silicon models are extremely useful in testing the ability of a model to function with real physical constraints such as noise and device imperfections (Mead, 1989). In addition, because silicon models operate in real time, feedback to the experimenter is immediate. Moreover, Very Large Scale Integrated (VLSI) circuits can be easily interfaced to mechanical actuators to build systems which interact with the environment, such as mobile robots (DeWeerth et al., 1991). Several types of spiking "neural" circuits have been successfully modelled in silicon hardware. Pulse stream encoding of information has been used in data communications applications and neural networks for a number of years (Murray et al., 1991; Mahowald et al., 1992). Ryckebusch et al. (1989) described silicon models of invertebrate central pattern generators using simple spiking neurons and synapses. Similar neuronal circuits have been used successfully in silicon models of auditory localization (Lazzaro and Mead, 1989) and the jamming-avoidance response of weakly-electric fish (LeMoncheck, 1992). A detailed model of a single neuron which explicitly included different membrane conductances and adaptation mechanisms was introduced by Mahowald and Douglas (1991). Our approach thus combined biological experiments, computer simulations, and silicon hardware designs, to study central pattern generators underlying terrestrial insect locomotion.

3.3 Methods

Electrophysiology

Experiments were performed on adult locusts *Schistocerca americana* of either sex, from our crowded laboratory colony. The results presented here were gathered from 44 different experiments.

The preparation. Experiments were performed on an *in vitro* thoracic preparation described previously (Ryckebusch and Laurent, 1993). Briefly, thoracic ganglia were removed from the thorax of the animal with the surrounding tracheal supply and air sacs undisturbed, and were pinned down in a chamber lined with Sylgard 184 (Dow Corning Co., Midland, MI). Leg motor nerves were carefully stripped of their surrounding connective tissue with a small hooked pin. The preparation was superfused with locust saline (mM: NaCl: 140; KCl: 5; $CaCl_2$: 5; $NaHCO_3$: 4; $MgCl_2$: 1; *N*-2-hydroxyethylpiperazine-*N'*-2-ethanesulfonic acid: 6.3; pH 7.0) supplemented with 2.5% (wt/vol) sucrose. Air was supplied to the ganglia by teasing open the tracheae at the surface of the saline. A stock solution of 10^{-2}M pilocarpine hydrochloride (Sigma) was prepared in advance, and was added to the saline to final bath concentrations of 10^{-5} to 10^{-4}M. The preparation remained healthy for at least 4 or 5 hours at 20 to 26°C.

Recordings. The electrical activity of different leg motor nerves was monitored extracellularly using polyethylene suction electrodes. Data were recorded on an eight-channel Digital Audio Tape recorder sampling at 5 kHz (Sony/Biologic), and were displayed on a Gould TA4000 chart recorder.

Anatomy and nomenclature. The muscles are numbered according to Snodgrass (1929), except where a variant is now more commonly used in the literature. The nerves are numbered according to Bräunig (1982). Motor neurons are designated by

commonly used abbreviations or by the name of the muscle group that they innervate. Detailed descriptions of the innervation of the leg musculature can be found in Campbell (1961), Bräunig (1982), and Siegler and Pousman (1990a).

Analysis. Electrophysiological recordings were analyzed off-line with a Macintosh II microcomputer, after digitization at 2 to 8 kHz with a National Instruments NBMIO16L AD/DA interface. The software packages used for data analysis were Spike Studio (Eli Meir, Cornell University), MatLab (The MathWorks), and Kaleidagraph (Abelbeck Software).

The centrally generated rhythm observed in the present experiments was characterized by two main phases, hereafter referred to as the **levator** and **depressor** phases, corresponding to the activities of levators and depressors of the trochanter. The onset of a burst of activity in trochanteral levators was chosen as the reference for the rhythmic activity. A period is defined as the interval from the onset of a levator burst to the onset of the next levator burst.

Computer simulations

Spike: Event-driven simulation. "Spike" is a fast event-driven simulator written by Lloyd Watts (Caltech, Synaptics), optimized for simulating networks of spiking neurons and synapses. The key simplifying assumption in Spike is that all currents injected into a cell may be composed of piecewise-constant pulses (i.e., boxcar pulses). All integrated membrane voltage trajectories are therefore piecewise linear in time. This simple representation is well-suited for investigating system-level questions that rely on detailed spiking behavior. The simulator operates by maintaining a queue of scheduled events. The occurrence of one event (i.e., an action potential) usually causes later events to be scheduled in the queue (i.e., end of refractory period, end of post-synaptic current pulse). The total current injected into a neuron is integrated

into the future to predict the time of firing, at which time a neuron spike event is scheduled. If any of the current components being injected into the cell subsequently change, the spike event is rescheduled. The simulator runs until the queue is empty or until the desired run-time has elapsed.

NeuraLOG: Neural schematic capture. "NeuraLOG" is a schematic entry tool, which allows the convenient entry of "neural" circuit diagrams, consisting of neurons, synapses, test inputs, and custom symbols. NeuraLOG is a customization by Lloyd Watts of the program AnaLOG, by John Lazzaro and Dave Gillespie (Caltech). The parameters of the neural elements are entered directly on the schematic diagram; these parameters include the neuron refractory period, duration and intensity of the post-synaptic current pulse following an action potential, saturation value of summating post-synaptic currents, tonic input currents, axonal delays, *et caetera.* Custom symbols can be defined, so that arbitrarily complex hierarchical designs may be made. For example, one can create a complex "neuron" (e.g., bursting neuron) containing many neuron and synapse primitive elements. Spiking inputs may be supplied as external stimuli in a number of formats, including single spikes, periodic spike trains, periodic bursts, (Poisson) random spike trains, and gaussian-jittered periodic spike trains. Textual input to Spike is also possible, to allow simulation of algorithmically-generated circuit topologies too complex to specify graphically.

NeuraLOG and Spike were both created by Lloyd Watts and are distributed under the GNU General Public Licence. Send email to lloyd@pcmp.caltech.edu for information.

Neuron and synapse models. The model neuron and synapse circuit primitives we used both in our simulations and in the VLSI implementation were developed by Lloyd Watts as abstract models which capture some of the basic characteristics of biological neurons and synapses. These circuit elements are the primitive elements in the NeuraLOG/Spike simulator described above. Since both the neuron and synapse

circuits were designed as electronic VLSI circuits, it is relatively straightforward to implement in VLSI a given model circuit which was designed and simulated using NeuraLOG/Spike. Detailed mathematical analysis of the neuron circuit at the transistor level can be found in Sarpeshkar et al. (1992). General descriptions of the circuit models and the simulation tools can be found in Watts (1992, 1993). We will briefly describe these circuits here in biological terms. The model neuron circuit is similar to a Hodgkin-Huxley sodium-potassium conductance pair. This neuron circuit takes as its input a current, and generates as its output a train of pulses whose height is determined by the voltage of the power supply (typically 5 volts). The pulses are fired only if the input node, which is integrating the input current, reaches the threshold voltage. The firing frequency increases with the input current until the upper frequency limit (saturation) set by the refractory period is reached. The neuron circuit has three parameters: a threshold, a pulse width, and the refractory period of the action potential. The circuit operations underlying the generation of a pulse can be described in biological terms as follows. A persistent "sodium conductance" causes the rising phase of the action potential. The "sodium conductance" activates, after a delay, a "potassium conductance" that is coupled to it. This "potassium conductance" restores the membrane potential to its "resting" value and causes the falling phase of the action potential. The "potassium conductance" inactivates slowly in a time-dependent (but not voltage-dependent) manner, causing a "refractory" period after the firing of the action potential.

A simplified synaptic cleft model is the basis for the synapse circuit. An action potential from the presynaptic "neuron" causes the release of "neurotransmitter" into the synaptic cleft, where it remains for a controlled duration. While "neurotransmitter" is in the cleft, a constant current is injected into the postsynaptic cell. The "synapse" circuit therefore has two parameters: the duration of a synaptic event and the synaptic current which flows into the postsynaptic cell. Any number of "synapses"

can be connected to a "neuron" circuit.

VLSI implementation

The VLSI implementation of the neuron circuit contains 8 transistors and can operate over wide ranges of firing frequency, pulse width, refractory period, and threshold. The firing frequency can be varied from 0.1–0.5Hz to 100 kHz. The pulse widths and refractory periods of the action potentials can be varied from a few tens of microseconds to hundreds of milliseconds. The threshold for firing can be varied from approximately 0.7 volts to the power supply voltage (5 volts). A typical neuron with its synaptic inputs measures approximately $100 \times 250\mu$m (Fig. 6B). The entire 3-neuron circuit contains 97 transistors and measures $400 \times 600\mu$m. VLSI circuits were designed using the layout editor LEdit (Tanner Research) on a Hewlett Packard workstation. The chip was fabricated in a standard 2-micron double-poly CMOS (Complementary Metal-Oxide Semiconductor) process on a 2×2mm 40-pin die (TinyChip) (Fig. 6A). Chip fabrication was provided by the Defense Advanced Research Projects Agency and through the MOSIS service. Data acquisition was performed using a Macintosh microcomputer with a National Instruments NBMIO16L AD/DA interface running MatLab (The MathWorks).

3.4 Results

Segment-specific rhythmic motor patterns

Metathoracic rhythm

The rhythmic patterns evoked in leg motor neurons in isolated metathoracic ganglia by pilocarpine have been described in detail in Ryckebusch and Laurent (1993). Those

Abbreviations

CI	common inhibitor
CMOS	Complementary Metal-Oxide Semiconductor
dep	depressor
D_f	fast depressor trochanteris
D_s	slow depressor trochanteris
lev	levator
troch	trochanter
VLSI	Very Large Scale Integrated

---

results are summarized here for the purposes of comparison.

The frequency of the pilocarpine-induced rhythm increased approximately linearly from 0 to 0.2 Hz with concentrations of pilocarpine from 10^{-5} to 10^{-4}M. For each hemiganglion, the rhythm was characterized by two main phases: a **levator** phase, during which the anterior coxal rotator, levators of the trochanter, flexors of the tibia, and common inhibitory motor neurons were active; and a **depressor** phase, during which depressors of the trochanter, extensors of the tibia, and depressors of the tarsus were active. During normal walking these two phases would correspond to the swing and stance phases of a step of the hind leg, respectively. Trochanteral depressor activity followed the trochanteral levator bursts with a short, constant interburst latency such that activity in the two antagonistic groups did not overlap. The levator phase was short in comparison to the cycle period (0.5 to 2 sec, or 10% to 20% of the period), and was independent of the cycle period. The interval between the end of a levator burst and the beginning of the following one thus increased with cycle period. The depressor phase was more variable and was usually shorter than the interval between successive levator bursts. A second depressor burst was sometimes observed during the latter half of a cycle. This second burst generally coincided with

a levator burst on the contralateral side and always ended before the onset of the ipsilateral levator burst.

All depressor trochanteris motor neurons were active during the same phase, although their spiking thresholds differed substantially. In inactive preparations (no pilocarpine), D_f was silent and D_s was tonically active. At low levels of activity, the tonic firing of D_s was interrupted during the bursts of trochanteral levator activity; this interruption was followed by a transient increase in firing frequency. Variations of the instantaneous firing frequency of D_s were mirrored by those of the membrane potential of D_f, which was hyperpolarized during a levator burst, and depolarized immediately after it. As the level of activity increased, the tonic firing of D_s ceased, and short, clearly defined, bursts of action potentials emerged. D_f action potentials were often observed when D_s reached its peak instantaneous firing frequency.

Prothoracic rhythm

We recorded extracellularly from leg motor nerves 4A (trochanteral levators) and 5A (trochanteral depressors) of isolated prothoracic ganglia. From nerve 4A, we recorded the activity of up to 10 motor neurons. From nerve 5A, we recorded the activity of the fast and slow trochanteral depressors D_f and D_s, and a common inhibitory motor neuron CI (Fig. 1). In inactive preparations (no pilocarpine), D_f was silent and D_s was tonically active. The prothoracic rhythmic motor patterns recorded in the presence of pilocarpine differed in several respects from the metathoracic ones. During rhythmic activity, D_s maintained a high tonic firing rate, and was periodically inhibited during the bursts of trochanteral levator activity (Fig. 1 (top)). The rhythmic activity could be elicited at lower concentrations of pilocarpine (*ca.* 10^{-5}M) than that which was typically used for the metathoracic ganglion (5×10^{-5}–10^{-4}M). The frequencies (inverse of cycle period) typically recorded were higher than those in the metathoracic ganglion at similar concentrations of pilocarpine. Although both pro-

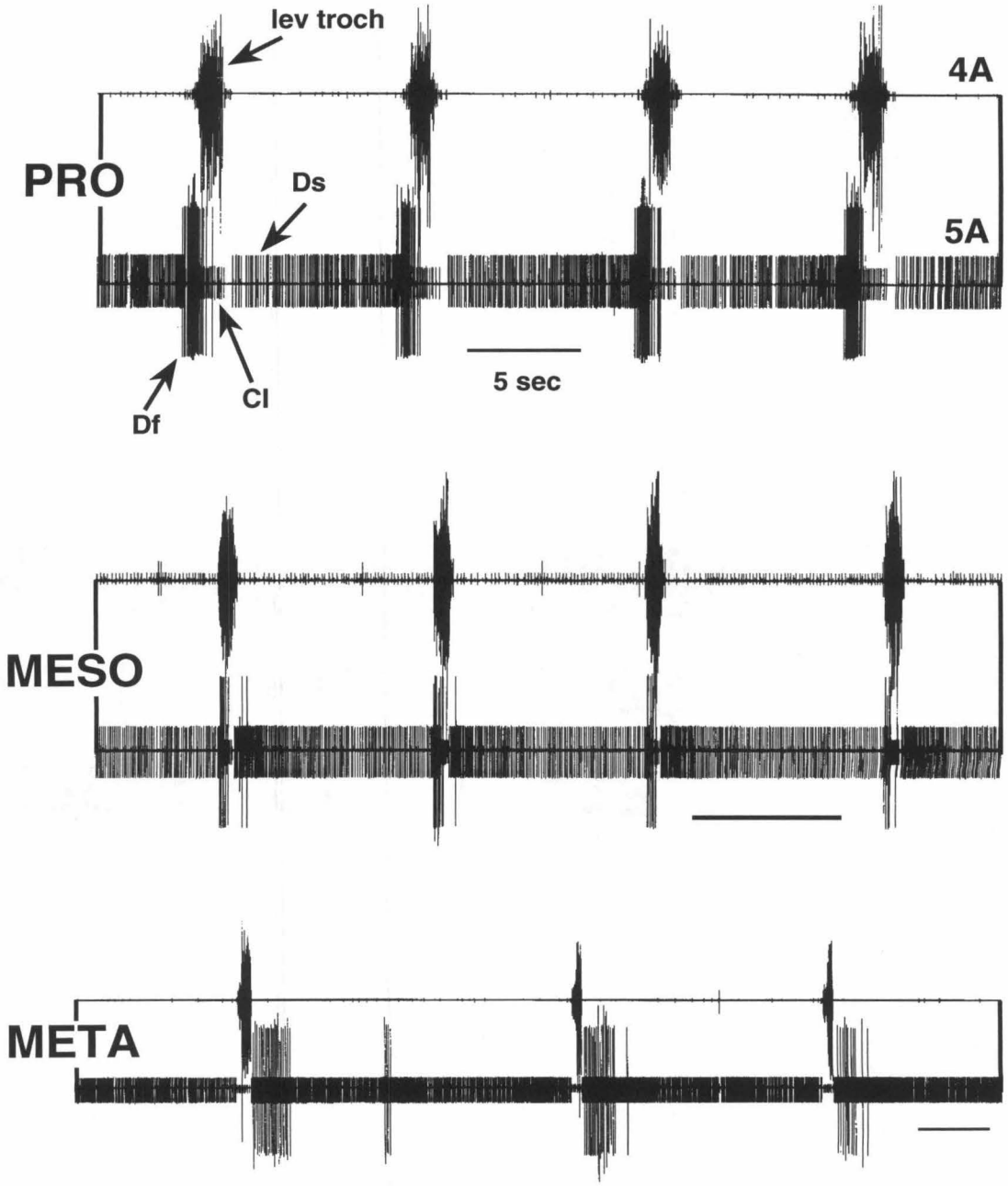

Figure 1

Figure 1. Rhythmic patterns of activity of levator and depressor trochanteris motor neurons in isolated pro-, meso-, and metathoracic ganglia. In each pair of traces, the top trace is an extracellular recording of nerve 4A (trochanteral levators) and the bottom trace is an extracellular recording of nerve 5A (trochanteral depressors, CI). Pilocarpine: 10^{-5}M (pro), 10^{-5}M (meso), 3×10^{-5}M (meta) (Scale bar: 5 sec).

thoracic trochanteral levator burst durations and interburst intervals were shorter than the metathoracic ones, the higher frequency was mainly due to shorter intervals between trochanteral levator bursts (Figs. 1 and 2). Whereas metathoracic D_s and D_f fired at the highest rate immediately after a trochanteral levator burst, the highest firing frequency of prothoracic D_s and D_f occurred *before* trochanteral levator bursts (Figs. 1 and 2). Overlap between levator and depressor activities was often observed at the beginning of a trochanteral levator burst (Fig. 2). In the isolated prothoracic ganglion, we typically did NOT observe a postinhibitory increase in depressor firing frequency after a trochanteral levator burst, although the latency between the end of a levator burst and resumption of tonic firing of D_s was shorter than that observed in the metathoracic ganglion (Fig. 2). Whereas in the metathoracic ganglion we often saw coupling between depressors and the contralateral levators (i.e., the firing frequency of depressors increased during a contralateral levator burst), we rarely saw such bilateral coupling in the prothoracic ganglion. (A detailed analysis of intersegmental coupling is the object of the following chapter.)

Mesothoracic rhythm

The rhythmic activity recorded in the mesothoracic ganglion was similar in most respects to that in the prothoracic ganglion, as described above. The main difference observed was that the depressor motor neurons (D_s and D_f) had marked peaks of ac-

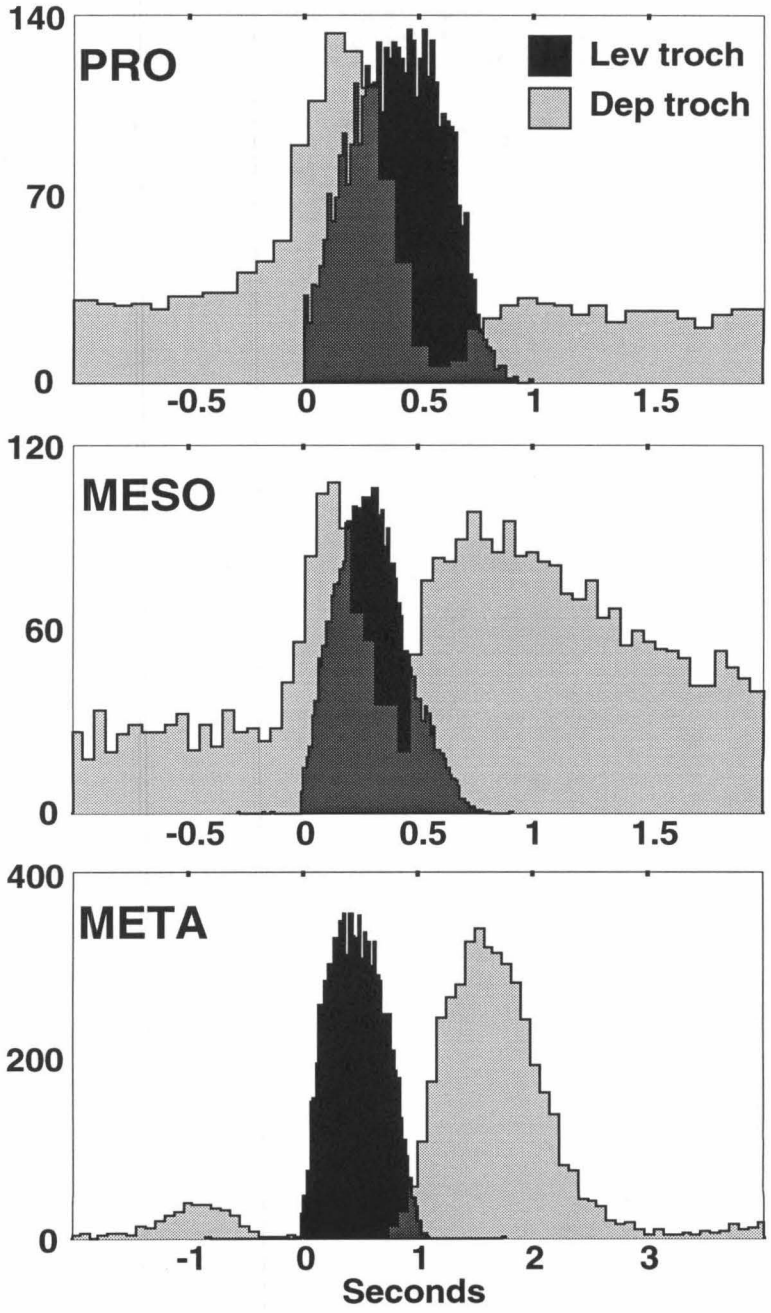
140
PRO
Lev troch
Dep troch
70
0
-0.5
0
0.5
1
1.5
120
MESO
60
0
-0.5
0
0.5
1
1.5
400
META
200
0
-1
0
1
2
3
Seconds

Figure 2

Figure 2. Spike frequency histograms of trochanteral levator and depressor motor neuron activity as shown in Fig. 1. Data is compiled from 30 (pro), 132 (meso) and 53 (meta) periods of activity from single continuous recordings. The reference is the onset of a burst of trochanteral levator action potentials. The scale on the ordinate is the total number of action potentials in each bin, and represents a cumulative total for all of the periods of activity that were analyzed.

tivity both immediately before and after a levator burst (Figs. 1 and 2). This pattern of activity was somewhat variable: In some preparations, the mesothoracic depressors fired maximally before the levator burst (as was described for the prothoracic ganglion); in other preparations, the depressors fired maximally after a levator burst (as was observed in the metathoracic ganglion); in still other preparations, depressor activity was equally high both before and after a levator burst. In most preparations, each of these patterns occurred at some time. The frequencies of the rhythmic activity were similar to those of the prothoracic ganglion, as described above.

A simple configurable model circuit

The aim of the simulation studies described here was to test model circuit designs which could produce the different motor patterns recorded in the isolated pro-, meso-, and metathoracic ganglia. The goal of this modelling study was therefore to explore possible circuit designs of a central pattern generator which would be flexible enough to produce all of these motor patterns. Such modulation of the motor pattern should be achievable by simple and biologically realistic mechanisms in the model circuit. The actual structures of the biological circuits, however, are unknown at this point. Such a circuit was designed using abstract models of neurons and synapses using the NeuraLOG/Spike circuit simulator (see Methods). It should be emphasized that this circuit was designed so that it would be both simple and easy to implement using

available VLSI technology (see below).

The bursting neuron

A bursting neuron, which produces rhythmic bursts of action potentials, was constructed using two primitive neuron circuits (Fig. 3A). Two neuron circuits were needed to obtain an equivalent neuron with enough state variables to generate bursting behavior. In Appendix B, we describe another bursting neuron model which uses only a single cell, but requires a more sophisticated model of the synapse. In the burster circuit (Fig. 3A), cell 1 makes a weak excitatory synapse onto cell 2. Cell 2, in turn, makes a strong inhibitory synapse onto cell 1. In addition, cell 1 makes an excitatory feedback synapse onto itself. In response to an excitatory input drive (such as a constant current or a train of action potentials fed through an excitatory synapse), cell 1 fires bursts of action potentials. The activity of cell 1 is taken to be the output of the bursting neuron. The firing frequency of cell 1 during a burst is determined by the magnitude of its positive feedback current. The duration of the burst is determined by the strength of the excitatory synapse from cell 1 to cell 2, and the interval between bursts is determined by the strength of the excitatory input drive into cell 1. The burst duration and interburst interval are therefore independently determined.

The central pattern generator circuit

The entire model circuit, shown in Fig. 3B, is composed of two bursting neurons as described above (Drive and Lev) and one non-bursting neuron (Dep). Lev represents the drive to the pool of trochanteral levator motor neurons, and Dep represents the drive to the pool of trochanteral depressor motor neurons. For simplicity, we will often refer to Dep and Lev as levator and depressor neurons. Since connections

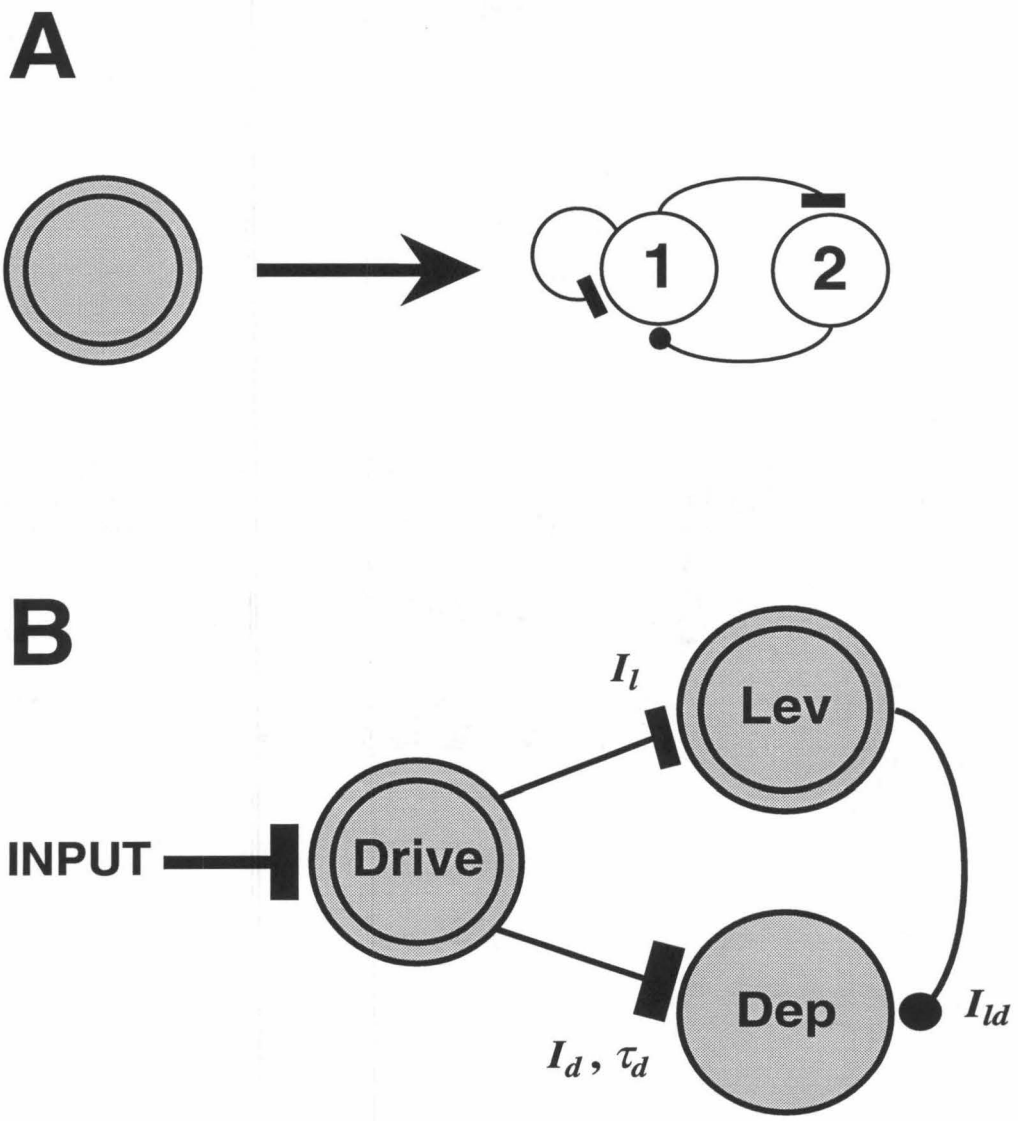

Figure 3

Figure 3. An abstract model circuit for generating pro-, meso-, and metathoracic motor patterns. **A.** A "bursting" neuron can be modeled by two "cells" connected by reciprocal synapses. Cell 1 makes a weak excitatory synapse onto cell 2. Cell 2 makes a strong inhibitory synapse onto cell 1. In addition, cell 1 makes an excitatory connection onto itself (positive feedback). With the addition of a small excitatory input drive into cell 1, the output of cell 1 consists of bursts of action potentials separated by a silent period. Note that in such a model circuit, cells 1 and 2 represent state variables rather than actual cells. **B.** Three-neuron model circuit, consisting of a "Drive" neuron and levator (Lev) and depressor (Dep) motor pool drivers. Drive and the levator motor pool driver are bursting neurons. Filled bars represent excitatory synapses, and filled circles represent inhibitory synapses. The three motor patterns (pro-, meso- and metathoracic) can be obtained by modifying the strength of the excitatory synapse between Drive and the levator neurons (I_l). For details see Results and Appendix.

between motor neurons do not occur in the locust circuits, we consider levator and depressor motor neurons to be followers, rather than fundamental components of the central pattern generating circuits. The connections shown between Lev and Dep in the model circuit are therefore not connections between pools of motor neurons, but between the central drives to these motor neurons.

In this model circuit, Drive makes excitatory synapses onto Lev and Dep, and Lev makes an inhibitory synapse onto Dep. The ability of this circuit to produce the different patterns of levator and depressor activity depends on the relative strengths of the excitatory synapses, I_l and I_d. In particular, by simply modifying the strength of I_l, the output of the circuit can be changed from a prothoracic-like pattern, where the activity of Dep precedes Lev, to a metathoracic-like pattern, where the activity of Dep follows the activity of Lev. Intermediate mesothoracic-like patterns are obtained in the transition region between prothoracic and metathoracic patterns. The operation of the model circuit can be understood as follows: Drive receives a constant depolarizing input, which causes it to burst rhythmically (see previous description of burster

neuron). When Drive is active, it excites both Lev and Dep. If I_l is weaker than I_d, Dep reaches threshold sooner than Lev, and fires as long as it is being driven. Once Lev reaches threshold, it fires a burst of action potentials, inhibiting Dep. Since Lev is a bursting neuron, its burst of activity eventually ends. This first pattern, shown in Fig. 4 (PRO), is similar to the prothoracic rhythmic pattern described above (Figs. 1 and 2). Note that Fig. 4 shows the outputs of two different depressor neurons (a "fast" depressor Dep_f and a "slow" depressor Dep_s) with different thresholds. The activities of these neurons differ only in that Dep_s fires tonically in its resting state. Compare with the activities of the biological neurons D_f and D_s (Fig. 1, lower traces).

If, on the other hand, I_l is stronger than I_d, Lev reaches threshold sooner than Dep. Once Lev begins to spike, Dep is inhibited. Only when Lev stops firing is Dep released from inhibition sufficiently to fire a burst of action potentials. This pattern, shown in Fig. 4 (META), is similar to the metathoracic rhythmic pattern described above and shown in Figs. 1 and 2. In order for Dep to fire a burst of action potentials upon release from inhibition, it must receive sufficient excitatory input to drive it to threshold. This can be accomplished in this model circuit in either of two ways. (*i*) If Drive has a longer burst duration than Lev ($t > t_l$), Dep will continue to receive excitatory input from Drive once it is no longer being inhibited by Lev. This is a simple condition to achieve, since the burst durations of Drive and Lev can be controlled independently. If, however, the burst duration of Drive is set too long, Lev may be depolarized enough to generate another burst, leading to anomalous "double bursts" in the activity of Lev. (*ii*) In the simulation, the excitation to Dep was prolonged by making the time constant of decay of the excitatory current I_d very long. As a consequence, Dep is being depolarized by a persistent excitatory current for a certain time τ_d after the Drive burst terminates. The mathematical analysis shown in Appendix A is general enough to allow one or both of the conditions to hold.

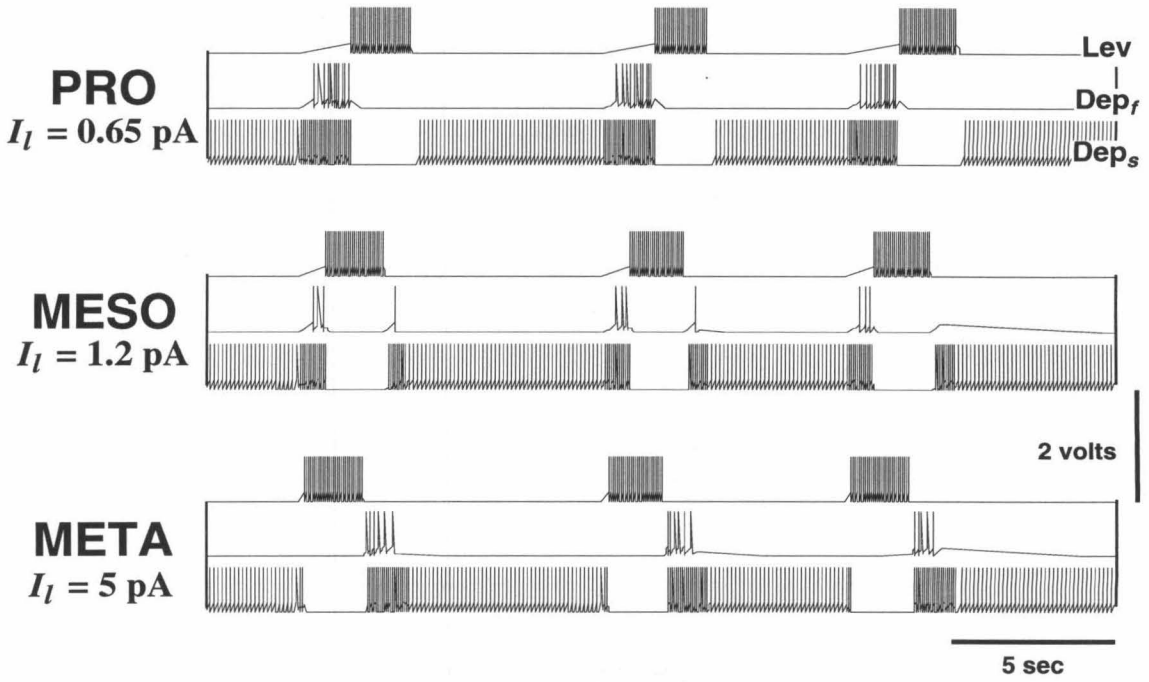

Figure 4. Results of the simulation of the model circuit shown in Fig. 3B using NeuraLOG/Spike. Shown are levator (Lev) and depressor (Dep) activities for three different values of I_l, the synaptic strength of the excitatory synapse from Drive to Lev (Fig. 3B). In this simulation, two different Dep neurons were simulated, one fast (Dep_f) and one slow (Dep_s). In the three sets of traces, the top trace is the output from Lev, the middle trace is the output from Dep_f, and the bottom trace is the output from Dep_s. Compare with Fig. 1 (Scale bars: 5 secs, 2 volts).

For intermediate values of the synaptic strength I_l, Dep fires a burst of action potentials both before and after a burst of activity in Lev. This output is therefore similar to the mesothoracic rhythmic pattern (Figs. 1, 2, and 4).

Spike frequency histograms of the simulation output are shown in Fig. 5. This figure should be compared with Fig. 2, which shows the spike frequency histograms of electrophysiological data from locust thoracic ganglia. One difference between the figures is the shape of the levator spike frequency histogram. This histogram is bell-shaped in Fig. 2, whereas it is square in Fig. 5. This difference is mainly due to the different numbers of neurons whose activity is represented in the histograms. In Fig. 2, data was obtaining by pooling all of the trochanteral levator action potentials on nerve 4A, which included up to 10 motor neurons with different thresholds. As can be seen from Fig. 1, a trochanteral levator burst consists of action potentials from many different motor neurons, with the largest number of neurons participating near the middle of a burst. In contrast, the simulation in Fig. 5 only included a single levator neuron (Lev). A similar bell-shaped distribution would be obtained by pooling the activities of many levator motor neurons driven by Lev, but with different thresholds.

In Fig. 2, substantial overlap between activities of the levators and depressors of the trochanter can be seen, particularly for the pro- and mesothoracic patterns. This overlap is much smaller in the simulation histograms in Fig. 5. Such overlap can be obtained in the simulation by weakening the inhibition between the levators and depressors, which would allow some co-activity between the antagonists (Fig. 3B).

VLSI implementation

We designed, fabricated, and tested a VLSI implementation of the simulated model circuit described above (see Methods). Fig. 6A shows a picture of the entire VLSI

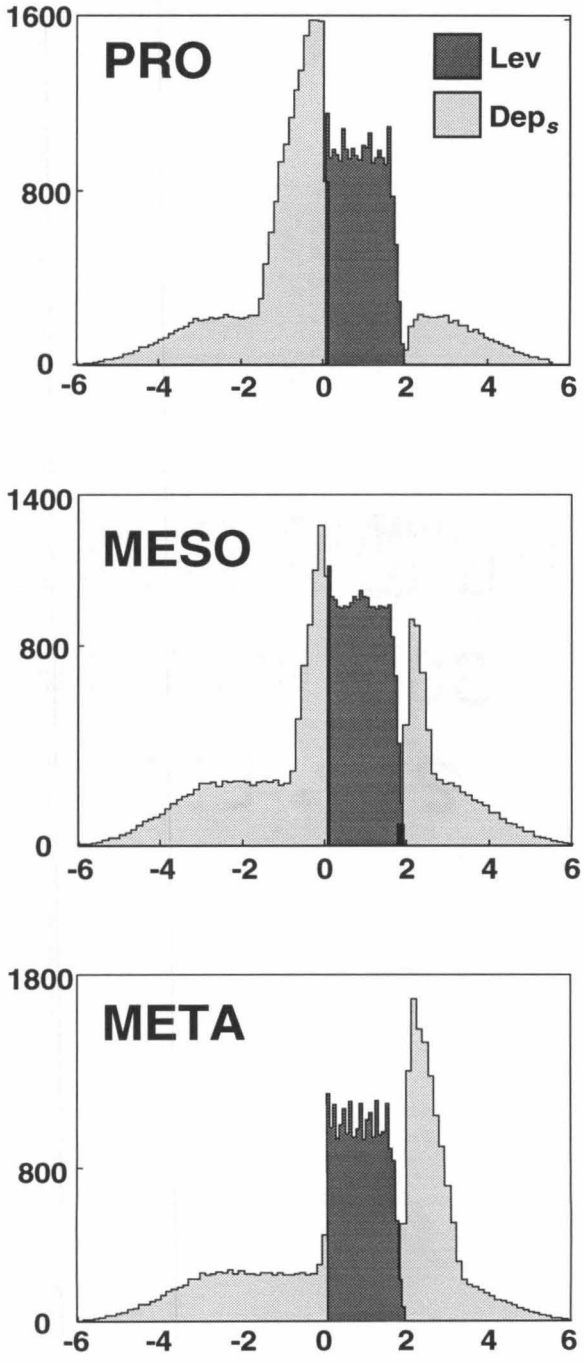
1600
PRO
Lev
Dep$_s$
800
0
-6
-4
-2
0
2
4
6
1400
MESO
800
0
-6
-4
-2
0
2
4
6
1800
META
800
0
-6
-4
-2
0
2
4
6

Figure 5

Figure 5. Spike frequency histograms of the simulated trochanteral levator and depressor neuron activities shown in Fig. 4. Data compiled from 238 periods of activity from single continuous output traces. The reference is the onset of a burst of trochanteral levator action potentials. The scale on the ordinate is the total number of action potentials in each bin, and represents a cumulative total for all 238 periods of activity that were analyzed. Compare with Fig. 2.

chip layout, and Fig. 6B, one of the depressor neuron layout. The electronic circuit implemented on the chip was essentially the same as the simulated circuit, since, as described in Methods, the circuit primitives used in the simulator were developed on the basis of existing electronic circuits. The different parameters in the model were represented as voltages which could be externally controlled. The synaptic strength I_l (Fig. 3B) was represented as a single voltage parameter. Fig. 7 shows voltage outputs of the chip operating at different frequencies. Fig. 7A, for example, shows the output from the levator and depressor drives for three different values of I_l. As was shown in the simulation (Figs. 4 and 5), as I_l is increased, the output of the circuit moves smoothly from a prothoracic (top) to a mesothoracic (middle), and finally to a metathoracic (bottom) rhythmic pattern. All other circuit parameters were unchanged. Figs. 7B and 7C show the same behavior as Fig. 7A, but at different time scales. In each case, the circuit parameters were adjusted for operation of the circuit at a given time scale, but only I_l was then modified to generate the pro-, meso-, and metathoracic rhythmic patterns. We verified that the chip can operate in a stable manner in the frequency range of 0.1 to 100Hz.

The circuit was most stable (i.e., the operating range of circuit parameters was widest) at higher frequencies of operations. In an attempt to quantify the decreased circuit stability at lower frequencies of operation, we studied the operating range of a single parameter (I_l) for different time scales of circuit operation (Fig. 8). We

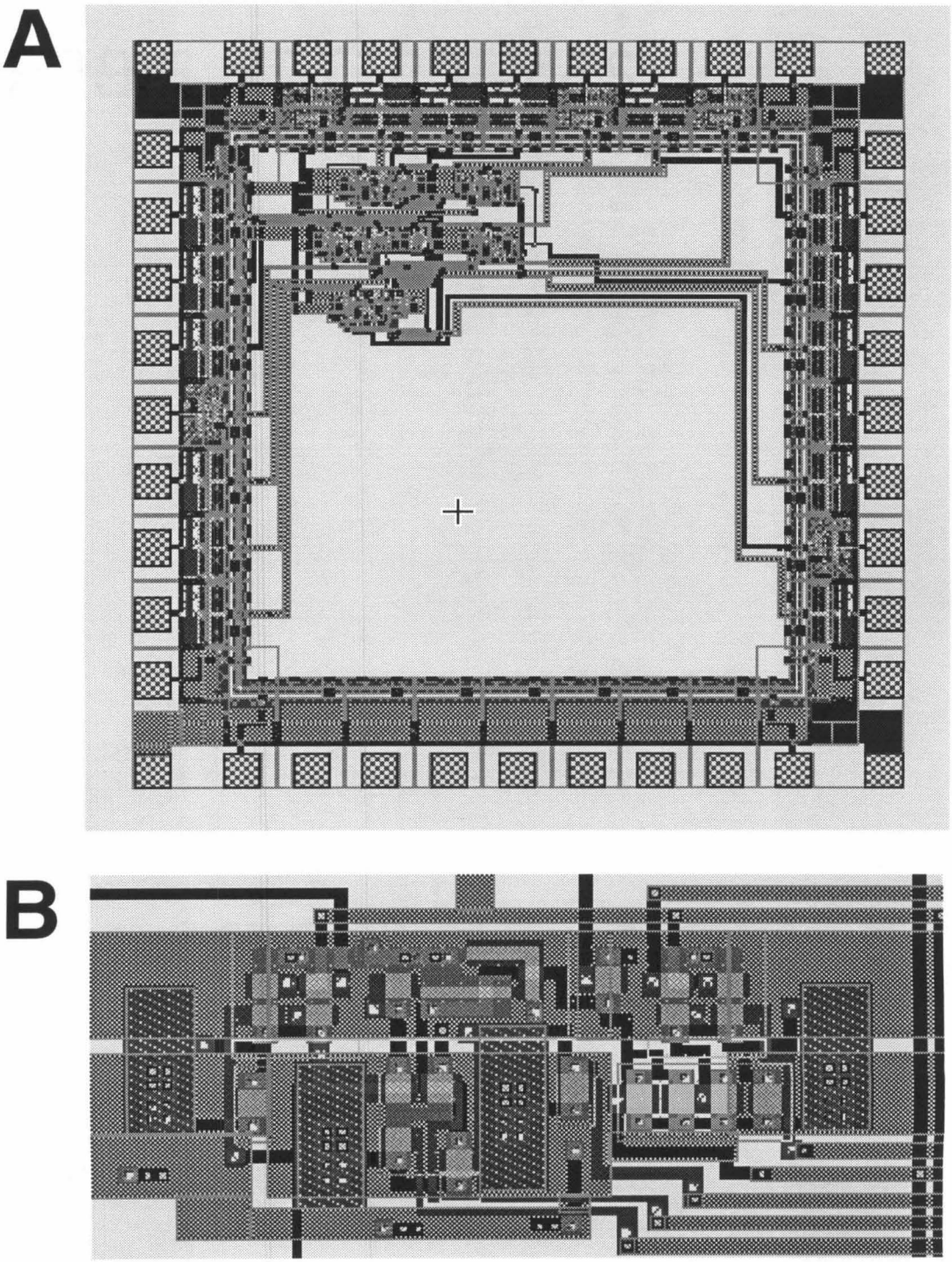

Figure 6

Figure 6. A VLSI implementation of the model circuit shown in Fig. 3. **A.** Graphical design of the entire chip, measuring 2 × 2mm. The model circuit is in the upper left corner of the chip. **B.** Expanded view of a single non-bursting neuron circuit.

chose the synaptic current I_l, since it is this parameter that determines the output of the circuit model. For each frequency of circuit operation, we measured the amount by which I_l needed to be changed to switch from a prothoracic to a metathoracic pattern (defined to be the "range" of I_l). On the chip, I_l is determined by externally setting the voltage on the gate of a single transistor. Since the synaptic currents in the chip could not be measured, I_l was estimated from the gate voltage and was normalized. The range of I_l was determined for five different frequencies of circuit operation (Fig. 8). As can be seen in Fig. 8, the range of I_l decreased monotonically as the cycle period increased. This is because slow operation of the circuit is achieved by reducing all currents in the electronic circuitry. Therefore, excursions in circuit parameters needed to switch between two states are correspondingly smaller. Since all of the currents in the circuit are smaller at lower frequencies, we would expect the operating ranges of all of the different circuit parameters to decrease in a similar way. This decrease in operating range of the parameters is closely related to the increased instability of the circuit at lower frequencies. When currents are very small, instabilities due to noise and device imperfections have a greater effect on circuit operation.

Mathematical analysis

We developed a simple theoretical analysis of the circuit model shown in Fig. 3B and described above. The mathematical details can be found in Appendix A. We computed expressions which describe the behavior of the circuit as I_l is varied. These

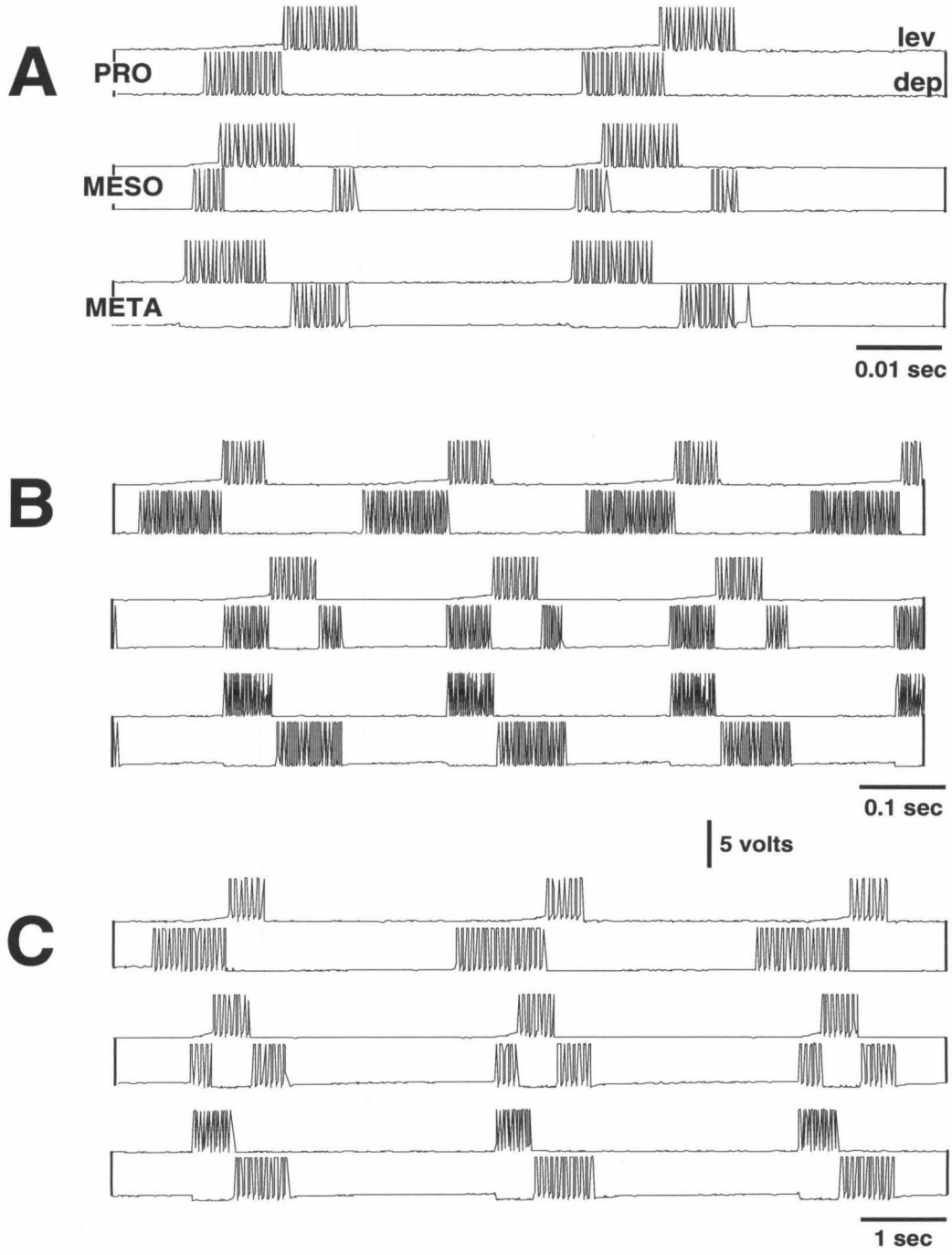

Figure 7

Figure 7. Output of the VLSI circuit. **A.** Output of electronic levator and depressor neurons for 3 different settings of the synaptic strength I_l (see Fig. 3). This synaptic strength is modified by changing the gate voltage on a single transistor. In the three sets of traces, top trace is output from a "levator" neuron and bottom trace is output from a "fast depressor" neuron. Compare with Figs. 1 and 4. **B–C.** Same figure as in **A**, except that the chip is operating at different time scales (note scale bars in **A**, **B**, and **C**). The circuit can operate over 4 orders of magnitude of frequency.

expressions express the widths of the bursts of activity of depressor drives before and after a levator burst as functions of I_l (Fig. 9A). In Fig. 9A, we can see that the width of the depressor burst which precedes a levator burst (w_1) decreases as I_l increases, and the width of the depressor burst which follows a levator burst (w_2) increases as I_l increases. Different regions of the graph (shaded area, delimited by asymptotes) correspond to the production of pro-, meso-, and metathoracic rhythmic patterns. For small values of I_l, $w_2 = 0$ and the depressor activity precedes the levator activity. This corresponds to the prothoracic rhythm. For intermediate values of I_l, both w_1 and w_2 are greater than zero, and the depressor activity both precedes and follows a levator burst. This corresponds to the mesothoracic rhythm. For large values of I_l, $w_1 = 0$ and the depressor activity follows the levator activity. This corresponds to the metathoracic rhythm. In Fig. 9B, we show measured values of w_1 and w_2 from the output of the integrated circuit as I_l is varied. The solid lines are fits of the forms given by the theoretical expressions for w_1 and w_2 (see Appendix A). Note that since I_l is controlled by a voltage, exact values of the current I_l could not be determined. The abscissa therefore represents a normalized current.

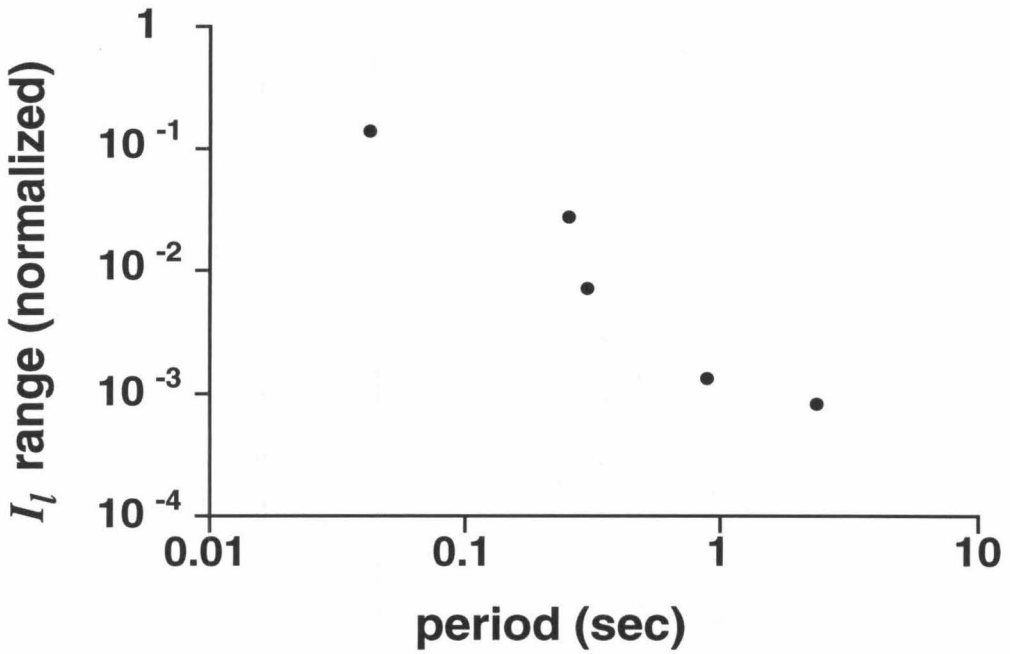

Figure 8. Range of the synaptic current I_l as a function of the period. The range of I_l is defined as the difference in synaptic current required to switch the circuit from a "prothoracic" rhythm to a "metathoracic" rhythm ($I_{l(meta)} - I_{l(pro)}$). Since the synaptic currents in the chip could not be measured, values of the currents were estimated from voltage measurements and normalized. The range was determined for five different time scales, represented on the abscissa as the period. Note that both the current range and the period are plotted on log scales. That the circuit is more stable at higher frequencies of operation (smaller periods) can be attributed to the larger ranges over which parameters can be modified at these frequencies.

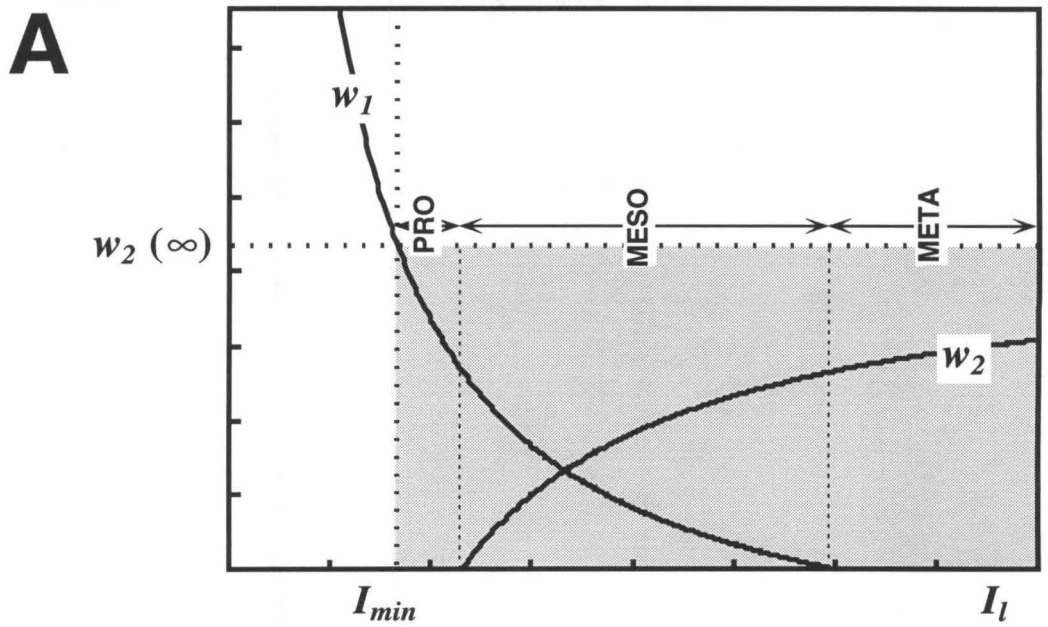

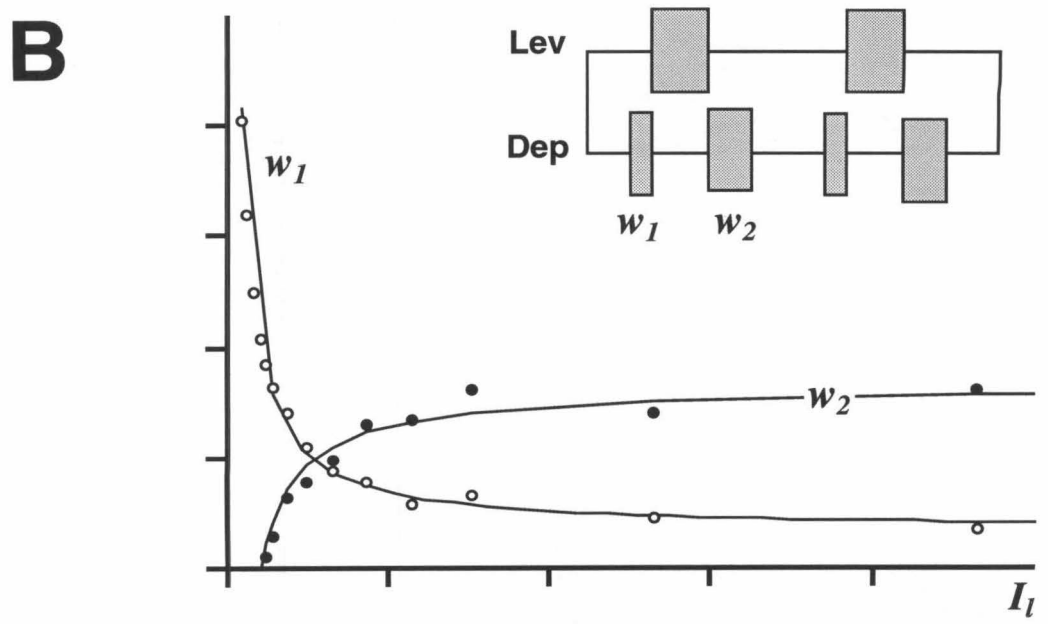

Figure 9

Figure 9. Comparison of chip performance and theoretical analysis. **A.** Graph of theoretical expressions for w_1 and w_2 (see Appendix and inset in Fig. 9B) as a function of the magnitude of I_l, the excitatory current from Drive to the levator motor pool driver (Fig. 3). Solutions lie within the shaded rectangle delimited by the asymptote $w_2(\infty)$ and the constraint I_{min}. See Results and Appendix for details. **B.** Measured values of w_1 and w_2 from integrated circuit output, as a function of the current I_l. Solid lines are fits of the form given by the theoretical expressions derived in the Appendix and plotted in **A**. Because I_l was modified by changing a voltage on the integrated circuit, exact current values could not be determined. The current on the abscissa is therefore a normalized current.

3.5 Discussion

We have shown that pilocarpine induces rhythmic activity in leg motor neurons of isolated locust pro-, meso-, and metathoracic ganglia. The patterns recorded in the three ganglia differed in their sensitivities to pilocarpine, their frequencies, and the phase relationships of motor neuron antagonists. The different patterns we observed could be generated by a simple adaptable model circuit, which was both simulated and implemented in VLSI hardware.

Locomotor rhythm generation in thoracic segments

Given that locomotor rhythms could be induced by pilocarpine in the isolated locust metathoracic ganglion (Ryckebusch and Laurent, 1993), it is perhaps not surprising that such rhythms could also be recorded in isolated pro- and mesothoracic ganglia. This result supports the idea that there exist distinct pattern generating circuits for leg movements in each thoracic ganglion or hemiganglion. This is in contrast to other insect central pattern generators (CPGs), such as those underlying flight and ventilation. The flight central pattern generator, which controls two sets of wings in

the locust, is known to be distributed in both the meso- and the metathoracic ganglia (Robertson and Pearson, 1983; 1985; Robertson, 1986). It has been established that ventilatory rhythms are produced by a dominant central pattern generator in the metathoracic ganglion; indeed, respiratory rhythms recorded in the pro- and mesothoracic ganglia cease when the connectives to the metathoracic ganglion are sectioned (Farley et al., 1967; Miller, 1960, 1966, 1967).

Perhaps more surprising is our finding that the phases and frequencies of the evoked rhythms differ in the three thoracic ganglia. These differences in rhythmic patterns may reflect the intrinsic physical differences between the three pairs of insect legs. The front legs are oriented toward the front of the body, whereas the hind legs are oriented toward the rear. This implies that the intrinsic locomotor rhythms for these legs must differ, as the sequence of levator and depressor activity (protraction and retraction) would be different during a step. Cruse (1976) has found that the three pairs of legs in stick insects have different functions during walking and the maintenance of posture. During horizontal walking, the foreleg has primarily a feeler function, while the middle leg has a supportive function and the hind leg has both supportive and propulsive functions. These roles can change, however, if the insect walks on a non-horizontal surface, which implies that individual segmental oscillators, already tuned in a segment-specific manner, in addition must have the capability of adapting their output in response to the changing functional role of the limb which they move.

Differences in intrinsic frequencies of the segmental rhythms might also be related to the morphological differences of the limbs. It has been observed in behavioral experiments that, during tethered walking, the insect hind leg can exhibit either 1:1 or 1:2 coupling with the front and middle legs (N. Hatsopoulos, personal communication; Graham 1978a,b); i.e., the front and middle legs occasionally make two steps for one step of the hind leg. Since the hind leg is longer than the front or middle legs,

it compensates for a missed step by making a larger amplitude step at the next cycle. That the step frequencies of the hind leg are lower than those of the front and middle legs in walking animals is consistent with the finding that locomotor patterns recorded from isolated metathoracic ganglia are slower than those produced by the pro- and mesothoracic ganglia. Several models of insect walking have in fact proposed a anterior-posterior gradient of frequencies for the thoracic segments, with the hind segment having the lowest intrinsic frequency (Wilson, 1966; Graham, 1977; reviewed in Graham, 1985). Such a frequency gradient appears to be necessary to produce appropriate phase lags and coupling between the legs, and can also explain the occasional absences of rear leg protractions. It will be interesting to study the patterns of activity of the other motor neuron pools such as the tibial and tarsal motor neurons and compare them to the corresponding metathoracic patterns (Ryckebusch and Laurent, 1993). We already established, however, that the phase relationships between trochanteral antagonists are tuned in a segment-specific manner.

Adaptable neural circuits

Our basic assumption in designing a model pattern generating circuit was that the locomotor circuits in segmentally homologous thoracic ganglia were likely to be very similar, despite the different rhythmic output patterns they generated. In the model we devised, the output pattern could be switched between those characteristic of the pro-, meso-, and metathoracic ganglia by modifying a single synaptic coupling parameter in the circuit. There are now numerous examples of biological pattern generating circuits which can produce several rhythmic patterns: the pyloric and gastric mill rhythms in the stomatogastric system of crabs (Weimann et al., 1991); withdrawal and swimming in *Tritonia* (Getting and Dekin, 1985a); forward and backward scaphognathite beating in crabs (Simmers and Bush, 1983); jumping and kicking in

the locust (Gynther and Pearson, 1989), to name only a few. In some of these systems, the switch from one pattern to another is accomplished under the action of a neuromodulator which alters cellular and synaptic properties of the circuit elements. For example, the crustacean gastric mill motor pattern can be switched from "squeezing" to "cut-and-grind" mode under the action of the peptide proctolin (Heinzel and Selverston, 1988; Heinzel, 1988). Although in most systems the detailed mechanisms by which neuromodulators alter circuit properties are not known, the modification of a synaptic strength to alter circuit dynamics has been demonstrated in the crustacean stomatogastric nervous system, where application of the peptide proctolin potentiates the inhibitory synapse from the inferior cardiac (IC) neuron to the gastric mill (GM) neurons, causing the GM neurons to switch from a gastric to a pyloric pattern of activity (Weimann, 1992).

Although any biological pattern generator is likely to be far more complex than the simple model which we have designed, some of the mechanisms we propose could be imbedded in a larger neural circuit. Some simple central pattern generator circuits, such as that underlying feeding in the snail *Lymnaea stagnalis* (Benjamin and Elliott, 1989) have been shown to use mechanisms similar to those employed by our model circuit. The Slow Oscillator (SO) in *Lymnaea* plays a role much like that of Drive in our model circuit. SO initiates, maintains, and controls the frequency of the snail feeding pattern, provided it receives a constant depolarizing input. SO is the primary source of excitatory drive to a small network of interneurons forming the central pattern generator, which in turn provides the drive to a set of buccal motor neurons. The interneurons (N1, N2, and N3) which form the core of the central pattern generator produce rhythmic output as a result of their intrinsic properties (e.g., endogenous bursting, postinhibitory rebound, plateau potentials) as well as their synaptic connections. N1 and N2 form a network reminiscent of the design of our two-neuron "bursting" neuron, with slow excitation from N1 to N2 and delayed inhibition

from N2 to N1. N3 is first inhibited by N1, and then produces a postinhibitory burst of action potentials, which is similar to the Lev–Dep interaction in our model network.

Design of realistic walking robots

The VLSI implementation of the model circuit we designed operated robustly over 4 orders of magnitude of frequency, despite physical constraints such as noise and device imperfections. The chip exhibited the behavior predicted by theoretical calculations and computer simulations. Because a complete understanding of biological sensory-motor systems requires an understanding of the real-world context within which they operate, physical models of biological circuitry can be valuable tools for the neurobiologist. Designing physical devices such as sensory systems and mechanical actuators that interact with the real world need not be the exclusive domain of the engineer. Physical devices such as walking robots could provide biologists with a platform on which to test ideas about the design of biological circuitry. We will use such techniques, for example, to explore the intersegmental coupling between thoracic locomotor circuits, as well as the role of sensory information in shaping motor outputs. We believe that such an interdisciplinary approach will help to uncover the design principles of the biological circuit while, at the same time, allowing the design of more adaptable walking robots.

Appendix A: A mathematical description of the levator-depressor model

Variables

C: Capacitance of neurons

V_T: Neuron spike threshold

I_l: Magnitude of excitatory synaptic current from Drive to Lev

I_d: Magnitude of excitatory synaptic current from Drive to Dep

I_{ld}: Magnitude of inhibitory synaptic current from Lev to Dep

τ_d: Duration of synaptic current from Drive to Dep

w_1: Duration of Dep burst preceding Lev burst

w_2: Duration of Dep burst following Lev burst

t: Duration of Drive burst

t_l: Duration of Lev burst

Assumptions

1. The excitatory synapse from Drive to Dep is strong (I_d is large). We assume that $I_d \gg I_l$ for the pro- and mesothoracic solutions.

2. Inhibition of Dep by Lev is stronger than the excitatory drive to Dep ($|I_{ld}| > I_d$).

3. The synaptic current I_d persists for a time τ_d. All other synaptic currents decay quickly.

Derivations

Given the above assumptions, one can derive the following expressions for w_1 and w_2:

$$w_1 = \frac{CV_T}{I_l} - \frac{CV_T}{I_d} \tag{1}$$

$$w_2 = t + \tau_d - t_l - (\frac{CV_T}{I_l} - \frac{CV_T}{I_d}) \tag{2}$$

We can see from (2) that $w_2 > 0$ if t or τ_d are sufficiently large, as was described above (see Results). $t > t_l$ if the Drive burst is longer than the Lev burst. τ_d is large is the same as saying that the excitatory drive to Dep has a slow time constant of decay. One or both of these conditions need to be true to obtain a positive value for w_2.

Constraints

For this circuit to operate in the desired range, the current I_l must satisfy the following constraint, represented graphically in Fig. 9A by a vertical dashed line:

$$I_l > I_{min} = \frac{CV_T}{t} \tag{3}$$

This constraint expresses the requirement that the time needed for Lev to charge its membrane to threshold must be less than t, the duration of the Drive burst. If $I_l < I_{min}$, Lev will remain silent, and Dep will receive excitatory input from Drive but no inhibition.

Asymptotes:

$$w_2(\infty) = \lim_{I_l \to \infty} w_2 = t + \tau_d - t_l + \frac{CV_T}{I_d} \tag{4}$$

$$\lim_{I_l \to \infty} w_1 = -\frac{CV_T}{I_d} \tag{5}$$

Solutions of interest

1. Prothoracic solution ($w_2 = 0$)

   This solution will occur when

$$I_{min} < I_l < \frac{CV_T}{t - t_l + \tau_d} \tag{6}$$

   The solution only exists when $t_l > \tau_d$ (i.e., if the duration of a Lev burst is longer than the duration of the excitatory drive to Dep).

2. Mesothoracic solution ($w_1 > w_2$)

$$\frac{CV_T}{t - t_l + \tau_d} < I_l < \frac{2CV_T}{t - t_l + \tau_d} \tag{7}$$

3. Mesothoracic solution ($w_1 \leq w_2$)

$$\frac{2CV_T}{t - t_l + \tau_d} \leq I_l < I_d \tag{8}$$

4. Metathoracic solution ($w_1 = 0$)

   This solution will occur when $I_l \geq I_d$.

Appendix B: A bursting neuron using summating synapses

We describe here an alternative design for a bursting neuron using new features recently incorporated in the NeuraLOG/Spike simulator. In the earlier version of the simulator, synaptic events consisted of square pulses of "neurotransmitter" with a fixed amplitude and duration (see Methods). These events did not summate; i.e., if two presynaptic action potentials occurred in close succession, the amplitude of the "neurotransmitter" released at the synapse as a result was no greater than that caused by a single action potential. The only effect of a presynaptic train of action potentials was to prolong the duration of the presence of "neurotransmitter" in the "synaptic cleft." The design of a bursting neuron as a two-neuron circuit was a direct consequence of this limitation of the simulator. Indeed, to build a neuron capable of slow membrane potential oscillations, a mechanism is needed for storing the "history" of the activity of the neuron. In biological neurons, this can be accomplished by the accumulation of intracellular calcium caused by the generation of action potentials. The intracellular calcium concentration is a representation of the time integral of the spiking history of the neuron. In the bursting neuron circuit described above (see Fig. 3A and Results), Cell 2 was used to store information about the activity of Cell 1. Repeated action potentials from Cell 1 led to the gradual depolarization of Cell 2.

A new feature of NeuraLOG/Spike allows the "neurotransmitter" at a "synaptic cleft" to summate. If a second action potential occurs before the end of the pulse of "neurotransmitter" due to the first action potential, the net amount of "neurotransmitter" during that time will be twice as large. In addition to the magnitude and duration of a synaptic event, the number of pulses which can be summated (i.e., the

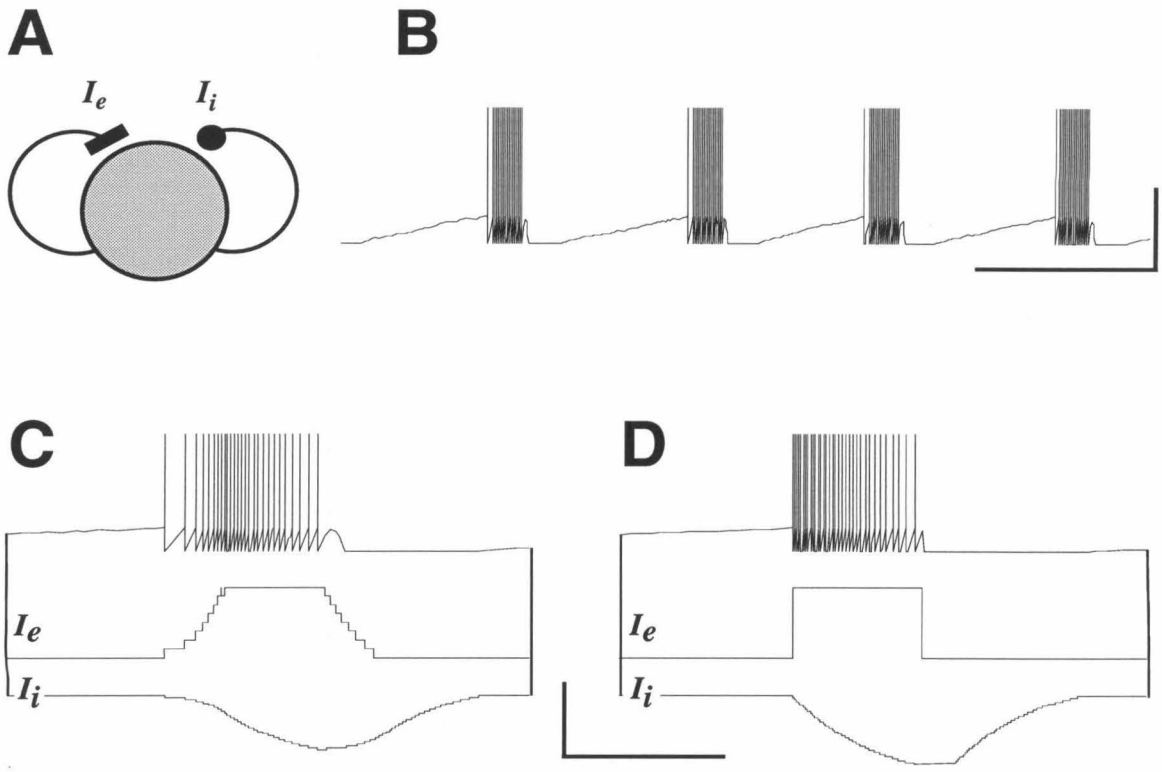

Figure 10. An alternative model for the bursting neuron. **A.** Using an improved synapse model (see Appendix B), a bursting neuron can be represented by a single neuron with excitatory and inhibitory feedback conductances. **B.** Output of the bursting neuron in response to a constant excitatory input, simulated using NeuraLOG/Spike (Scale bars: 1 volt, 10 sec). **C–D.** Expanded view of a single burst (top trace), excitatory (middle), and inhibitory (bottom) feedback currents for different characteristics of the excitatory feedback current I_e, as described in Appendix B (Scale bars: 1 volt, 2 sec). Note that, here, different firing patterns *within* a burst can be achieved by changing the properties of the excitatory feedback I_e.

maximum amount of neurotransmitter in the synaptic cleft) can now also be specified as parameters in the simulator. This new feature allows a bursting neuron to be implemented by a single "neuron" circuit (Fig. 10A) with excitatory and inhibitory feedback conductances. When the neuron has reached threshold in response to an excitatory current input, it will begin to fire action potentials at a rate determined by the characteristics of the excitatory feedback in much the same way as the previous bursting neuron circuit (Fig. 3A). While the neuron is firing, a slow feedback inhibition builds up. The summating property of the synapse allows the inhibition to slowly increase during the course of the burst. As the cumulative inhibition increases, the frequency of action potentials decreases until the neuron eventually stops firing (Fig. 10B). The firing frequency of the neuron during a burst thus depends on the interaction between the excitatory and inhibitory feedback. Figs. 10C and D show how the characteristics of a burst can be modified by changing the excitatory feedback conductance. If this excitatory feedback is small and slowly increasing, the firing frequency of the neuron will increase during the burst, reach a peak, and then decrease again (Fig. 10C). If, on the other hand, this excitatory feedback very quickly reaches its maximum amplitude, the firing frequency of the neuron will be highest at the beginning of a burst, and will slowly decrease during the course of a burst (Fig. 10D). Although the ability of NeuraLOG/Spike to simulate summating synapses makes it possible to simulate much more sophisticated circuits, this new feature will currently not be useful to the VLSI chip designer who uses NeuraLOG/Spike to develop hardware models, since there does not yet exist a VLSI circuit implementation of the summating synapse.

Chapter 4

Coordination of Segmental Leg Central Pattern Generators

4.1 Summary and conclusions

1. Rhythmic activity of leg motor neurons could be evoked in isolated locust thoracic ganglia as well as in preparations of 2 or 3 connected thoracic ganglia superfused with the muscarinic agonist pilocarpine. Rhythms were always more regular and reliably elicited in single isolated ganglia. When the ganglia were connected, rhythmic activity of leg motor neurons was not usually simultaneously evoked in all 6 hemiganglia. Typically, some of the hemiganglia were rhythmically active, while others showed tonic or highly irregular activity.

2. Action potentials from leg motor neuron pools were recorded extracellularly from motor nerves and cross-correlated using standard algorithms. The following correlations were observed between activities of motor neurons in different hemisegments:

   (a) Within a segment, trochanteral levators were coactive with contralateral

trochanteral depressors. This correlation was strong in the metathoracic ganglion, and weaker in the pro- and mesothoracic ganglia.

(b) Coupling between levators on opposite sides of the same segment was variable in the pro- and mesothoracic ganglia, as phase relationships between levators were different in each preparation and could also change during the course of an experiment. In the metathoracic ganglion, levators on opposite sides were never coactive.

(c) Trochanteral levators were often active within a short latency of levator bursts in an ipsilateral adjacent hemiganglion. This correlation appeared to be weak, as it was not observed in all preparations. In addition, levators in one segment often seemed to be inhibited during levators bursts in the ipsilateral adjacent segment.

(d) Trochanteral levators were strongly coupled to ipsilateral adjacent trochanteral depressors, for all three thoracic ganglia.

3. The phase relationships between motor neuron activities revealed by cross-correlation is discussed in the context of what is known about the mechanisms underlying intersegmental coupling during legged locomotion.

4.2 Introduction

The need to coordinate different body parts during locomotion is common to many species, invertebrates and vertebrates alike. Although it is generally accepted that neural circuits (central pattern generators) exist that can produce the basic motor patterns underlying movement of individual limbs or body segments in the absence of sensory inputs (review: Delcomyn 1980), little is known about how pattern generators in different body segments are coordinated during locomotion. The mechanisms

underlying intersegmental coordination during locomotion are best understood in the context of locomotion in an aqueous environment (swimming) in both vertebrates (Roberts et al. 1986; Grillner et al. 1991) and invertebrates (crayfish: Stein 1971; Paul and Mulloney 1986; leech: Friesen 1989). In these systems, the central pattern generator is comprised of a chain of segmentally repeated pattern generators, each of which independently produces a rhythmic output appropriate for the movement of a single appendage or body segment. The coordination between body segments in nervous systems deprived of sensory feedback is similar to that observed in the intact animal, which indicates that intersegmental coordination can be achieved by central mechanisms alone (crayfish: Ikeda and Wiersma 1964; leech: Kristan and Calabrese 1976; Pearce and Friesen 1985; fish: Grillner et al. 1976; lamprey: Poon 1980; Wallén and Williams 1984; toad: Kahn and Roberts 1982). Although the neuronal basis of the intersegmental coordination is not completely understood in any of these systems, models have been proposed that can account for the coordination in terms of known circuit components such as intersegmental neurons and their connections (lamprey: Matsushima and Grillner 1992; leech: Friesen 1989).

Evidence for central control of intersegmental coordination in terrestrial walking is more scarce (reviews: arthropods: Cruse 1990; Graham 1985; vertebrates: Grillner 1981; Rossignol et al. 1993). Although segments of the nervous system can produce motor patterns appropriate for the movement of a single limb in the absence of sensory inputs (insects: Pearson and Iles 1970; Bässler and Wegner 1983; Ryckebusch and Laurent 1993; crayfish: Sillar and Skorupski 1986; cat: Grillner and Zangger 1979; chick: Jacobson and Hollyday 1982), coordination between individual limb pattern generators is often weak (Grillner and Zangger 1979) or behaviorally inappropriate (Sillar and Skorupski 1986; Sillar et al. 1987; Bässler and Wegner 1983). The most thorough studies of intersegmental coordination in an insect have been carried out in stick insects (review: Cruse 1990), but the relative influences of central and sensory

mechanisms have not been investigated.

In locusts, we have recently developed a preparation in which sustained rhythmic activity appropriate for leg movement during walking can be evoked in motor neurons of isolated thoracic ganglia (Ryckebusch and Laurent 1993). This preparation now makes it possible to study the central mechanisms underlying intersegmental coordination of the legs in an isolated insect nervous system. Here we show evidence for central coordination of leg motor patterns in isolated locust thoracic nerve cords. Understanding the relative contributions of central and sensory mechanisms in generating appropriately coordinated leg movements should help us to gain insights not only about the nature of terrestrial walking, but about how the nervous system integrates information from different sources to produce well-adapted behavior.

4.3 Methods

Electrophysiology

Experiments were performed on adult locusts *Schistocerca americana* of either sex, from our crowded laboratory colony. The results presented here were gathered from 44 insects.

The preparation. Experiments were performed on an *in vitro* thoracic preparation described previously (Ryckebusch and Laurent 1993). Briefly, sections of the thoracic nerve cord consisting of 2 or 3 thoracic ganglia were removed from the thorax of the animal with the surrounding tracheal supply and air sacs undisturbed, and were pinned down in a chamber lined with Sylgard 184 (Dow Corning Co., Midland, MI). Leg motor nerves were carefully stripped of their surrounding connective tissue with a small hooked pin. The preparation was superfused with locust saline (mM: NaCl: 140; KCl: 5; $CaCl_2$: 5; $NaHCO_3$: 4; $MgCl_2$: 1; *N*-2-hydroxyethylpiperazine-*N'*-2-

ethanesulfonic acid: 6.3; pH 7.0) supplemented with 2.5% (wt/vol) sucrose. Air was supplied to the ganglia by teasing open the tracheae at the surface of the saline. A stock solution of 10^{-2}M pilocarpine hydrochloride (Sigma) was prepared in advance, and was added to the saline to final bath concentrations of 10^{-5} to 10^{-4}M. The preparation remained healthy for at least 4 or 5 hours at 20 to 26°C.

Recordings. The electrical activity of leg motor nerves was monitored extracellularly using polyethylene suction electrodes. In all thoracic ganglia, recordings from trochanteral levator motor neurons were made from nerves 4A, and recordings from trochanteral depressor motor neurons were made from nerves 5A. Data were recorded on an eight-channel Digital Audio Tape recorder sampling at 5 kHz (Sony/Biologic), and were displayed on a Gould TA4000 chart recorder.

Anatomy and nomenclature. The muscles are numbered according to Snodgrass (1929), except where a variant is now more commonly used in the literature. The nerves are numbered according to Bräunig (1982). Motor neurons are designated by commonly used abbreviations or by the name of the muscle group that they innervate. Detailed descriptions of the innervation of the leg musculature can be found in Campbell (1961), Bräunig (1982), and Siegler and Pousman (1990).

Data analysis

For each extracellular recording, all of the action potentials that could be resolved were used in the analysis. These recordings usually contained action potentials of several motor neurons from the same pool. Recordings of nerve 4A contained action potentials from up to 10 trochanteral levator motor neurons, and recordings of nerve 5A contained action potentials from 2 trochanteral depressor motor neurons (D_s and D_f) and a common inhibitory motor neuron (CI).

Electrophysiological recordings were analyzed off-line after digitization at 5 kHz

with a National Instruments NBMIO16L AD/DA interface. The times of occurrence of action potentials were determined from the digitized extracellular recordings using Spike Studio (Eli Meir, University of Washington), and software written by Wyeth Bair (California Institute of Technology) was used to compute cross-correlations between spike trains.

Cross-correlations were computed using standard algorithms (Perkel et al. 1967; Glaser and Ruchkin 1976) with a bin width of 10 msec and were normalized by the expected value of the cross-correlation at 0 time lag under the assumption that the spike trains were independent Poisson processes. This normalization was based upon the observed mean firing rates of the two spike trains and their common duration (e.g., if the two spike trains were random and uncorrelated, their cross-correlation at 0 time lag would be equal to 1 after normalization). The resultant cross-correlation histograms were smoothed by convolving them with a Gaussian of unit area and a standard deviation of 100 msec. Since periods of rhythmic activity were always much greater than 100 msec, this smoothing preserved all fluctuations in the cross-correlograms relevant to the present analysis.

Cross-correlation of neuronal spike trains

The data analysis methods we used in previous studies of the rhythmic patterns recorded in single isolated thoracic ganglia relied on our ability to unambiguously identify "bursts" of activity in different sets of motor neurons. The rhythmic patterns were then characterized by comparing the onsets and durations of bursts of activity in different pools of motor neurons (Ryckebusch and Laurent 1993). Because of the irregularity of the activity patterns recorded in chains of 2 or 3 thoracic ganglia, these methods were not appropriate for the analysis of the present experiments. It was often difficult to define a "burst" of activity in a pool of motor neurons because

the activity in each pool was irregular, ranging from low-frequency tonic firing of a few motor neurons to high-frequency bursts of action potentials from many motor neurons. A cross-correlation analysis of neuronal spike trains was judged to be more appropriate for these data, since such an analysis could be performed objectively on all of the activity patterns we recorded, irrespective of whether they could be characterized as "rhythmic."

To verify that cross-correlation histograms (cross-correlograms) were consistent with and comparable to latency histograms, we applied both techniques to a set of extracellular recordings obtained from isolated metathoracic ganglia (Fig. 1). In Fig. 1, three pairs of neuronal spike trains were analyzed using both techniques. Shown in Fig. 1A is the spike-latency histogram for the right trochanteral depressor D_s relative to the onsets of bursts of action potentials in right trochanteral levators, which were used as a reference for the rhythmic activity. As reported previously (Ryckebusch and Laurent 1993), the activity of the metathoracic depressor D_s was inhibited during a trochanteral levator burst, and was greatest immediately following the levator burst. The average duration of levator bursts in this case was approximately 1 second. Fig. 1B shows the cross-correlogram of the same two spike trains used in Fig. 1A. Note that the general shapes of the two histograms are similar, but that the histogram of Fig. 1A is shifted to the right compared to the one in Fig. 1B. This is due to the fact that in Fig. 1A we compared each spike onset time to a burst onset time, whereas in Fig. 1B we compared the onset times of two spikes (bin width: 10 msec). The histogram in Fig. 1A is therefore shifted to the right by an amount that depends on the exact structure of the burst of action potentials in the motor pool used as a reference. The magnitude of this shift is comparable to the duration of a burst in the reference motor pool. Although spike-latency and cross-correlograms are not related by a simple translation, for cases in which the reference bursts are short compared to the period, the two histograms have very similar shapes, as shown in

Fig. 1. Figs. 1C and D compare the activities of metathoracic trochanteral depressors on the right and levators on the left, and Figs. 1E and F compare the activities of metathoracic trochanteral levators on the left and right.

Cross-correlations of two highly structured neuronal spike trains are nonetheless difficult to interpret. Standard statistical tests generally cannot be devised, since the sampling distributions of the spike trains are unknown. Even in the absence of a rigorous statistical test, the cross-correlation technique provides powerful information about temporal relationships between neuronal spike trains. As can be seen from the examples shown in Fig. 1, cross-correlograms of spike trains that have been shown by other methods to be interdependent exhibit large peaks and troughs. The following procedure was used to evaluate the significance of modulations in the cross-correlograms:

Only salient features in the cross-correlograms that occurred near 0 time lag (time lag much less than 50% of the estimated cycle period) were examined. The cross-correlogram of two highly structured spike trains usually exhibits many peaks and troughs, particularly if the spike trains are from pacemaker neurons with similar oscillation frequencies (see discussion of Figs. 2 and 3 below and Perkel et al. 1967). These modulations generally occur at all time lags, and their size relative to significant peaks depends on the amount of noise in the signals and the sample sizes. The cross-correlograms we obtained could be separated into two broad categories: *(1).* Histograms in which there were no large peaks or troughs near 0 time lag. Although these histograms were often highly structured with many peaks and troughs, the fluctuations were distributed uniformly at all time lags. We never saw a histogram with an isolated peak or trough at a time lag greater than 50% of the average period. These histograms were assumed to show no significant correlations between the spike trains. *(2).* Histograms with a peak or a trough near 0 time lag that was larger than all other peaks. The correlation or anticorrelation was then confirmed

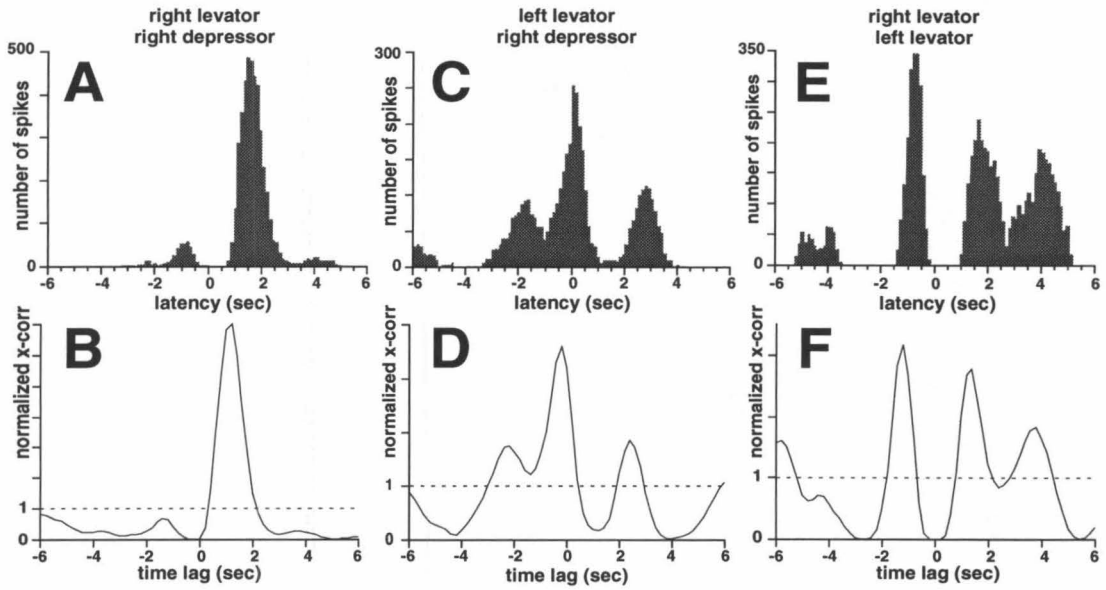

Figure 1. Comparison of spike-latency histograms and cross-correlation histograms. Data were obtained from simultaneous recordings from nerves R5A (right trochanteral depressors, CI), $L3B_2$ (left trochanteral levators) and $R3B_2$ (right trochanteral levators) of an isolated metathoracic ganglion in 5×10^{-5}M pilocarpine. In all spike-latency histograms (**A**, **C**, **E**), spike latencies were computed from the onset of a burst in metathoracic trochanteral levators. In all cross-correlograms (**B**, **D**, **F**), time lags were relative to action potentials from the metathoracic trochanteral levators used as a reference in the corresponding spike-latency histogram. The cross-correlations were normalized as described in Methods. **A-B**. Metathoracic right depressor D_s (4764 spikes) relative to metathoracic right levators (53 cycles; 9049 spikes). **C-D**. Metathoracic right depressor D_s (4764 spikes) relative to metathoracic left levators (46 cycles; 6898 spikes). **E-F**. Metathoracic left levators (46 cycles; 6898 spikes) relative to metathoracic right levators (53 cycles; 9049 spikes). Note that whereas the general shapes of the spike-latency and cross-correlograms are similar, the spike-latency histograms are slightly shifted to the right (discussed in Methods).

by visual inspection of the extracellular recordings of spike trains from which the data were obtained. Large single peaks at 0 time lag in cross-correlograms always corresponded to visibly synchronized activity of the extracellular spike trains. For example, Fig. 2A shows synchronized activity of the mesothoracic depressor D_s and prothoracic levators. For every burst of activity of prothoracic levators (middle trace, asterisks), there is a corresponding increase in the spike frequency of mesothoracic D_s (top trace). The cross-correlogram of these two spike trains is shown in Fig. 2B. Note that this histogram shows a peak at 0 time lag that is larger than any other peaks in the histogram. Fig. 2C shows the cross-correlogram of the activity of the prothoracic depressor D_s (bottom trace) relative to the prothoracic levators. In this histogram we can see a large trough at 0 time lag, which corresponds to an interruption of the tonic activity of prothoracic D_s during a prothoracic levator burst (Fig. 2A, middle and bottom traces). The smaller peaks preceding and following the inhibition are less apparent in Fig. 2A, since this is only a small portion of the 250-second recording used to compute the cross-correlogram. (The cross-correlation thus illustrates the general trend in relationships between spike trains and corresponds well to the general impression one receives from visually inspecting large amounts of data, even though this trend may not be apparent in any small subset of data.) Although these criteria were subjective, they were chosen conservatively; accordingly, it is likely that subtle relationships in our data were left undetected.

4.4 Results

Rhythmic activity in isolated thoracic ganglia

Rhythmic activity in leg motor neurons of thoracic ganglia that are completely isolated from each other and from their normal peripheral inputs can be elicited when

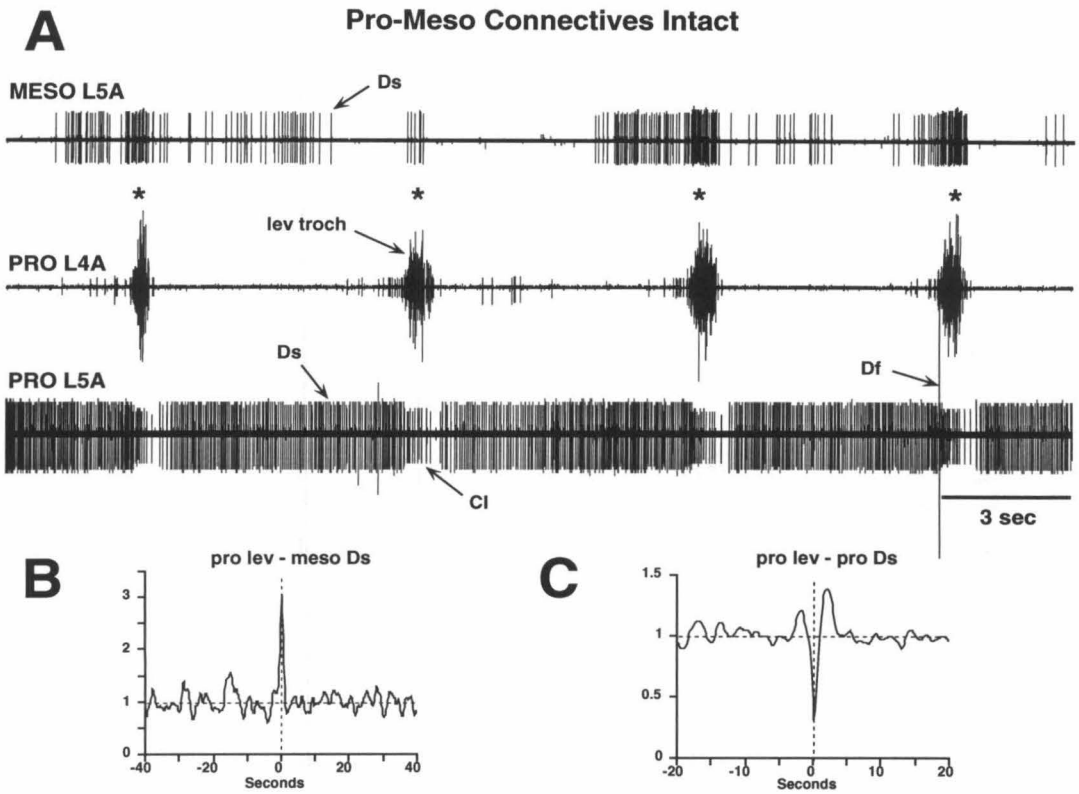

Figure 2. Correlated motor neuron activity in a semi-isolated thoracic nerve cord (pro-, meso-, and metathoracic ganglia). **A**. Extracellular recordings are from mesothoracic nerve L5A (trochanteral depressors, CI), prothoracic nerve L4A (trochanteral levators), and prothoracic nerve L5A (trochanteral depressors, CI). Pilocarpine 1.5×10^{-5}M. (Time scale: 3 sec). Asterisks indicate correlated activity of prothoracic trochanteral levators and the mesothoracic trochanteral depressor D_s. **B**. Cross-correlogram of the activity of mesothoracic depressor D_s (A, top trace) relative to the activity of prothoracic levators (A, middle trace). **C**. Cross-correlogram of the activity of prothoracic depressor D_s (A, bottom trace) relative to the activity of prothoracic levators (A, middle trace). Compare this figure with Fig. 3.

Abbreviations

CI	common inhibitory motor neuron
dep	depressor
D_f	fast depressor trochanteris
D_s	slow depressor trochanteris
L	left
lev	levator
meso	mesothoracic
meta	metathoracic
pro	prothoracic
R	right
troch	trochanter

---

the preparation is superfused with the muscarinic agonist pilocarpine. These rhythmic patterns have been described in detail elsewhere (Ryckebusch and Laurent 1993; Ryckebusch et al. 1994). In this paper we focus exclusively on the coordination of levators and depressors of the trochanter, whose alternating activity during each cycle describes the walking rhythm well (Ryckebusch and Laurent 1993). The rhythmic activity recorded in each hemiganglion consisted of a short **levator** phase, during which a brief burst of activity was recorded in trochanteral levator motor neurons, alternating with a longer **depressor** phase, during which activity was recorded in the slow and fast trochanteral depressors (D_s and D_f). During normal walking, these two phases correspond to the swing and stance phases of hind leg stepping, respectively (Burns 1973; Burns and Usherwood 1979). Although alternation of the trochanteral motor neuron antagonists was observed in all three thoracic ganglia, the details of the rhythmic pattern differed (Ryckebusch et al. 1994). In particular, there was an anterior to posterior shift in the activity patterns of the trochanteral depressors relative to the levator bursts. Whereas metathoracic D_s and D_f fired at their highest rates immediately *after* a trochanteral levator burst, the highest firing frequencies

of the prothoracic D_s and D_f occurred *before* each trochanteral levator burst. The rhythmic activity recorded in the mesothoracic ganglion was similar in most respects to that in the prothoracic ganglion, but D_s and D_f had marked peaks of activity both immediately *before and after* a levator burst.

Effects of sectioning thoracic connectives on rhythmic activity

In preparations consisting of two or three connected thoracic ganglia, the patterns of rhythmic activity were highly variable. Although we could record simultaneous activity of motor neurons in all six hemiganglia, in most preparations rhythmic activity could only be elicited in a subset of these hemiganglia. Rhythmic activity was usually highly irregular, and in some hemiganglia only tonic activity was recorded. Simultaneous rhythms in different hemiganglia generally had different average frequencies. These patterns of activity often spontaneously changed during the course of an experiment and could be modified by altering the bath concentration of pilocarpine.

Sectioning the connectives between ganglia usually led to drastic changes in the patterns of activity, including the emergence of rhythmic activity in previously quiescent hemiganglia. Ongoing rhythmic activity usually became more regular, with more uniform burst shapes and durations and less variable bursting frequencies than were observed before the section. Extracellular recordings and corresponding cross-correlograms for prothoracic levators and mesothoracic depressors before and after sectioning the pro-meso connectives are illustrated in Figs. 2 and 3. The correlated activity between prothoracic levators and mesothoracic depressors is apparent both in the extracellular recordings (Fig. 2A, asterisks) and in the cross-correlogram (Fig. 2B). Sectioning the pro-meso connectives had two major effects: *(i)* a stable rhythmic pattern emerged in the mesothoracic motor neurons, while the prothoracic rhythm was

relatively unchanged (Fig. 3A); and *(ii)* evidence of correlated activity in mesothoracic depressors and prothoracic levators disappeared (Fig. 3B). Note that the mesothoracic depressor D_s no longer fired at a higher frequency during a prothoracic levator burst (Fig. 3A), as it did before the section (Fig. 2A); as a result, the large peak at 0 time lag is absent from the post-section cross-correlogram (Fig. 3B). Fig. 3B also illustrates one of the difficulties of interpreting cross-correlograms of rhythmic spike trains. After sectioning the connectives, the pro- and mesothoracic ganglia were rhythmically active with similar average frequencies. Therefore, although the ganglia were isolated from each other and were therefore functionally independent, the cross-correlogram of the activities of prothoracic levators and mesothoracic depressors exhibited regularly spaced peaks. Because these peaks were of uniform amplitude over all time lags, however, they were easily distinguishable from single central peaks.

Intrasegmental correlations

Levators and contralateral depressors: The smallest preparation from which we recorded was a single thoracic ganglion, which is composed of a pair of fused hemiganglia. Coupling between pattern generators in the two hemiganglia was often apparent, and has been described in detail in our studies of rhythms evoked in isolated metathoracic ganglia (Ryckebusch and Laurent 1993). In particular, we found that the activity of levators of the trochanter was strongly coupled to activity of contralateral depressors of the trochanter (Figs. 1C and D). There is a large component of trochanteral depressor activity that is synchronized with contralateral trochanteral levator activity. Such coupling between levators and contralateral depressors was also observed in the pro- and mesothoracic ganglia, although not as consistently as in the metathoracic ganglion. Examples of coupling between the activities of levators and contralateral depressors for the pro- and mesothoracic ganglia are shown in Figs. 4A and B, re-

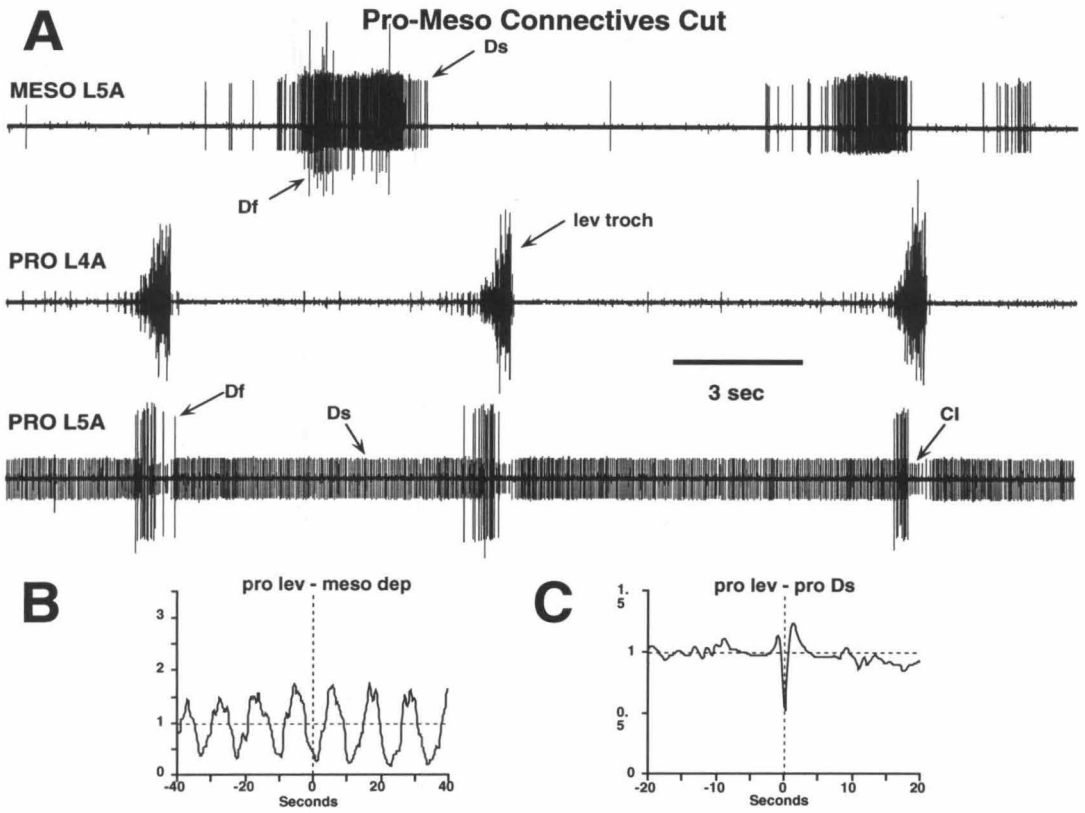

Figure 3. Intrasegmental correlations in motor neuron activity disappear when ganglionic connectives are sectioned. **A**. Same preparation and nerves as shown in Fig. 2, after sectioning the connectives between the pro- and mesothoracic ganglia. (Time scale: 3 sec). **B**. Cross-correlogram of the activity of mesothoracic depressor D_s (A, top trace) relative to the activity of prothoracic levators (A, middle trace). Note the emergence of regular peaks in the histogram compared to Fig. 2B, and the disappearance of the central peak at 0 time lag (discussed in Results). **C**. Cross-correlogram of the activity of prothoracic depressor D_s (A, bottom trace) relative to the activity of prothoracic levators (A, middle trace). Note that there is almost no change in this cross-correlogram compared to Fig. 2C.

spectively.

Levators and contralateral levators: Rhythmic activity of trochanteral levators was not strongly coupled to the rhythmic activity of levators in the contralateral hemiganglion; in fact, the intrinsic frequencies of the rhythms on the left and right were generally different. However, levators on opposite sides were never coactive in the metathoracic ganglion (Fig. 1E-F), and phase-locking between rhythms on the left and right was occasionally observed. In the pro- and mesothoracic ganglia, the coupling between levators on opposite sides was even more variable. Generally, levator activity on opposite sides appeared to be anticorrelated, but in some cases synchronous activity was also observed (Fig. 5). Fig. 5 shows cross-correlograms of mesothoracic levators on the left and right sides calculated from four discrete recordings ($\approx$ 300 sec each) in the same experiment. Initially, the levators were anticorrelated, as can be seen from the trough in the cross-correlogram at 0 time lag in Fig. 5A. Later, the trough at 0 time lag disappeared, and a peak appeared (Figs. 5B-C). Still later, the left and right levator motor neurons were bursting synchronously (Fig. 5D). (The regularly spaced peaks in the cross-correlograms (e.g., Fig. 5B) are due to the fact that both motor pools were bursting rhythmically with similar cycle periods (2–3 sec). Thus, several possible phase relationships occurred between levators on opposite sides of an isolated pro- or mesothoracic ganglion, in contrast to isolated metathoracic ganglia (see above).

Intersegmental correlations

Coupling between levators in adjacent segments

In most experiments, activity between levators on the same side of different segments appeared to be uncorrelated. Sometimes, however, levator activity in one segment immediately preceded or followed levator activity in an adjacent segment, with a short

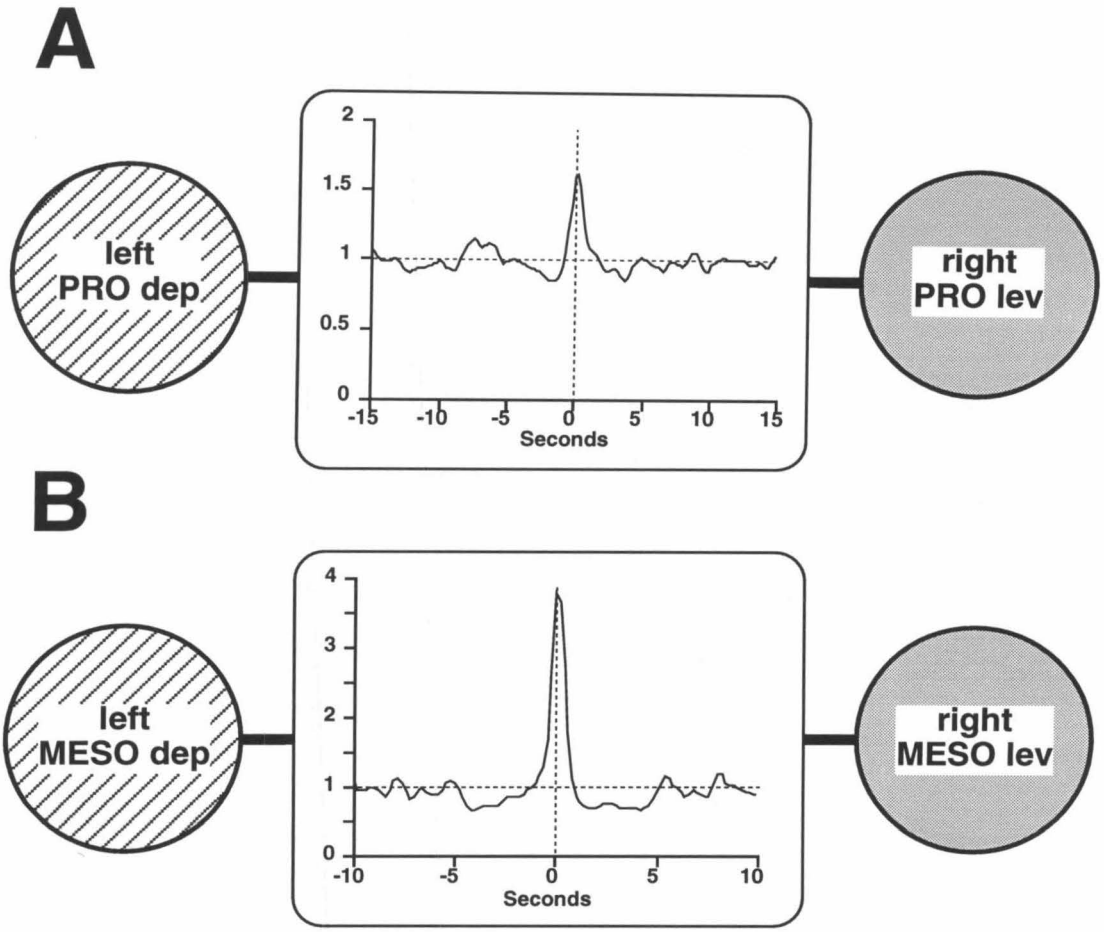

Figure 4. Coupling between thoracic levators and contralateral depressors. **A**. Cross-correlogram of the activity of prothoracic depressors on the left relative to levators on the right. Histogram was computed from 360-second continuous recordings of prothoracic levators (4129 spikes) and depressors (4496 spikes). Pilocarpine 2×10^{-5}M. **B**. Cross-correlogram of the activity of mesothoracic levators on the right relative to depressors on the left. Histogram was computed from 270-second continuous recordings of mesothoracic levators (8258 spikes) and depressors (3201 spikes). Pilocarpine 10^{-5}M.

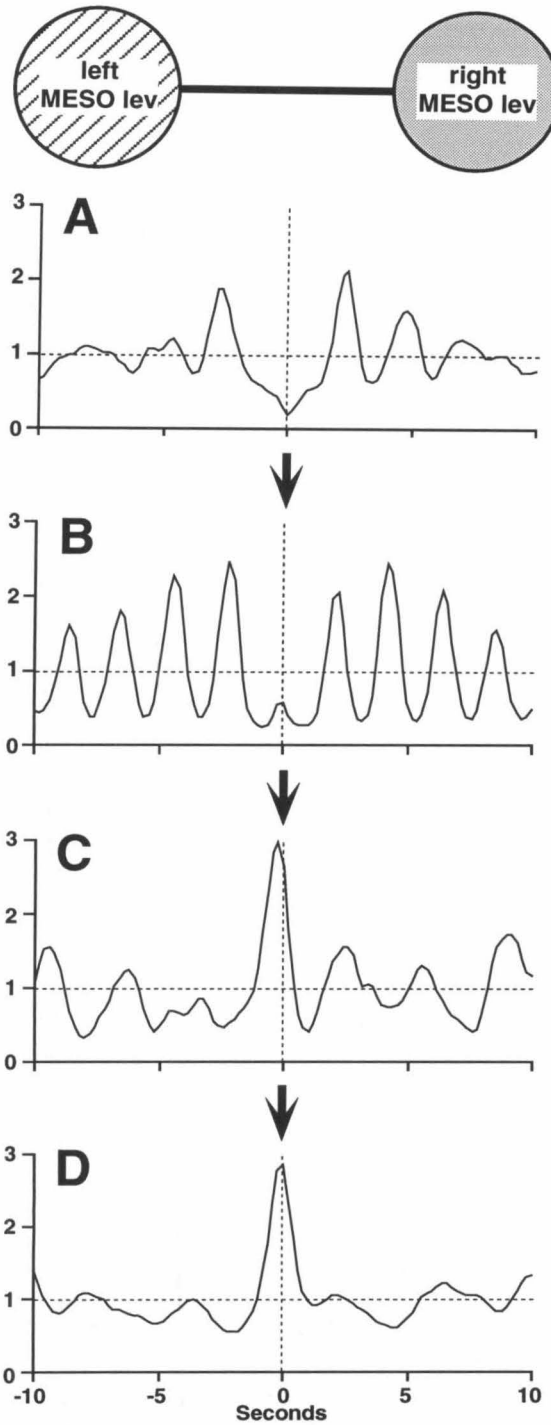

Figure 5

Figure 5. Coupling between left and right mesothoracic levators changes with time. **A**. Cross-correlogram of the activity of mesothoracic levators on the left relative to levators on the right. Histogram was computed from 270-second continuous recordings of left (13890 spikes) and right (8258 spikes) mesothoracic levators. Pilocarpine 10^{-5}M. **B**. As in **A**, later in the experiment, histogram was computed from 297-second continuous recordings of left (13692 spikes) and right (6960 spikes) mesothoracic levators. Both sets of motor neurons were rhythmically active with similar periods (2–3 seconds), giving rise to regular oscillations in the cross-correlogram. **C**. Later in the experiment, histogram was computed from 351-second continuous recordings of left (8204 spikes) and right (5144 spikes) mesothoracic levators. **D**. Later in the experiment, histogram was computed from 506-second continuous recordings of left (10525 spikes) and right (15852 spikes) mesothoracic levators. Note that absolute peak amplitudes cannot be compared in **A**–**D**, since the normalization factor for each cross-correlogram was different.

latency (1–3 sec; see below). In the cross-correlograms, this can be seen as a peak near, but not at, 0 time lag (Figs. 6A,C). In addition, there was often an inhibitory trough in the histogram at 0 time lag (Fig. 7B).

Coupling between pro- and mesothoracic levators: The most commonly seen sequence was activity in prothoracic levators that *preceded* mesothoracic levator activity (Fig. 6A), although the reverse was occasionally observed. In some cases, there was also a trough in the cross-correlogram corresponding to anticorrelated activity at 0 time lag (Figs. 6A, 7B). This correlation disappeared after the thoracic connectives were sectioned (Fig. 6B).

Coupling between meso- and metathoracic levators: The most commonly seen sequence was activity in mesothoracic levators that *followed* metathoracic levator activity (Fig. 6C), although the reverse was occasionally observed. In some cases (not shown), there was strong evidence of anticorrelated activity at 0 time lag (i.e., a trough in the cross-correlogram).

Coupling (as evidenced in cross-correlograms) was apparent even when rhythmic

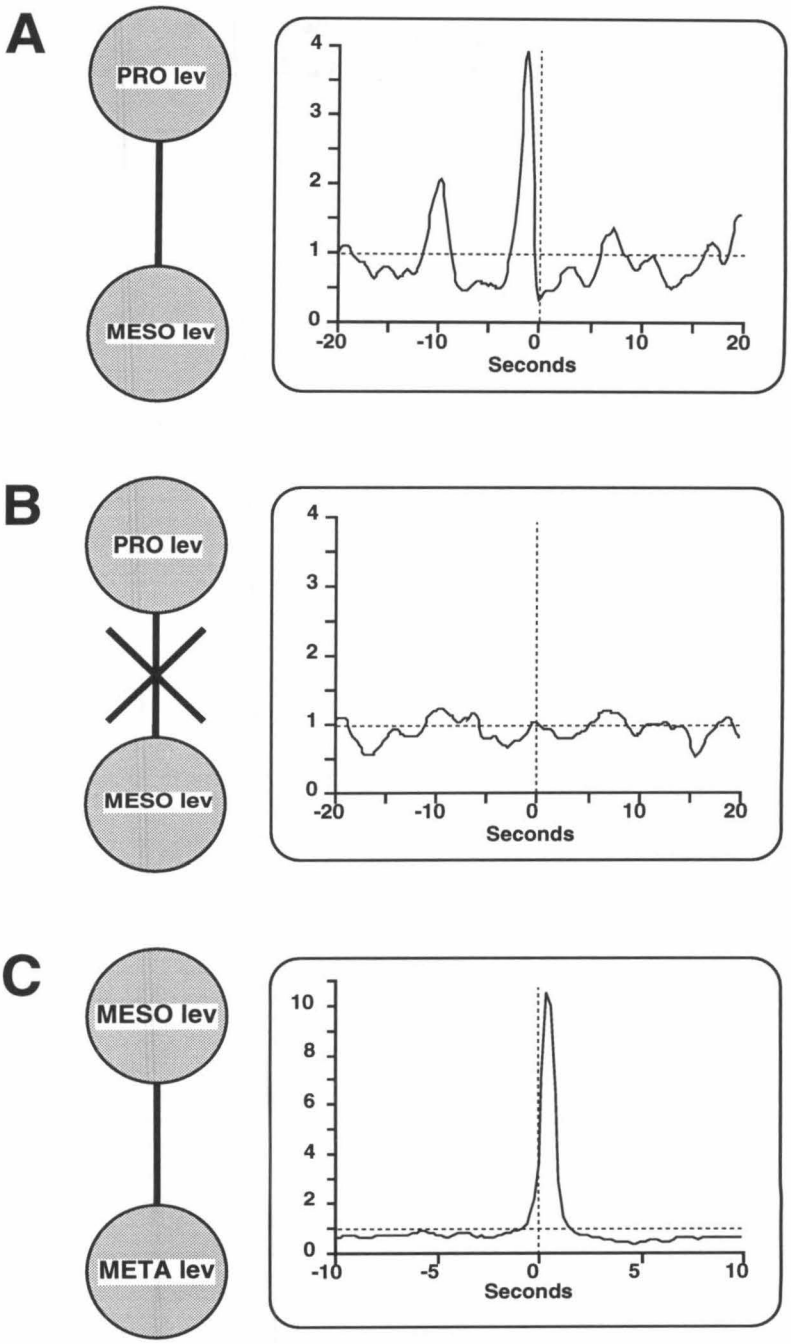
A
PRO lev
MESO lev
4
3
2
1
0
-20
-10
0
10
20
Seconds
B
PRO lev
MESO lev
4
3
2
1
0
-20
-10
0
10
20
Seconds
C
MESO lev
META lev
10
8
6
4
2
0
-10
-5
0
5
10
Seconds

Figure 6

Figure 6. Coupling between pro- and mesothoracic levators. **A**. Cross-correlogram of prothoracic levators relative to mesothoracic levators (prothoracic levators *precede* mesothoracic levators). Histogram was computed from 318-second continuous recordings of mesothoracic (3852 spikes) and prothoracic (8797 spikes) levators. Pilocarpine 3×10^{-5}M. **B**. Same experiment as **A**, after cutting the pro-meso thoracic connectives. Histogram was computed from 192-second continuous recordings of mesothoracic (15218 spikes) and prothoracic (3227 spikes) levators. **C**. Coupling between meso- and metathoracic levators. Cross-correlogram of mesothoracic levators relative to metathoracic levators (mesothoracic levators *follow* metathoracic levators). Histogram was computed from 188-second continuous recordings of mesothoracic (2706 spikes) and metathoracic (634 spikes) levators.

activity was not clearly seen in extracellular recordings from one of the hemiganglia. In Fig. 7, for example, bursting activity was recorded in the mesothoracic but not the prothoracic ganglion, but prothoracic activity was clearly modulated during bursts of activity in the mesothoracic levators (Fig. 7A, asterisks). The trough at 0 time lag and peak in the activity of prothoracic levators preceding mesothoracic levator bursts was similar to cross-correlations from experiments in which both pro- and mesothoracic segments were rhythmically active (Fig. 6A). After sectioning the pro-meso connectives, the modulation of the activity of prothoracic levators disappeared (Figs. 7C and D).

Coupling between levators and depressors on the same side of adjacent segments

A burst of activity in trochanteral levators in one segment was correlated with an increase of the firing frequency of trochanteral depressors (usually D_s) in the adjacent ipsilateral segment (Fig. 2A, top two traces). This coupling between levators in one segment and depressors in an adjacent segment was observed in most prepara-

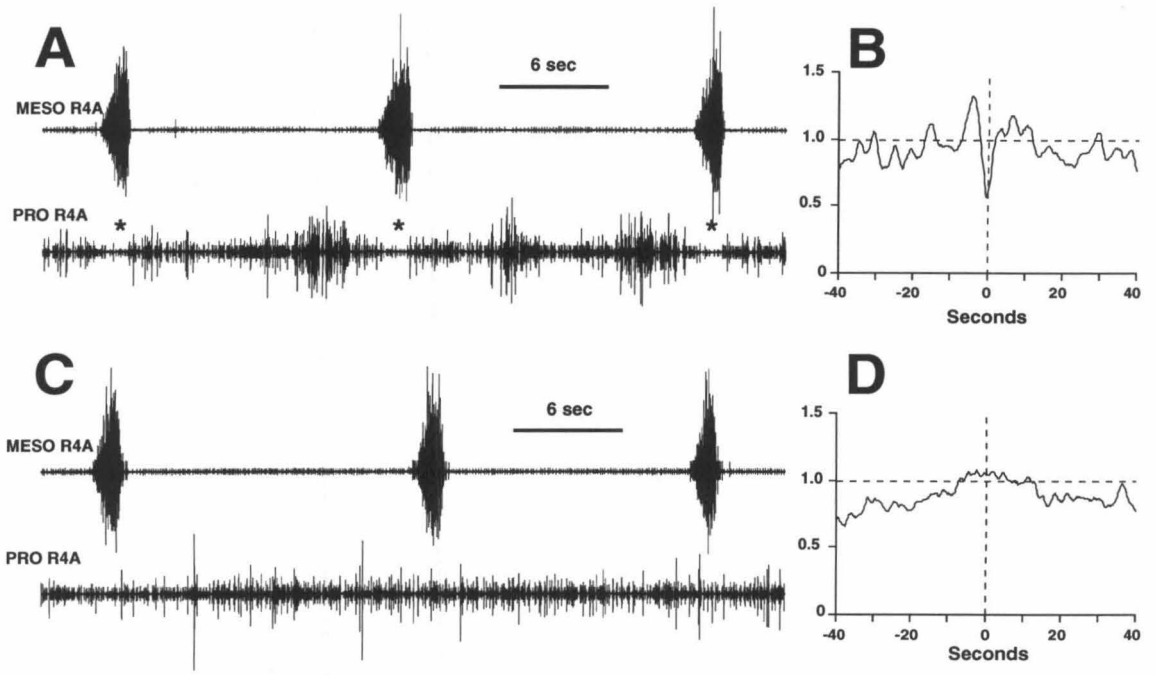

Figure 7. Modulated tonic activity of prothoracic levators during mesothoracic activity. **A**. Extracellular recordings from mesothoracic nerve R4A (trochanteral levators) and prothoracic nerve L4A (trochanteral levators). Pilocarpine 1.5×10^{-5}M. (Time scale: 6 sec). **B**. Cross-correlogram of prothoracic levator spikes relative to mesothoracic levator spikes (the peak in the histogram indicates that prothoracic levators tend to *precede* mesothoracic levators). **C**. Same preparation and nerves as shown in **A**, after sectioning the connectives between the pro- and mesothoracic ganglia. Extracellular recordings are from mesothoracic nerve R4A (trochanteral levators) and prothoracic nerve L4A (trochanteral levators). Pilocarpine 1.5×10^{-5}M. (Time scale: 6 sec). **D**. Cross-correlogram of prothoracic levator spikes relative to mesothoracic levator spikes. Compare to **B**.

tions, and appeared to be unaffected by the presence or absence of the third thoracic segment. Cross-correlations of the activity of levators in one segment and depressors in an ipsilateral adjacent segment showed a large peak at 0 time lag. Fig. 8 shows cross-correlograms for 4 different levator/depressor pairs, obtained from different experiments: prothoracic levators and mesothoracic depressors (Fig. 8A); mesothoracic levators and prothoracic depressors (Fig. 8B); mesothoracic levators and metathoracic depressors (Fig. 8C); and metathoracic levators and mesothoracic depressors (Fig. 8D).

Correlations between non-adjacent hemisegments

The significance of correlations between motor neuron activities in non-adjacent hemiganglia was more difficult to assess. This is because in most cases in which "significant" correlations between two "distant" motor pools were observed, it could be argued that the correlation was an indirect result of shorter-range correlations through an indirect pathway linking the two motor neuron pools. Simultaneous recordings of three motor neuron pools in two adjacent hemisegments of the same ganglion (mesothoracic levators and depressors on the left and mesothoracic levators on the right) illustrates this ambiguity (Fig. 9). As previously reported (Ryckebusch et al. 1994), mesothoracic depressors were inhibited during ipsilateral levator bursts, and showed increased activity both immediately before and after each levator burst (Fig. 9A). Mesothoracic levators were coactive with contralateral depressors (Fig. 9C; see also Fig. 4B). The cross-correlogram of right and left mesothoracic levators (Fig. 9B) shows inhibition at 0 time lag flanked by excitatory peaks, much like the histogram in Fig. 9A. Taken alone, this histogram would appear to indicate the existence of inhibitory coupling between left and right mesothoracic levators. In the context of the other two histograms (Figs. 9A and C), however, we could argue

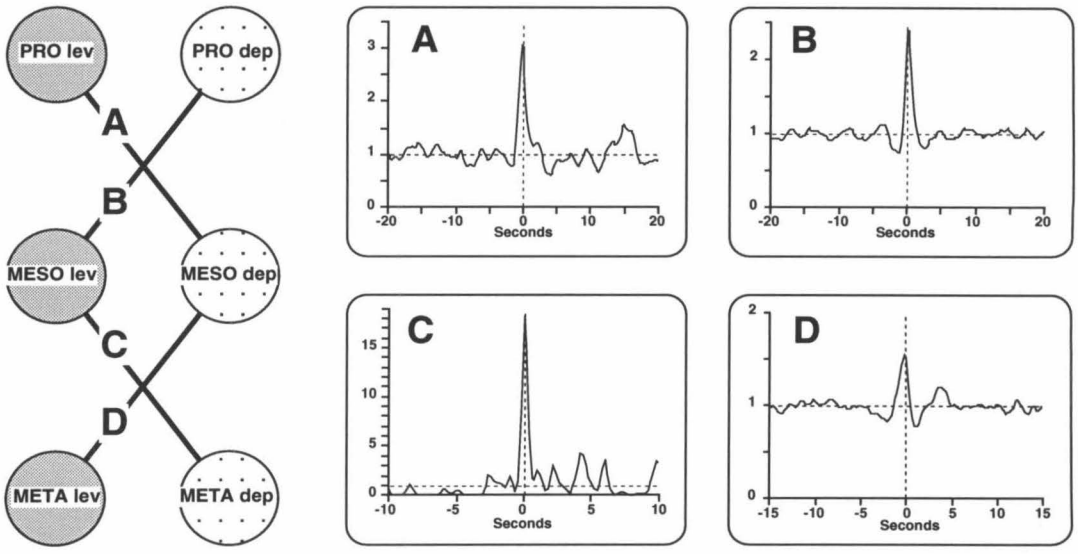

Figure 8. Coupling between trochanteral levators and depressors in ipsilateral adjacent segments. Cross-correlograms from four different preparations. **A**. Cross-correlogram of prothoracic levators relative to mesothoracic depressors. Histogram was computed from continuous recordings of mesothoracic depressors (10224 spikes) and prothoracic levators (12292 spikes). Pilocarpine 1.5×10^{-5}M. **B**. Cross-correlogram of mesothoracic levators relative to prothoracic depressors. Histogram was computed from 618-second continuous recordings of mesothoracic levators (28732 spikes) and prothoracic depressors (16543 spikes). **C**. Cross-correlogram of metathoracic depressor D_f relative to mesothoracic levators. Histogram was computed from 393-second continuous recordings of mesothoracic levators (5815 spikes) and metathoracic depressor D_f (206 spikes). **D**. Cross-correlogram of mesothoracic depressors relative to metathoracic levators. Histogram was computed from 618-second continuous recordings of metathoracic levators (8705 spikes) and mesothoracic depressors (18598 spikes).

that given that mesothoracic levators and contralateral depressors tended to be coactive (Fig. 9C), the cross-correlogram between left and right levators should resemble the cross-correlogram between left levators and depressors (Fig. 9A). Without additional information, it is not possible to determine which two of the three correlations show significant coupling, or if all three correlations are indicative of independent coupling pathways. In this case, we have been able to demonstrate relationships similar to those shown in Fig. 9A and C in preparations in which only one of the two mesothoracic hemiganglia was rhythmically active (not shown). This indicates that the coupling between mesothoracic levators and either ipsilateral (Fig. 9A) or contralateral (Fig. 9C) depressors does not depend on the existence of rhythmic contralateral levator activity.

In some preparations, "diagonal" coupling was observed, either between mesothoracic levators and contralateral pro- or metathoracic levators, or between prothoracic levators and contralateral metathoracic levators. As discussed above, however, it was not possible in any of these cases to establish whether this coupling was independent of shorter-range interactions. Fig. 10 shows pairwise cross-correlations between right mesothoracic levators and left prothoracic levators (Fig. 10C) along with correlations along a second, indirect pathway (Figs. 10A-B). Prothoracic levator activity preceded activity in ipsilateral mesothoracic levators (Fig. 10A; see also Fig. 6A), and mesothoracic levators on the right preceded mesothoracic levators on the left (Fig. 10B). These cross-correlations are consistent with Fig. 10C, which shows that left prothoracic levators tended to be coactive with right mesothoracic levators.

4.5 Discussion

We have shown that locomotor rhythms elicited in leg motor neurons of different hemisegments in isolated thoracic nerve cords are centrally coupled. A summary

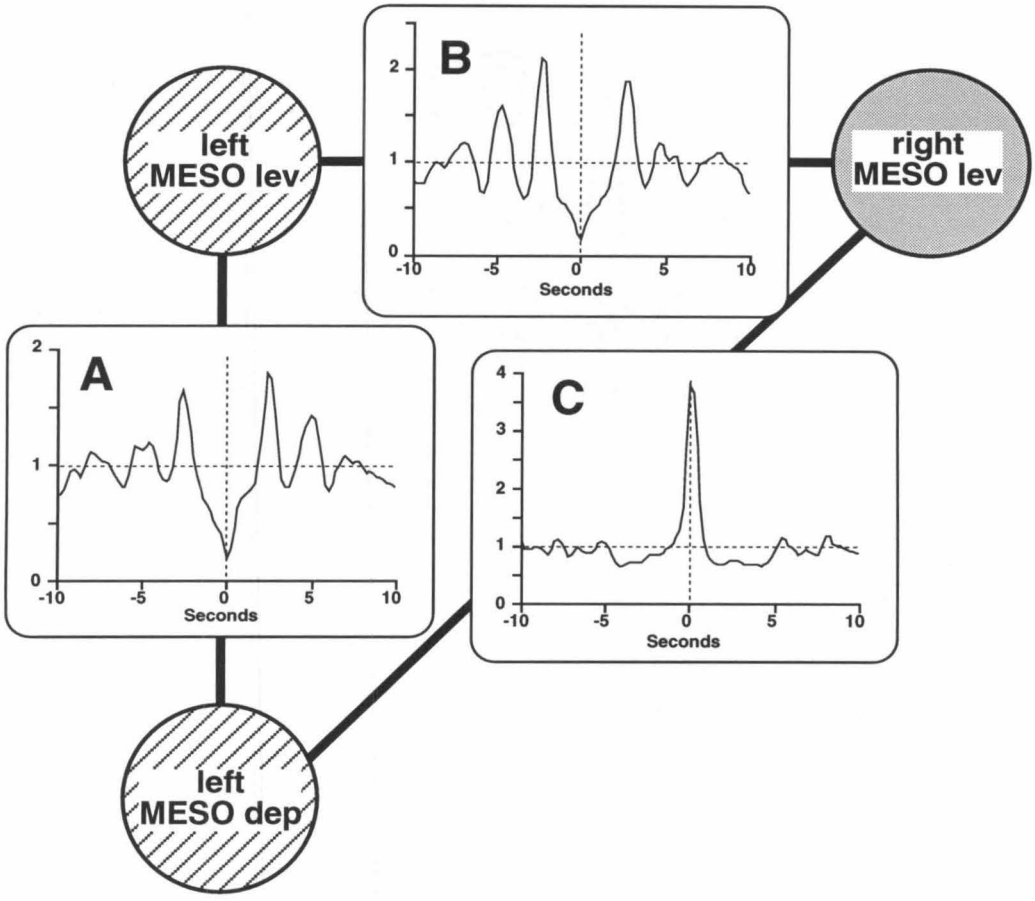

Figure 9. Coupling between mesothoracic trochanteral levators and depressors. Cross-correlograms from 270-second simultaneous recordings of mesothoracic levators (13890 spikes) and depressors (3201 spikes) on the left, and levators on the right (8258 spikes). Pilocarpine 10^{-5}M. **A**. Cross-correlogram of levators on the left relative to depressors on the left. **B**. Cross-correlogram of levators on the right relative to levators on the left. **C**. Cross-correlogram of levators on the right relative to depressors on the left.

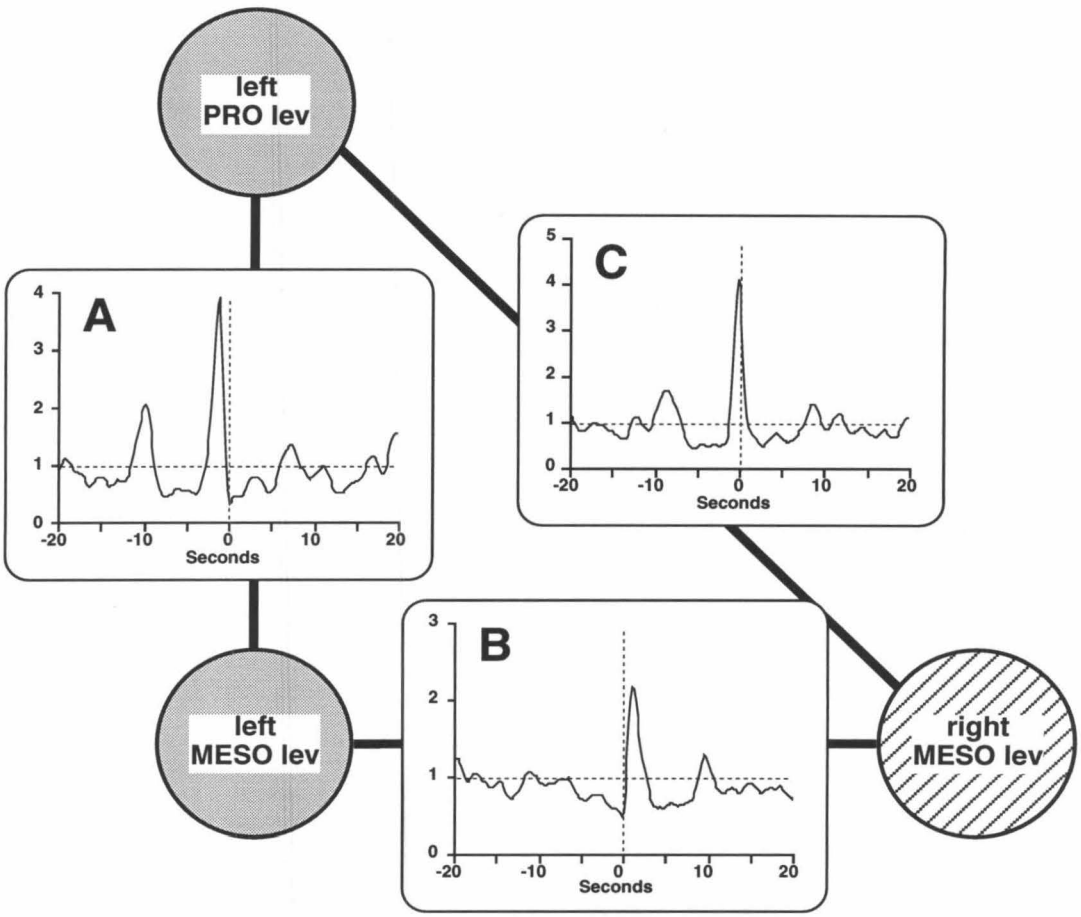

Figure 10. Coupling between mesothoracic trochanteral levators and contralateral meso- and prothoracic levators. Cross-correlograms from 318-second simultaneous recordings of mesothoracic levators on the left (3852 spikes) and right (10851 spikes), and prothoracic levators on the left (8797 spikes). Pilocarpine 3×10^{-5}M. **A**. Cross-correlogram of prothoracic levators on the left relative to mesothoracic levators on the left. **B**. Cross-correlogram of mesothoracic levators on the left relative to mesothoracic levators on the right. **C**. Cross-correlogram of prothoracic levators on the left relative to mesothoracic levators on the right.

of the major functional relationships between motor neuron pools as revealed by cross-correlation analysis is shown schematically in Fig. 11. Connections between motor neuron pools represent the phase relationships between the motor neurons, not actual neural pathways, which are unknown. Trochanteral levators tended to be coactive with trochanteral depressors in the ipsilateral adjacent hemiganglion and the contralateral hemiganglion of the same segment. Activity of trochanteral levators in adjacent hemiganglia on the same side was not usually synchronous, but mesothoracic levators tended to burst immediately after either pro- or metathoracic levator bursts. The coupling of levators in the two hemiganglia of the same segment was variable over long stretches of time, but not on a cycle-by-cycle basis, particularly in the pro- and mesothoracic ganglia.

Limitations of the cross-correlation technique

We have used cross-correlation analysis to assess functional relationships between motor neuron pools in different segments of isolated thoracic nerve cords. Cross-correlation analysis is one of the most useful techniques for exhibiting interdependencies between noisy spike trains, although the interpretation of cross-correlograms is sometimes difficult (see Methods). The question of how to determine whether a structure in a cross-correlogram is statistically significant has often been raised, but so far no generally recognized solution has been presented (Perkel et al. 1967; Glaser and Ruchkin 1976; Aertsen et al. 1989). One is left with the empirical procedure of comparing a peak or a trough near 0 time lag with the magnitudes of fluctuations in eccentric positions of the correlograms. This is potentially problematic when cross-correlating the activities of neurons with pacemaker-like properties, for the resulting histograms often show large and regular modulations, even when those neurons are known to be independent (Perkel et al. 1967). These limitations can be overcome,

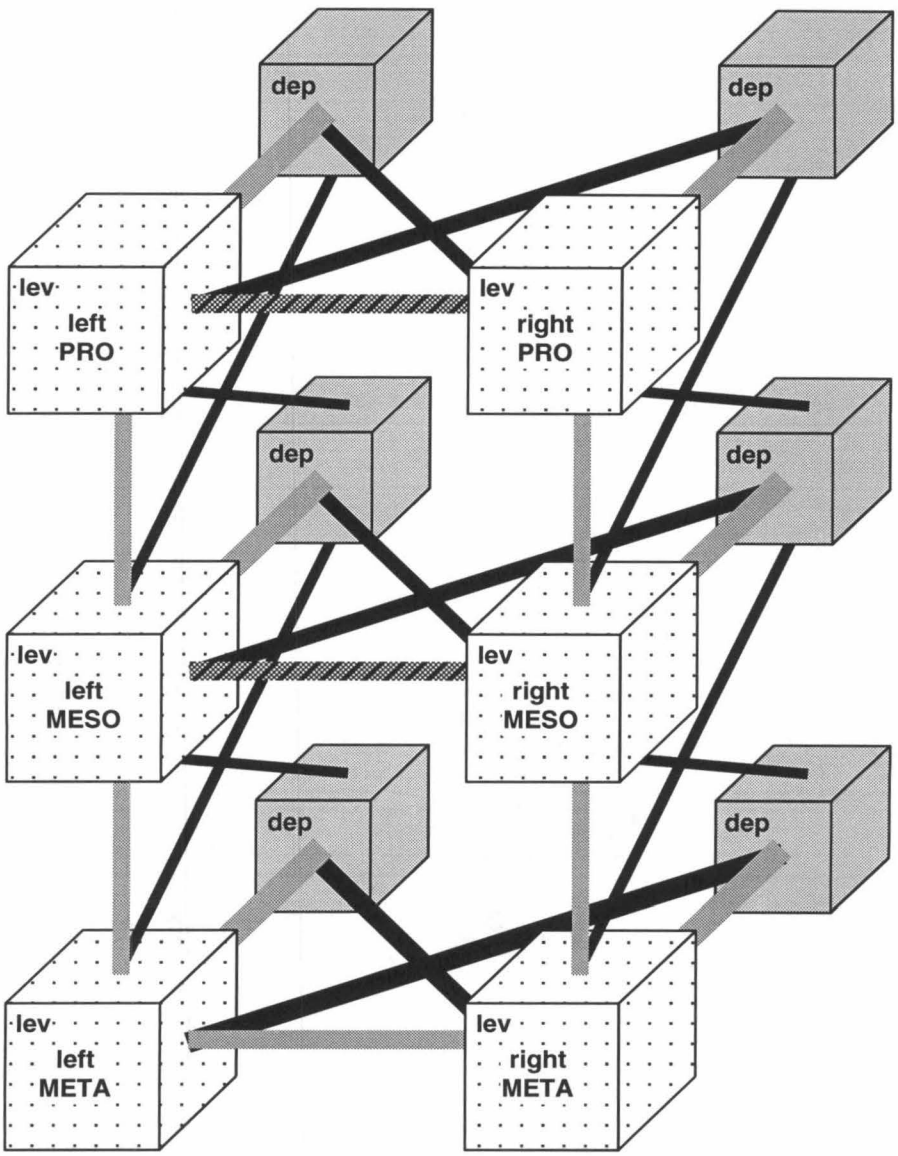

Figure 11. Schematic representation of correlations between trochanteral motor neuron pools (see also Ryckebusch and Laurent 1993; Ryckebusch et al. 1994). Solid black lines: synchronous activity (excitatory coupling). Grey lines: anticorrelated activity (inhibitory coupling which can be asymmetrical, such as that observed between trochanteral levators and depressors). Dashed lines: inhibition and time-delayed excitation. Striped black/grey lines: variable coupling.

however, if cross-correlation is combined with other analysis techniques and is interpreted cautiously.

One goal of cross-correlation analysis is to derive information on potential neuronal connectivity from physiological data. If two neurons receive a common excitatory input from unknown sources, they will have more synchronous spikes than statistically expected, and their cross-correlation function will correspondingly show a sharp central peak. If several neuronal processing stages lie between the locus of common input and the neurons recorded from, the central peak will be widened to a variable extent. Although it is less obvious, common inhibitory inputs will also produce a central peak in the cross-correlogram. Likewise, several different circuit configurations can result in a central trough in the cross-correlogram. Accordingly, although we may conclude that a central peak or trough is indicative of common inputs, it is impossible to determine uniquely the underlying circuit by spike-train analysis without complete knowledge of the states of all of the circuit elements. Cross-correlograms with more complicated shapes are in general ambiguous, so that conclusions can only be drawn from such data in conjunction with additional information. Therefore, although the results presented here suggest possible neural pathways for intersegmental coordination, definitive conclusions about underlying neuronal connections awaits the identification and characterization of neurons that can be shown to coordinate local pattern generators in the absence of sensory inputs.

Intersegmental coordination and the implications for behavior

The central coupling between different motor neuron pools described here, while not sufficient to account for the coordination of the legs observed during walking, is consistent with results obtained by others in intact and deafferented insects. Ipsilateral

intersegmental coupling has been shown to be stronger than contralateral coupling in several arthropod preparations (Sillar et al. 1987; Pearson and Iles 1973; Dean 1989). Although we see weak or variable coupling between contralateral levators, the two sides do not appear to be completely independent. That the levators on opposite sides are never coactive in the metathoracic ganglion suggests that there could be inhibitory coupling between the drives to levators on the left and right. On the other hand, the variable nature of the coupling between left and right sides observed in the pro- and mesothoracic ganglia (Fig. 5) indicates that the coupling between ganglia could be dynamic in nature, subject to change as required to modify the patterns of coordination of the legs. Simultaneous protractions of the left and right legs maintained for several cycles were occasionally observed in walking stick insects (Graham 1972). In other systems, particularly the crustacean stomatogastric nervous system, which controls movements of the foregut, it has been shown that the phase relationships between elements of a central pattern generator are subject to modification by endogenous neuromodulators (Marder and Weimann 1992).

The coupling observed between levators in adjacent hemisegments on the same side was similar to that seen in deafferented headless cockroaches (Pearson and Iles 1973), in which mesothoracic bursts tended to occur immediately after the end of the metathoracic burst. The tendency of levator burst activity in the different segments not to overlap indicates that the central coupling between the local pattern generators in the different segments is likely to be inhibitory. In addition, the tendency of prothoracic and metathoracic bursts to occur before mesothoracic bursts indicates that the coupling could be asymmetrical. That the burst in one segment tended to immediately follow the burst in the adjacent segment could be explained by a postinhibitory rebound mechanism of the sort suggested by Pearson and Iles (1973). Inhibitory coupling followed by asymmetrical delayed excitation between ipsilateral adjacent legs has been demonstrated in the stick insect, but it is not known whether

this coupling is achieved by sensory or central mechanisms, or a combination of the two (review: Cruse 1990).

Our results and those of previous studies (Ryckebusch and Laurent 1993; Pearson and Iles 1970) indicate that the drives to levator and depressor motor neurons are not symmetric. The occurrence of levator bursts appeared to be independent of the tonic firing rate of depressors or the presence or absence of depressor bursts timed with the rhythmic activity of other segments. Depressor activity, on the other hand, appeared to be modulated in time with the rhythmic activity of contralateral or ipsilateral levators, since an increase in depressor activity was always coupled to a contralateral levator burst or appeared in conjunction with an ipsilateral levator burst, and depressor activity was never inhibited in the absence of a corresponding ipsilateral levator burst. In isolated ganglia in which there was no rhythmic activity in levators on either side, only tonic activity was recorded in depressors.

Mechanisms proposed by Pearson and Iles (1970) based on their studies of leg motor rhythms in the cockroach are not sufficient to account for the asymmetric coupling between trochanteral levators and depressors we observed. They propose that a central pattern generator simultaneously excites the motor neurons active during the protraction phase (here: trochanteral levators) and inhibits antagonistic motor neurons active during the retraction phase (trochanteral depressors). A mechanism such as postinhibitory rebound was postulated to explain the postinhibitory burst of activity in depressors. This mechanism, however, cannot account for the observation in pro- and mesothoracic ganglia that depressors were also active *before* being inhibited during a levator burst. In a modelling study, we proposed that this result could be explained by concurrent excitation of both levators and depressors (Ryckebusch et al. 1994). In addition, since depressors appear to receive excitatory inputs during levator bursts in adjacent hemisegments, an additional excitatory drive to depressors from central pattern generators in adjacent segments would also be re-

quired. Evidence that intersegmental coordinating inputs are phasically active in the levator phase was obtained by Pearson and Iles (1973) in cockroaches. In recording from axons in the connectives that were rhythmically active in phase with walking rhythms, they reported that such axons always discharged in phase with levators in either segment and never with depressors.

The strong centrally mediated coordination between contralateral or adjacent levators and depressors stands in contrast to the weaker, variable coupling between levators. Since the legs of a locust must be capable of relatively independent movement to navigate on irregular terrain, it is sensible that leg protractions (levator phase) should be only weakly coupled centrally, relying more heavily on sensory information to achieve proper coordination. Leg protraction is potentially destabilizing, however, as weight is then shifted to other legs. Regardless of the sequence of leg protractions, stability must be maintained each time a leg is lifted by stiffening the joints of the remaining legs to bear the increased load and possibly prevent the protraction of adjacent legs. In the cockroach, increased load on a leg was shown to cause an increase in the firing rate of the slow depressor D_s (Pearson 1972). It is therefore likely that the increased activity of depressors—particularly the slow depressor D_s—during levator bursts in adjacent hemisegments at least partially subserves such a function. It has been assumed that load compensation in insects was mediated by feedback from sensory organs (Pearson 1972; Zill and Moran 1981). Based on our results, it appears likely that a central mechanism for maintaining stability exists as well.

Neural basis of intersegmental coordination

Motor neurons are driven either directly by central pattern generator neurons, or by other neurons which are themselves phasically driven by a central pattern generator. Direct connections between leg motor neurons have been reported only exceptionally

in insects (Siegler 1982; Burrows et al. 1989). It follows that central coupling between pools of motor neurons must be mediated by premotor interneurons, and can occur at different levels of premotor circuitry. Coordinating inputs carrying phasic information from one segmental pattern generator could be directly involved in shaping the rhythmic output of a pattern generator in another segment. In this case the rhythms generated by two connected segmental pattern generators would not be independent. Another possibility is that the motor neurons (or interneurons that drive them) are simultaneously receiving independent phasic inputs from several segmental pattern generators. In this case the output pattern of a motor neuron would represent the superposition of its different phasic inputs, which are themselves uncoordinated in the absence of sensory feedback. The fact that severing thoracic connectives leads to large changes in segmental rhythms, in most cases causing the rhythmic patterns to become more regular, indicates that this second possibility is not sufficient to explain the intersegmental coupling of motor outputs. Weak central coupling between segmental pattern generators and the absence of additional coordinating inputs from sensory pathways could explain the highly irregular rhythmic patterns we observed. In the absence of sensory feedback, rhythmic inputs to one pattern generator from another would occur at inappropriate times during the cycle, causing a disruption of otherwise "regular" rhythmic patterns. While motor neurons may be getting additional phasic inputs from other segments, it seems likely that the rhythmic output of a central pattern generator in one hemisegment is shaped in part by phasic inputs from other segments.

Intersegmental interneurons have been implicated in the coordination of motor behaviors in a number of insect preparations. In cockroaches, a large population of intersegmental interneurons (type-A thoracic interneurons or TI_As) has been identified that integrate inputs from different sources and project to local premotor and motor neurons in several ganglia, coordinating leg movements during the escape reflex

(Ritzmann and Pollack 1986, 1988, 1990; Ritzmann et al. 1991). In addition, Pearson and Iles (1973) have recorded from axons in the thoracic connectives whose activity patterns were modulated in phase with centrally-generated rhythms in the ipsilateral adjacent segments. The pattern generator underlying locust flight, which can produce well-coordinated motor patterns in the absence of sensory inputs, is distributed in all three thoracic ganglia, and includes many intersegmental interneurons (Robertson and Pearson 1983; review: Robertson 1986; but see Ronacher et al. 1988). In stick insects, it has been established that the various mechanisms responsible for the coordination of adjacent legs (Cruse 1990) are mediated primarily by neural signals travelling in the ipsilateral connectives (Dean 1989). It is not known, however, whether these coordinating signals are driven by sensory or central inputs. The neuronal basis of central coordination between pattern generators underlying leg movements in the locust is unknown, although several populations of intersegmental interneurons have been studied. In one study, at least 30 paired intersegmental interneurons with somata in the mesothoracic ganglion were shown to receive mechanosensory inputs from the middle leg and to project to the ipsilateral metathoracic hemiganglion, where they made synaptic contacts with the local interneurons and motor neurons controlling the hind leg (Laurent 1986, 1987, 1988; Laurent and Burrows 1989a, b). In another study, some 35 interneurons with somata in the metathoracic ganglion were shown to receive mechanosensory inputs from the hind leg and project to the mesothoracic ganglion in either the ipsilateral or the contralateral connective (Laurent and Burrows 1988b). Although it is not known if these neurons receive central inputs from local circuits controlling the legs in addition to the sensory inputs, their anatomical and physiological characteristics make them good candidates for the role of intersegmental coordinating interneurons.

Concluding remarks

The neuronal components of the pattern generators underlying leg movements have not been identified, and studies of intersegmental interneurons in insects suggest that the number of neurons involved in the coordination of these local circuits is likely to be very large (Rowell 1993; Laurent 1987; Laurent and Burrows 1988b; Ritzmann and Pollack 1988). Based on the results presented here, however, specific predictions can be made about the nature of the central coupling between segmental pattern generators. These predictions can be tested experimentally and through the use of computer models. In a previous study, we proposed a model for a hemisegmental pattern generator that could be configured to generate different motor patterns appropriate for each pair of legs (Ryckebusch et al. 1994). These hemisegmental models could now be connected into a larger circuit to test our hypotheses about the central coupling between pattern generators. Such a model will be the focus of future work.

Chapter 5

Conclusions

Detailed discussions of the results described in this thesis can be found in the individual chapters. Accordingly, I will briefly summarize here the major contributions of this work and directions for future research.

5.1 Central control of leg movements during walking

In Chapter 1, I showed that the motor patterns underlying the movement of individual legs during walking in locusts can be generated by segmental central pattern generators. This is the first clear demonstration that isolated thoracic ganglia of insects can produce rhythmic patterns appropriate for walking. The early studies that provided the most convincing evidence for the existence of CPGs were done in cockroach preparations in which the thoracic nervous system was only partly isolated from peripheral and descending inputs. In addition, the rhythmic activity recorded in leg motor neurons was sporadic and highly irregular (Pearson 1972; Pearson and Iles 1970, 1973). The weakness of the evidence obtained in cockroaches, together with

the failure to demonstrate walking-like motor patterns in other isolated insect nervous systems (Bässler and Wegner 1983) led several researchers to reject the hypothesis that leg movements in insects were under the control of central pattern generators, or that the rhythmic patterns observed were related to walking (Bässler and Wegner 1983; Pearson 1985; Zill 1986). An alternative explanation supported by the results presented here is that the central pattern generators require excitatory stimulation in order to be activated, and that this stimulation is absent in highly dissected preparations. Such stimulation is likely to come from the sub- and supraoesophageal ganglia, as evidenced by early studies which showed that walking was inhibited when the connectives between the suboesophageal ganglion and the thoracic nerve cord were severed (Roeder 1937), but facilitated when the connectives between the supra- and suboesophageal ganglia were cut (Roeder 1937; Graham 1979a, b). It is now well established that external stimuli such as electrical stimulation of neural pathways or bath-applied pharmacological agents can be used to activate endogenous rhythms. In the present study, such external stimulation was provided by bath application of the muscarinic cholinergic agonist pilocarpine, which further suggests that the pathways that activate the locomotor rhythms could be cholinergic. The work described in Chapter 2 suggests several directions for future studies:

The role of descending inputs in the initiation and maintenance of walking

The roles of the sub- and supraoesophageal ganglia in the initiation and maintenance of walking have not been studied sufficiently. Electrically stimulating the connectives between the sub- and prothoracic ganglia can evoke leg motor rhythms in isolated locust thoracic nerve cords (unpublished observation), which suggests that it should be possible to identify neurons in the sub- and supraoesophageal ganglia projecting to the thoracic ganglia that are involved in the initiation or modification of walking rhythms. In parallel, the identification of cholinergic neurons and their postsynaptic

targets is needed to elucidate the role of muscarinic agonists in the initiation of motor rhythms. The electrically-evoked motor rhythms were not blocked by the muscarinic antagonist atropine (unpublished observation), which suggests that the descending control of locomotor rhythms may not be mediated by the same muscarinic cholinergic pathways activated by pilocarpine.

Interneuronal basis for central pattern generation

Much is known about the different populations of interneurons in thoracic ganglia of locusts (review: Burrows 1992). Spiking local interneurons integrate sensory information about the movement and position of a leg. They make synapses onto nonspiking local interneurons, which also receive direct afferent input (Burrows et al. 1988; Laurent and Burrows 1988), and organize movements in sets of coordinated motor pool activations (Burrows 1980; Burrows and Siegler 1976). Intersegmental interneurons are responsible for controlling the gain of local reflexes in phase with sensory activity in adjacent segments (Laurent 1987; Laurent and Burrows 1989a, b). It is likely that these different populations of interneurons are involved in the generation and control of rhythmic motor outputs during locomotion, in addition to their participation in sensory-motor reflex pathways. Now that rhythmic patterns can be evoked in isolated thoracic ganglia, the contributions of each of these populations to the generation of the rhythmic motor pattern can be determined.

Because synaptic connections between motor neurons have only rarely been found, the walking rhythm must be generated by networks of spiking or nonspiking local interneurons. Based on what we know about the local circuits underlying leg movement in the locust, a central pattern generator circuit seems most likely to be composed of spiking local interneurons. These interneurons are known to make connections among themselves, as well as to non-spiking interneurons, motor neurons, and intersegmental interneurons (Burrows 1992). In addition, it has recently been

shown that spiking local interneurons receive rhythmic synaptic inputs during fictive walking in the preparation described here (Wolf and Laurent 1994). Although the source of these rhythmic inputs is not known, only sensory afferents and other spiking local interneurons are known to make synapses onto this population of interneurons. Because (1) these rhythmic inputs were recorded in a deafferented preparation and (2) connections from non-spiking interneurons to spiking local interneurons have never been found, it appears likely that the rhythmic drive to local spiking interneurons comes from other local spiking interneurons. The non-spiking interneurons, which receive inputs from the spiking local interneurons and provide most of the synaptic input to motor neurons, may be responsible for the precise shaping of the final motor pattern.

Integration of central and sensory signals

Much is already known about leg sensory receptors and the effects of sensory inputs on thoracic interneurons (Burrows 1992). The differences reported here between the "fictive" rhythm and walking allow us to make predictions about which phases of the motor pattern are likely to be most heavily influenced by sensory feedback (discussed in Chapter 2). These predictions can be tested by stimulating different sensory inputs and observing the effects on the centrally-generated motor pattern. In addition, a large body of work has established that sensory inputs are also modulated by CPGs, which gate sensory function according to the phase of the movement cycle in which the input occurs (review: Sillar 1991). The modulation or gating of sensory pathways can occur at several levels. For example, primary afferent terminals seem to be an important site for phasic modulation of reflex function, as it has been shown in several preparations that sensory terminals are subject to rhythmic synaptic depolarization (PAD) during centrally-generated locomotor rhythms (review: Sillar 1991; Sillar and Skorupski 1986; Gossard et al. 1991). In the locust, depolarizing synaptic potentials

have been recorded in afferent terminals as well (Burrows and Laurent 1993), but it is not known whether such potentials are phasically modulated during fictive locomotor rhythms.

5.2 Segment-specific tuning of fictive motor patterns

In Chapter 3, I showed that the centrally-generated rhythmic patterns evoked in the three thoracic ganglia are different. These differences are likely to reflect the different morphologies and functional roles of the three pairs of legs during walking. It seems, then, that the central nervous system is tuned to produce segment-specific patterns of motor output. I then proposed an abstract model circuit which can produce the different motor patterns when a single circuit parameter is modified. This model was tested using computer simulations and was also implemented in hardware using VLSI technology. Since the three thoracic ganglia are segmentally homologous, the design of the model circuit was based on the assumption that much of the underlying circuitry should be conserved in the three thoracic ganglia, and therefore that a single circuit design should be capable of producing the range of behaviors we observed. This model demonstrated that a simple neural mechanism can be used to switch the output of a single circuit from one output state to another. It has been shown in other systems that central pattern generators can switch between different output patterns under the influence of endogenous neuromodulators (see for example Marder and Weimann 1992). It seems likely that much of the flexibility observed in behaving walking animals might come about through constant modulation of central pattern generator circuits which, under the impoverished conditions imposed in laboratory studies, might otherwise generate only a single fixed pattern.

Comparison of fictive motor rhythms to leg movements during walking

The three pairs of legs in the locust are highly specialized, and differ in their geometries as well as their positions relative to the body. Since the joint angles and movements during a step of the three pairs of legs are different, the activities of the leg muscles during walking can be expected to differ accordingly. In a previous study, the activity patterns of tibial motor neurons of the three segments were compared in a walking locust (Burns and Usherwood 1979). In that study, the timing of the flexor and extensor motor neuron activities relative to the protraction and retraction phases of a step differed in a segment-specific manner. A similar study should be carried out for the trochanteral motor neurons, in order to establish whether the segment-specific motor patterns we report here are actually related to the different functional roles of the legs during walking. If the differences in the fictive segmental motor patterns are consistent with differences in the activities of muscles during walking, this would indicate that a representation of the functional roles of the three pairs of legs exists in the central nervous system.

Neuromodulation of segmental motor patterns

Work on the crustacean stomatogastric nervous system has shown that a single neural circuit can produce different output patterns in the presence of different neuromodulatory substances, many of which are naturally present in the nervous system (review: Marder and Weimann 1992). These substances modify cellular and synaptic parameters to reconfigure the network of neurons and their connections, forming different functional circuits. The modification of the synaptic parameter which allowed our model circuit to switch between different thoracic motor patterns could be accomplished by similar mechanisms in a real nervous system. Accordingly, a study of the effects of different neuromodulators on the segment-specific thoracic motor patterns

in the locust might provide some insight about the underlying neural circuit. Indeed, if the different motor patterns were produced by modifications of a single circuit under the action of a neuromodulator, such modifications might be achieved by exposing the thoracic neuropil to the appropriate substance.

Origin of segment-specific tuning of motor patterns

One fascinating question which arises from this study is whether the segment-specific patterns reported here are present when the locust hatches, or rather if they appear during post-embryonic development. To address this question, pro- meso- and metathoracic motor patterns could be compared in the different instars of the post-embryonic locust.

5.3 Coordination of segmental central pattern generators

Lastly, I have shown that there exists central coupling between the different hemisegmental central pattern generator circuits, and that this coupling, although weak, would be appropriate for the coordination of the legs to ensure stability and maintenance of posture during walking.

Interneuronal basis of intersegmental coordination

The neuronal basis of the central coordination between leg central pattern generators in the locust is unknown, although several populations of intersegmental interneurons have been studied (see Chapter 4 and Laurent 1986, 1987, 1988; Laurent and Burrows 1988b, 1989a, b). Although it is not known if these neurons receive central inputs from local circuits controlling the legs, their anatomical and physiological

characteristics make them good candidates for the role of intersegmental coordinating interneurons. In an isolated preparation of coupled thoracic ganglia, it should now be possible to identify those neurons involved in intersegmental coordination by finding intersegmental interneurons that are rhythmically driven by the segmental oscillator in one segment and can modify the rhythmic motor pattern in a different segment.

Models of coordination of segmental central pattern generators

A number of models have been advanced to describe the essential features of coordinated locomotion in insects (review: Graham 1985). These models were for the most part mechanistic in nature, and their aim was to reproduce the qualitative aspects of insect walking. Accordingly, sensory and central mechanisms were not usually distinguished, and no attempt was made to build a detailed neuronal model of a central pattern generator. The work presented here should allow much more detailed models to be developed. Now that central pattern generating circuitry can be studied in the absence of sensory inputs, eventually it will be possible to build a model of an individual central pattern generator based on the properties and interconnections of known populations of interneurons (Burrows 1992), once their roles in generating leg motor rhythms have been determined. In addition, the central coupling between segmental pattern generator circuits presented here should form a basis for developing a detailed model of intersegmental coupling between the CPGs for different legs which clearly distinguishes central and sensory mechanisms for intersegmental coordination.

The demonstration that segmental central pattern generators contribute to shaping many aspects of walking in insects confirms that central pattern generation is a principle common to many animal nervous systems. Indeed, nervous systems which differ in many fundamental respects appear to all have evolved the same basic mechanism to generate robust yet flexible movements, consisting of a central circuit which generates basic patterns that can be modulated as needed by other neural pathways.

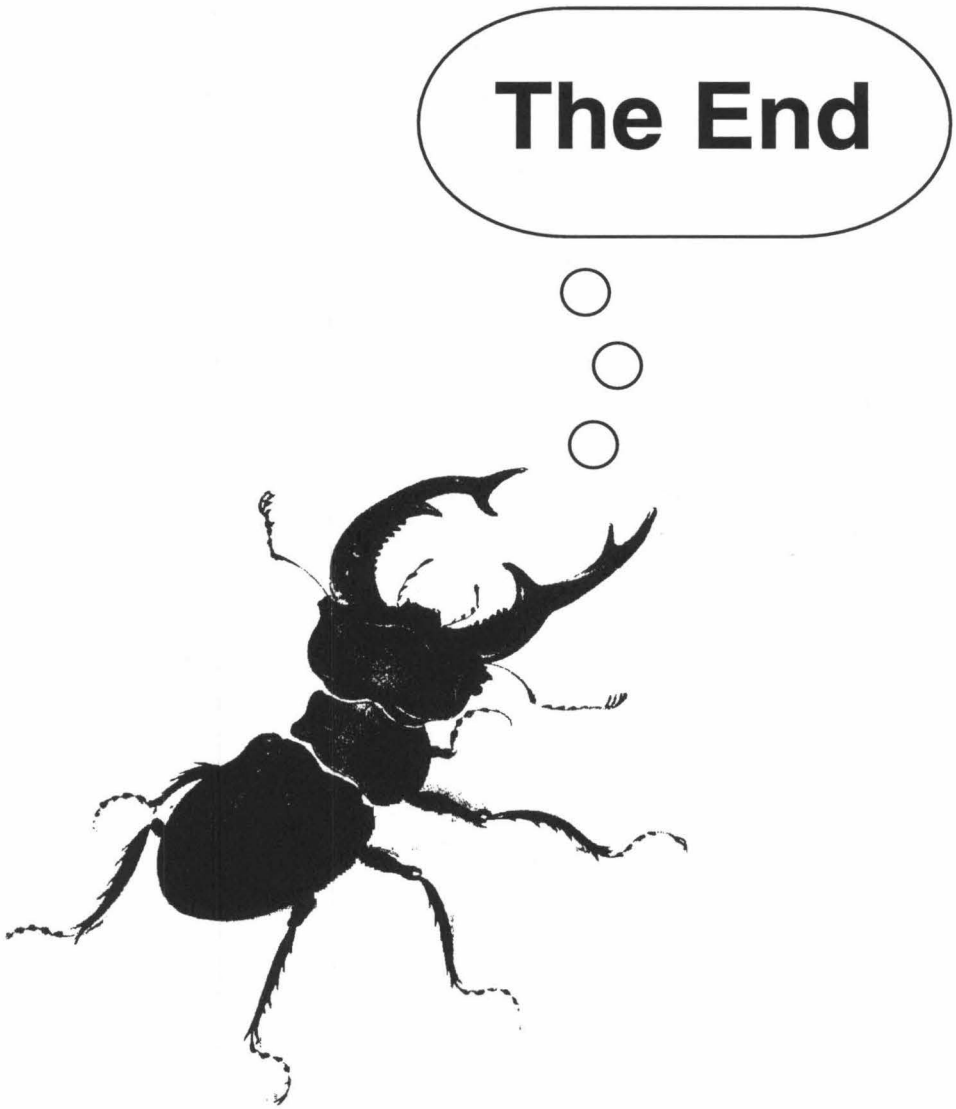
The End

Bibliography

Aertsen AMHJ, Gerstein GL, Habib MK and Palm G. Dynamics of neuronal firing correlation: modulation of "effective connectivity." *J Neurophysiol* **61**:900–917, 1989.

Arshavsky YI, Orlovsky GN, Panchin YV, Roberts A and Soffe SR. Neuronal control of swimming locomotion: analysis of the pteropod mollusc *Clione* and embryos of the amphibian *Xenopus*. *Trends Neurosci* **16**:227–233, 1993.

Barbeau H and Rossignol S. Initiation and modulation of the locomotor pattern in the adult chronic spinal cat by noradrenergic, serotonergic, and dopaminergic drugs. *Brain Res* **546**:250–260, 1991.

Bässler U and Wegner U. Motor output of the denervated thoracic ventral nerve cord in the stick insect *carausius morosus*. *J Exp Biol* **105**:127–145, 1983.

Benjamin PR and Elliott CJH. Snail feeding oscillator: The central pattern generator and its control by modulatory interneurons. In: *Neuronal and Cellular Oscillators*, JW Jacklet, ed. New York:Marcel Dekker, pp 173–214, 1989.

Bräunig P. The peripheral and central nervous organization of the locust coxo-trochanteral joint. *J Neurobiol* **13**:413–433, 1982.

Breer H and Knipper M. Characterization of acetylcholine release from insect synaptosomes. *Insect Biochem* **14**:337–344, 1984.

Breer H and Sattelle DB. Molecular properties and functions of insect acetylcholine receptors. *J Insect Physiol* **33**:771–790, 1987.

Burns MD. The control of walking in orthoptera. I. Leg movements in normal walking. *J Exp Biol* **58**:45–58, 1973.

Burns MD and Usherwood PNR. The control of walking in orthoptera. II. Motor neurone activity in normal free-walking animals. *J Exp Biol* **79**:69–98, 1979.

Burrows M. Co-ordinating interneurones of the locust which convey two patterns of motor commands: their connexions with ventilatory motorneurones. *J Exp Biol* **63**:735–753, 1975.

Burrows M. The control of sets of motoneurones by local interneurones in the locust. *J Physiol* **298**:213–233, 1980.

Burrows M. The physiology and morphology of median nerve motor neurones in the thoracic ganglia of the locust. *J Exp Biol* **96**:325–341, 1982.

Burrows M. Local circuits for the control of leg movements in an insect. *Trends Neurosci* **15**:226–232, 1992.

Burrows M and Hoyle G. Neural mechanisms underlying behavior in the locust *Schistocerca gregaria.* III. Topography of limb motorneurons in the metathoracic ganglion. *J Neurobiol* **4**:167–186, 1973.

Burrows M and Laurent G. Synaptic potentials in the central terminals of locust proprioceptive afferents generated by other afferents from the same sense organ.

J Neurosci **13**:808–819, 1993.

Burrows M, Laurent GJ and Field LH. Proprioceptive inputs to nonspiking local interneurones contribute to local reflexes of a locust hindleg. *J Neurosci* **8**:3085–3093, 1988.

Burrows M and Siegler MVS. Transmission without spikes between locust interneurones and motoneurones. *Nature* **262**:222–224, 1976.

Burrows M, Watson AHD and Brunn DE. Physiological and ultrastructural characterization of a central synaptic connection between identified motor neurons in the locust. *Eur J Neurosci* **1**:111–126, 1989.

Calabrese RL and Arbas EA. Central and peripheral oscillators generating heartbeat in the leech *Hirudo medicinalis.* In: *Cellular and Neuronal Oscillators*, JW Jacklet, ed., New York: Marcel Dekker, 237–267, 1989.

Campbell JI. The anatomy of the nervous system of the mesothorax of *locusta migratoria migratorioides* R. & F. *Proc R Zool Soc London* **137**:403–432, 1961.

Chrachri A and Clarac F. Fictive locomotion in the fourth thoracic ganglion of the crayfish, *Procambarus clarkii. J Neurosci* **10**:707–719, 1990.

Cruse H. The function of the legs in the free walking stick insect, *Carausius morosus. J Comp Physiol*, **112**:235–262, 1976.

Cruse H. What mechanisms coordinate leg movement in walking arthropods? *Trends Neurosci* **13**:15–21, 1990.

Dale N and Roberts A. Excitatory amino acid receptors in *Xenopus* embryo spinal cord and their role in the activation of swimming. *J Physiol* **348**:527–543, 1984.

David JA and Pitman RM. The pharmacology of muscarinic receptors on the soma membrane of an identified cockroach (*Periplaneta americana*) motoneuron *in vitro*. *J Physiol Lond* **446**:326, 1992.

Dean J. Leg coordination in the stick insect *Carausius morosus*: effects of cutting thoracic connectives. *J Exp Biol* **145**:103–131, 1989.

Delcomyn F. Neural basis of rhythmic behavior in animals. *Science* **210**:492–498, 1980.

Delcomyn F. Motor activity during searching and walking movements of cockroach legs. *J Exp Biol* **133**:111–120, 1987.

Delcomyn F and Usherwood PNR. Motor activity during walking in the cockroach *periplaneta americana*. I. Free walking. *J Exp Biol* **59**:629–642, 1973.

DeWeerth SP, Nielsen L, Mead CA and Åström KJ. A simple neuron servo. *IEEE Trans on Neural Networks*, **2**:248–251, 1991.

Elson RC and Selverston AI. Mechanisms of gastric rhythm generation in the isolated stomatogastric ganglion of spiny lobsters: bursting pacemaker potentials, synaptic interactions and muscarinic modulation. *J Neurophysiol* **68**:890–907, 1992.

Farley RD, Case JF and Roeder KD. Pacemaker for tracheal ventilation in the cockroach, *Periplaneta americana*. (L). *J Insect Physiol*, **13**:1713–1728, 1967.

Friesen WO. Neuronal control of leech swimming movements. In: *Cellular and Neuronal Oscillators*, JW Jacklet, ed., New York: Marcel Dekker, 269–316, 1989.

Getting PA. Comparative analysis of invertebrate central pattern generators. In: *Neural Control of Rhythmic Movements in Vertebrates*, edited by AH Cohen, S

Rossignol, and S Grillner, New York: Wiley, 101–127, 1988.

Getting PA and Dekin MS. Mechanisms of pattern generation underlying swimming in *Tritonia*. IV. Gating of central pattern generator. *J Neurophysiol*, **53**:466–480, 1985a.

Getting PA and Dekin MS. *Tritonia* swimming: A model system for integration within rhythmic motor systems. In AI Selverston (Ed), *Model Neural Networks and Behavior*, New York, NY: Plenum Press, 1985b.

Glaser EM and Ruchkin DS. *Principles of Neurobiological Signal Analysis.* New York: Academic Press, 1976.

Gossard J-P, Cabelguen J-M and Rossignol S. An intracellular study of muscle primary afferents during fictive locomotion in the cat. *J Neurophysiol* **65**:914–926, 1991.

Graham D. A behavioural analysis of the temporal organization of walking movements in the 1st instar and adult stick insect (*Carausius morosus*). *J Comp Physiol* **81**:23–52, 1972.

Graham D. Simulation of a model for the coordination of leg movement in free walking insects. *Biol Cybern*, **26**:187–198, 1977.

Graham D. Unusual step patterns in the free walking grasshopper *Neoconocephalus robustus*. I. General features of the step patterns. *J Exp Biol*, **73**:147–157, 1978a.

Graham D. Unusual step patterns in the free walking grasshopper *Neoconocephalus robustus*. II. A critical test of the leg interactions underlying different models of hexapod co-ordination. *J Exp Biol*, **73**:159–172, 1978b.

Graham D. Effects of circum-oesophageal lesion on the behaviour of the stick insect *Carausius morosus*. I. Cyclic behaviour patterns. *Biol Cybernetics* **32**:139–145, 1979a.

Graham D. Effects of circum-oesophageal lesion on the behaviour of the stick insect *Carausius morosus*. II. Changes in walking co-ordination. *Biol Cybernetics* **32**:147–152, 1979b.

Graham D. Pattern and control of walking in insects. *Advances in Insect Physiology* **18**:31–140, 1985.

Gray J, Lissmann HW and Pumphrey RJ. The mechanism of locomotion in the leech (*Hirudo medicinalis* Ray). *J Exp Biol* **15**:408–430, 1938.

Grillner S. Control of locomotion in bipeds, tetrapods and fish. In *Handbook of Physiology*, Section 1, Vol 2, VB Brooks, ed. Bethesda, MD: Amer Physiol Soc, 1179–1236, 1981.

Grillner S, Perret C and Zangger P. Central generation of locomotion in the spinal dogfish. *Brain Res* **109**:255–269, 1976.

Grillner S and Wallén P. Central pattern generators for locomotion, with special reference to vertebrates. *Ann Rev Neurosci*, **8**:233–261, 1985.

Grillner S, Wallén P, Brodin L and Lansner A. Neuronal network generating locomotor behavior in lamprey: circuitry, transmitters, membrane properties, and simulation. *Ann Rev Neurosci* **14**:169–199, 1991.

Grillner S and Zangger P. On the central generation of locomotion in the low spinal cat. *Exp Brain Res* **34**:241–261, 1979.

Grillner S and Zangger P. How detailed is the central pattern generator for locomotion? *Brain Res* **88**:367–371, 1975.

Gundelfinger ED. How complex is the nicotinic receptor system of insects? *Trends Neurosci* **15**:206–211, 1992.

Gynther IC and Pearson KG. An evaluation of the role of identified interneurons in triggering kicks and jumps in the locust. *J. Neurophysiol*, **61**:45–57, 1989.

Hale JP and Burrows M. Innervation patterns of inhibitory motor neurones in the thorax of the locust. *J Exp Biol* **117**:401–413, 1985.

Harris-Warrick RM and Marder E. Modulation of neural networks for behavior. *Ann Rev Neurosci*, **14**:39–57, 1991.

Harris-Warrick RM, Nagy F and 'Nusbaum MP. Neuromodulation of stomatogastric networks by identified neurons and transmitters. In: *Dynamic Biological Networks: The Stomatogastric Nervous System*, RM Harris-Warrick, E Marder, AI Selverston, M Moulins, eds. Cambridge: MIT Press, pp 87–137, 1992.

Heinzel H-G. Gastric mill activity in the lobster. II. Proctolin and octopamine initiate and modulate chewing. *J Neurophysiol*, **59**:551–565, 1988.

Heinzel H-G and Selverston AI. Gastric mill activity in the lobster. III. Effects of proctolin on the isolated central pattern generator. *J Neurophysiol*, **59**:566–585, 1988.

Heitler WJ and Burrows M. The locust jump. I. The motor programme. *J Exp Biol* **66**:203–219, 1977.

Hoyle G. The neuromuscular mechanism of an insect spiracular muscle. *J ins Physiol*

3:378–394, 1959.

Hughes GM. The co-ordination of insect movements. I. The walking movements of insects. *J Exp Biol* **29**:267–284, 1952.

Ikeda K and Wiersma CAG. Autogenic rhythmicity in the abdominal ganglia of the crayfish: the control of swimmeret movements. *Comp Biochem Physiol* **12**:107–115, 1964.

Jacobson RD and Hollyday M. Electrically evoked walking and fictive locomotion in the chick. *J Neurophysiol* **48**:257–270, 1982.

Kahn JA and Roberts A. The central nervous origin of the swimming motor pattern in embryos of *Xenopus laevis*. *J Exp Biol* **99**:185–196, 1982.

Kater SB and Rowell CHF. Integration of sensory and central programmed components in generation of cyclical feeding activity of *Helisoma trivolvis*. *J Neurophysiol* **36**:142–155, 1973.

Kopell N. Toward a theory of modelling central pattern generators. In: *Neural Control of Rhythmic Movements in Vertebrates*, edited by AH Cohen, S Rossignol, and S Grillner, New York: Wiley, 1988, 369–413, 1988.

Kristan WB Jr and Calabrese RL. Rhythmic swimming activity in neurones of the isolated nerve cord of the leech. *J Exp Biol* **65**:643–668, 1976.

Laurent G. Thoracic intersegmental interneurones in the locust with mechanoreceptive inputs from a leg. *J Comp Physiol* **159**:171–186, 1986.

Laurent G. The morphology of a population of thoracic intersegmental interneurones in the locust. *J Comp Neurol* **256**:412–429, 1987.

Laurent G. Local circuits underlying excitation and inhibition of intersegmental interneurones in the locust. *J Comp Physiol A* **162**:145–157, 1988.

Laurent G. Voltage-dependent nonlinearities in the membrane of locust nonspiking local interneurons, and their significance for synaptic integration. *J Neurosci* **10**:2268–2280, 1990.

Laurent G and Burrows M. Direct excitation of nonspiking local interneurones by exteroceptors underlies tactile reflexes in the locust. *J Comp Physiol* **162**:563–572, 1988a.

Laurent G and Burrows M. A population of ascending intersegmental interneurones in the locust with mechanosensory inputs from a hind leg. *J Comp Neurol* **275**:1–12, 1988b.

Laurent G and Burrows M. Distribution of intersegmental inputs to nonspiking local interneurons and motor neurons in the locust. *J Neurosci* **9**:3019–3029, 1989a.

Laurent G and Burrows M. Intersegmental interneurons can control the gain of reflexes in adjacent segments of the locust by their action on nonspiking local interneurons. *J Neurosci* **9**:3030–3039, 1989b.

Laurent G and Hustert R. Motor neuronal receptive fields delimit patterns of motor activity during locomotion of the locust. *J Neurosci* **8**:4349–4366, 1988.

Lazzaro J and Mead CA. A silicon model of auditory localization. *Neural Computation*, **1**:47–57, 1989.

LeMoncheck JE. An analog VLSI model of the jamming avoidance response in electric fish. *IEEE Journal of Solid State Circuits*, **27**(6), 1992.

Lewis GW, Miller PL and Mills PS. Neuromuscular mechanisms of abdominal pumping in the locust. *J Exp Biol* **59**:149–168, 1973.

Mahowald M and Douglas R. A silicon neuron. *Nature*, **354**:515–518, 1991.

Mahowald MA, Douglas RJ, LeMoncheck JE and Mead CA. An introduction to silicon neural analogs. *Semin Neurosci*, **4**:83–92, 1992.

Marder E and Paupardin-Tritsch D. The pharmacological properties of some crustacean neuronal acetylcholine, γ-aminobutyric acid, and L-glutamate responses. *J Physiol* **280**:213–236, 1978.

Marder E and Weimann JM. Modulatory control of multiple task processing in the stomatogastric nervous system. In: *Neurobiology of Motor Programme Selection*, J Kien, C McCrohan, and B Winlow, eds. New York: Pergamon Press, pp 3–19, 1992.

Matsushima T and Grillner S. Neural mechanisms of intersegmental coordination in lamprey: local excitability changes modify the phase coupling along the spinal cord. *J Neurophysiol* **67**:373–388, 1992.

Mead CA. *Analog VLSI and Neural Systems.* Addison-Wesley: Reading, MA, 1989.

McClellan AD. Movements and motor patterns of the buccal mass of *Pleurobranchaea* during feeding, regurgitation and rejection. *J Exp Biol*, **98**:195–211, 1982.

Miller PL. Respiration in the desert locust. II. The control of the spiracles. *J Exp Biol* **37**:237–263, 1960.

Miller PL. The regulation of breathing in insects. *Adv Insect Physiol*, **3**:279–354, 1966.

Miller PL. The derivation of the motor command to the spiracles of the locust. *J Exp Biol*, **46**:349–371, 1967.

Murray A, Del Corso D and Tarassenko L. Pulse-stream VLSI neural networks mixing analog and digital techniques. *IEEE Trans Neural Networks*, **2**:193–204, 1991.

Myers T and Retzlaff E. Localization and action of the respiratory centre of the Cuban burrowing cockroach. *J Insect Physiol* **9**:607–614, 1963.

Nagy F and Dickinson PS. Control of a central pattern generator by an identified modulatory interneurone in crustacea. I. Modulation of the pyloric motor output. *J Exp Biol* **105**:33–58, 1983.

Paul DH and Mulloney B. Intersegmental coordination of swimmeret rhythms in isolated nerve cords of crayfish. *J Comp Physiol A* **158**:215–224, 1986.

Pearce RA and Friesen WO. Intersegmental coordination of the leech swimming rhythm. I. Roles of cycle period gradient and coupling strength. *J Neurophysiol* **54**:1444–1459, 1985.

Pearson KG. Central programming and reflex control of walking in the cockroach. *J Exp Biol* **56**:173–193, 1972.

Pearson KG. Are there central pattern generators for walking and flight in insects? In: *Feedback and Motor Control in Invertebrates and Vertebrates.* WJP Barnes and M Gladden, eds. Croom Helm: London, 307–316, 1985.

Pearson KG and Iles JF. Discharge patterns of coxal levator and depressor motoneurones of the cockroach, *Periplaneta americana. J Exp Biol* **52**:139–165, 1970.

Pearson KG and Iles JF. Nervous mechanisms underlying intersegmental co-ordination

of leg movements during walking in the cockroach. *J Exp Biol* **58**:725–744, 1973.

Pearson KG and Rossignol S. Fictive motor patterns in chronic spinal cats. *J Neurophysiol* **66**:1874–1887, 1991.

Perkel DH, Gerstein GL and Moore GP. Neuronal spike trains and stochastic point processes. II. Simultaneous spike trains. *Biophys J* **7**:419–440, 1967.

Pflüger H-J and Burrows M. Locusts use the same basic motor pattern in swimming as in jumping and kicking. *J Exp Biol* **75**:81–93, 1978.

Phillips CE. Organization of motor neurons to a multiply innervated insect muscle. *J Neurobiol* **12**:269–280, 1981.

Poon MLT. Induction of swimming in lamprey by L-DOPA and amino acids. *J Comp Physiol* **136**:337–344, 1980.

Rand RH, Cohen AH and Holmes PJ. Systems of coupled oscillators as models of central pattern generators. In: *Neural Control of Rhythmic Movements in Vertebrates*, edited by AH Cohen, S Rossignol, and S Grillner, New York: Wiley, 1988, 333–367, 1988.

Reingold SC and Camhi JM. A quantitative analysis of rhythmic leg movements during three different behaviors in the cockroach *Periplaneta americana*. *J Insect Physiol* **23**:1407–1420, 1977.

Ritzmann RE and Pollack AJ. Identification of thoracic interneurons that mediate giant interneuron-to-motor pathways in the cockroach. *J Comp Physiol A* **159**:639–654, 1986.

Ritzmann RE and Pollack AJ. Wind activated thoracic interneurons of the cockroach.

II. Patterns of connection from ventral giant interneurons. *J Neurobiol* **19**:589–611, 1988.

Ritzmann RE and Pollack AJ. Parallel motor pathways from thoracic interneurons of the ventral giant interneuron system of the cockroach, *Periplaneta americana. J Neurobiol* **21**:1219–1235, 1990.

Ritzmann RE, Pollack AJ, Hudson SE and Hyvonen A. Convergence of multi-modal sensory signals at thoracic interneurons of the escape system of the cockroach, *Periplaneta americana. Brain Res* **563**:175–183, 1991.

Roberts A, Soffe SR and Dale N. In *Neurobiology of Vertebrate Locomotion.* S Grillner et al, eds. Macmillan. 279–306, 1986.

Robertson RM. Neuronal circuits controlling flight in the locust: central generation of the rhythm. *Trends Neurosci* **9**:278–280, 1986.

Robertson RM and Pearson KG. Interneurons in flight system of the locust: distribution, connections and resetting properties. *J Comp Neurol*, **215**:33–50, 1983.

Robertson RM and Pearson KG. Neural circuits in the flight system of the locust. *J Neurophysiol*, **53**:110–128, 1985.

Roeder KD. The control of tonus and locomotor activity in the praying mantis (*Mantis religiosa L.*) *J Exp Zool* **76**:353–374, 1937.

Ronacher B, Wolf H and Reichert H. Locust flight behavior after hemisection of individual thoracic ganglia: evidence for hemiganglionic premotor centers. *J Comp Physiol A* **163**:749–759, 1988.

Rossignol S, Lund JP and Drew T. The role of sensory inputs in regulating patterns

of rhythmical movements in higher vertebrates: A comparison between locomotion, respiration, and mastication. In: *Neural Control of Rhythmic Movements in Vertebrates*, edited by AH Cohen, S Rossignol, and S Grillner, New York: Wiley, 201–283, 1988.

Rossignol S, Saltiel P, Perreault M-C, Drew T, Pearson K and Bélanger M. Intralimb and interlimb coordination in the cat during real and fictive rhythmic motor programs. *Sem Neurosci* **5**:67–75, 1993.

Rowell CHF. Intersegmental coordination of flight steering in locusts. *Sem Neurosci* **5**:59–66, 1993.

Runion HI and Usherwood PNR. Tarsal receptors and leg reflexes in the locust and grasshopper. *J Exp Biol* **49**:421–436, 1968.

Ryckebusch S, Bower JM and Mead C. Modeling small oscillating biological networks in analog VLSI. In D. S. Touretzky (ed.) *Advances in Neural Information Processing Systems 1.* Morgan Kauffman: San Mateo, CA. pp. 384–393, 1989.

Ryckebusch S and Laurent G. Pilocarpine induces rhythmic activity in isolated thoracic ganglia of locusts. *Soc Neurosci Abstr* **17**:1581, 1991.

Ryckebusch S, Laurent G. Rhythmic patterns evoked in locust leg motor neurons by the muscarinic agonist pilocarpine. *J Neurophysiol* **69**:1583–1595, 1993.

Ryckebusch S and Mead C. An analog VLSI model for oscillatory biological neural circuits. In *Journées d'Electronique 1989: Réseaux de neurones artificiels.* Presses Polytechniques Romandes: Lausanne, Switzerland. pp. 303–312, 1989.

Ryckebusch S, Wehr M and Laurent G. Distinct rhythmic locomotor patterns can

be generated by a simple adaptive neural circuit: biology, simulation, and VLSI implementation. Submitted to *J Computational Neuroscience*, 1994.

Sarpeshkar R, Watts L and Mead CA. Refractory Neuron Circuits. Internal Memorandum, Physics of Computation Laboratory, California Institute of Technology, 1992.

Selverston AI, Russell DF, Miller JP and King DG. The stomatogastric nervous system: structure and function of a small neural network. *Prog Neurobiol* **7**:215–290, 1976.

Seymour KJ. The neural control of oviposition in the locust *Schistocerca gregaria. Ph.D. Dissertation* Jesus College, University of Cambridge, 1990.

Sherman E, Novotny M and Camhi J. A modified walking rhythm employed during righting behavior in the cockroach *Gromphadorhina portentosa. J Comp Physiol* **113**:303–316, 1977.

Shik ML and Orlovsky GN. Neurophysiology of locomotor automatism. *Physiol Rev* **56**:465–501, 1976.

Siegler MVS. Electrical coupling between supernumerary motor neurones in the locust. *J Exp Biol* **101**:105–119, 1982.

Siegler MVS and Pousman CA. Motor neurons of grasshopper metathoracic ganglion occur in stereotypic anatomical groups. *J Comp Neurol* **297**:298–312, 1990a.

Siegler MVS and Pousman CA. Distribution of motor neurons into anatomical groups in the grasshopper metathoracic ganglion. *J Comp Neurol* **297**:313–327, 1990b.

Sillar KT. Spinal pattern generation and sensory gating mechanisms. *Curr Opinion*

Neurobiol **1**:583–589, 1991.

Sillar KT, Clarac F and Bush BMH. Intersegmental coordination of central neural oscillators for rhythmic movements of the walking legs in crayfish, *Pacifastacus leniusculus*. *J Exp Biol* **131**:245–264, 1987.

Sillar KT and Skorupski P. Central input to primary afferent neurons in crayfish, *Pacifastacus leniusculus*, is correlated with rhythmic motor output of thoracic ganglia. *J Neurophysiol* **55**:678–688, 1986.

Simmers AJ and Bush BMH. Motor programme switching in the ventilatory system of *Carcinus maenas*: The neuronal basis of bimodal scaphognathite beating. *J Exp Biol*, **104**:163–181, 1983.

Snodgrass RE. The thoracic mechanism of a grasshopper, and its antecedents. *Smithsonian Misc Coll* **82**:1–111, 1929.

Sqalli-Houssaini Y, Cazalets J-R and Clarac F. Oscillatory properties of the central pattern generator for locomotion in neonatal rats. *J Neurophysiol* **70**:803–813, 1993.

Stein PSG. Intersegmental coordination of swimmeret motoneuron activity in crayfish. *J Neurophysiol* **34**:310–318, 1971.

Stevenson PA and Kutsch W. A reconsideration of the central pattern generator concept for locust flight. *J Comp Physiol A* **161**:115–129, 1987.

Suzue T. Respiratory rhythm generation in the *in vitro* brain stem-spinal cord preparation of the neonatal rat. *J Physiol* **354**:173–183, 1984.

Székely G, Czéh G and Vörös G. The activity pattern of limb muscles in freely

moving normal and deafferented newts. *Exp Brain Res* **9**:53–62, 1969.

Thompson WJ and Stent GS. Neuronal control of heartbeat in the medicinal leech. I. Generation of the vascular constriction rhythm by heart motor neurons. *J Comp Physiol* **111**:261–279, 1976.

Trimmer BA and Weeks JC. Effects of nicotinic and muscarinic agents on an identified motoneurone and its direct afferent inputs in larval *Manduca sexta*. *J Exp Biol* **144**:303–337, 1989.

Trimmer BA and Weeks JC. The mechanism of an excitability change induced by muscarinic receptors in an identified insect motoneuron. *Soc Neurosci Abstr* **17**:199, 1991.

Turrigiano GG and Heinzel H-G. Behavioral correlates of stomatogastric network function. In *Dynamic Biological Networks: The Stomatogastric Nervous System*, edited by RM Harris-Warrick et al., Cambridge, MA: MIT Press, 197–220, 1992.

Tyrer NM and Gregory GE. A guide to the neuroanatomy of locust suboesophageal and thoracic ganglia. *Phil Trans R Soc Lond B* **297**:91–123, 1982.

Viala G and Buser P. Activités locomotrices rhythmiques stéréotypées chez le lapin sous anesthésie légère. Etude de leurs caractéristiques générales. *Exp Brain Res* **8**:346–363, 1969.

Wallén P and Williams TL. Fictive locomotion in the lamprey spinal cord *in vitro* compared with swimming in the intact and spinal animal. *J Physiol* **347**:225–239, 1984.

Wang X-J and Rinzel J. Spindle rhythmicity in the reticularis thalami nucleus:

synchronization among mutually inhibitory neurons. *Neuroscience*, **53**:899–904, 1993.

Watts L. (in press) Event-Driven Simulation of Networks of Spiking Neurons. *Neural Information Processing Systems, 1993.*

Watts L. Designing Networks of Spiking Silicon Neurons and Synapses. *Proceedings of Computation and Neural Systems Meeting CNS*92*, Kluwer: San Francisco, CA, 1992.

Weimann JM. Multiple task processing in neural networks: Numerous central pattern generators in the stomatogastric nervous system of the crab, *Cancer borealis*, Ph.D. Thesis, Department of Biology, Brandeis University, 1992.

Weimann JM, Meyrand P and Marder E. Neurons that form multiple pattern generators: identification and multiple activity patterns of gastric/pyloric neurons in the crab stomatogastric system. *J Neurophysiol*, **65**:111–122, 1991.

Wiens TJ. Common and specific inhibition in leg muscles of decapods: sharpened distinctions. *J Neurobiol* **20**:458–469, 1989.

Wilson DM. The central nervous control of flight in a locust. *J Exp Biol* **38**:471–490, 1961.

Wilson DM. Insect walking. *Ann Rev Entomol* **11**:103–122, 1966.

Wolf H. Activity patterns of inhibitory motoneurones and their impact on leg movement in tethered walking locusts. *J Exp Biol* **152**:281–304, 1990.

Wolf H. Reflex modulation in locusts walking on a treadwheel—intracellular recordings from motoneurons. *J Comp Physiol* **170**:443–462, 1992.

Wolf H and Laurent G. Rhythmic modulation of the responsiveness of locust sensory local interneurons by walking pattern generating networks. *J Neurophysiol* **71**:110–118, 1994.

Zill SN. A model of pattern generation of cockroach walking reconsidered. *J Neurobiol* **17**:317–328, 1986.

Zill SN and Moran DT. The exoskeleton and insect proprioception. III. Activity of tibial campaniform sensilla during walking in the American cockroach, *Periplaneta americana*. *J Exp Biol* **94**:57–75, 1981.